E.G.Gordeev, V.P.Ananikov
Russ. Chem. Rev., 2020, **89** (12) 1507 – 1561

https://doi.org/10.1070/RCR4980

Widely accessible 3D printing technologies in chemistry, biochemistry and pharmaceutics: applications, materials and prospects

Evgeniy G. Gordeev, Valentine P. Ananikov*

N.D.Zelinsky Institute of Organic Chemistry, Russian Academy of Sciences
Leninsky prosp. 47, 119991 Moscow, Russian Federation

Representative examples of the application of 3D printing in organic synthesis, biochemistry, biotechnology, analytical chemistry, pharmaceutics and chemical education are considered. It is shown that additive technologies open up new prospects for the development of these fields of science. The characteristics of widely used 3D printing methods (fused deposition modelling and stereolithography) are discussed in the context of chemical applications. It is noted that the key feature of these methods is the wide accessibility of technologies and materials.
The bibliography includes 498 references.

Contents

1. Introduction 1507
2. Methods of 3D printing 1509
3. Polymer materials for 3D printing 1514
3.1. Thermoplastic polymers as materials for fused deposition modelling 1515
3.2. Materials for robocasting 1523
3.3. Materials for photopolymerization methods 1524
4. Application of 3D printing in chemistry and related fields 1525
4.1. Additive technologies in chemical synthesis 1526
4.2. Additive technologies in analytical chemistry 1531
4.3. Additive technologies in biochemistry and biotechnology 1536
4.4. Additive technologies in pharmaceutics 1540
4.5. Additive technologies in chemical education 1544
5. Conclusion 1548
List of abbreviations and symbols 1549

1. Introduction

Additive manufacturing (AM), also known in the literature and mass media as 3D printing, has currently spread to all levels of material production, starting from large industrial plants using expensive equipment and ending with individual consumers who use inexpensive 3D printers or assemble quite functional 3D printers by themselves from available parts.[1–3] Despite the fact that the first patents related to commercial 3D printing refer to mid-1980s (earlier invented devices that have not found commercial use can be traced down to the beginning of the 1950s),[4] the common use of this technology started only recently.[5] The transition of 3D printing to a sort of personal technology is caused by the rapid appearance of quite a number of manufacturers who develop and sell inexpensive personal 3D printers (for a price comparable with the price of a personal computer). This is, in turn, is caused by expiration of the key patent restrictions on some additive technologies, reduction in the cost of element base of 3D printers and wide distribution of three-dimensional modelling software, which is an integral part of 3D printing technology.

Additive technologies are based on layer-by-layer forming of an object according to a computer model (Fig. 1). This is done by gradual building-up and subsequent curing of a material in some way.[6] It can be said that the object is grown in the build chamber of a 3D printer, with the utilization efficiency of the construction material reaching 100% in most cases. Computer representation of a product model is an integral part of any 3D printing method.

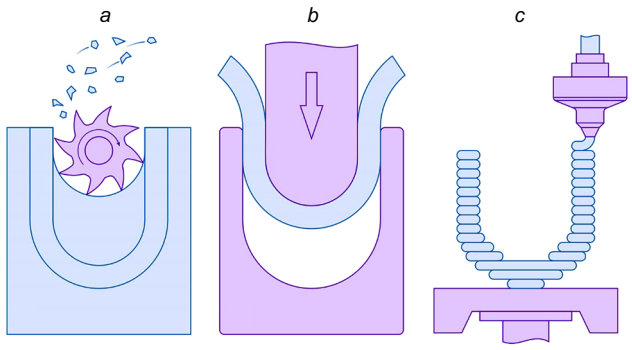


Figure 1. Schematic view of various manufacturing methods. (*a*) Subtractive methods, (*b*) forming (exemplified by stamping), and (*c*) additive methods. The item material is drawn in blue, and the process equipment material is drawn in violet.

E.G.Gordeev. PhD in Chemistry, Senior Researcher at the Laboratory of Metal-Complex and Nanoscale Catalysts, ZIOC RAS.
E-mail: gordeev_e@ioc.ac.ru
Current research interests: molecular modelling, quantum chemistry, reaction mechanisms, additive technologies.
V.P.Ananikov. Academician, Doctor of Chemical Sciences, Head of the same Laboratory, ZIOC RAS.
E-mail: val@ioc.ac.ru
Current research interests: catalysis, organic synthesis, nanotechnologies, NMR spectroscopy, mass spectrometry, electron microscopy, additive technologies.

Translation: Z.P.Svitanko

Received 14 July 2020

© 2020 Uspekhi Khimii, ZIOC RAS, Russian Academy of Sciences and IOP Publishing Limited

A comparison of additive technologies with conventional manufacturing methods shows a number of fundamental advantages of 3D printing, which implies that advancement of 3D printing may bring about a new industrial revolution.[7] For example, subtractive manufacturing methods (Fig. 1 *a*) based on removal of extra material from a billet (milling, turning, *etc.*) are characterized by large amounts of waste, irrational use of materials and the need for expensive and difficult to operate processing equipment to manufacture items of complex shape. Most often, the implementation of subtractive manufacturing methods requires a separate work space and highly skilled personnel. Forming methods (stamping, injection moulding, extrusion, *etc.*, Fig. 1 *b*) require complex shape-forming tooling (injection moulds, forming stamps, *etc.*), the manufacture of which is also sophisticated and expensive.

Additive technologies are free from the above drawbacks: 3D printing generates virtually no waste and 3D printers have modest installation requirements (such as dimensions, power consumption, sound insulation, *etc.*), which allows the use of these technologies in general-purpose rooms. Owing to the absence of waste, expensive construction materials (*e.g.*, some engineering plastics) are used much more efficiently for 3D printing than for subtractive technologies.

The additive technology principle, that is, layer-by-layer building of an object (Fig. 1 *c*), allows for manufacturing items of any geometrical complexity using the same 3D printer, including implementation of geometric shapes that cannot be attained by conventional subtractive technologies: parts with closed cavities of a complex topology, three-dimensionally branched channel structures, *etc.*[8–11] Furthermore, the additive method is suitable for manufacturing porous structures; objects made of mechanically weak materials (wax, gels, biological materials); and objects consisting of several different materials. Some 3D printing technologies have so high spatial resolution that it is possible to manufacture millimetre- or even micrometre-scale parts.[12–14]

An important feature of 3D printing is the high quality of the resulting objects even when inexpensive personal 3D printers are used. Therefore, additive technologies can be considered to be a part of a new manufacturing paradigm, as any person can fabricate an object not inferior (or only slightly inferior) to the one manufactured industrially. In view of these extensive opportunities for 3D printing, interest in this class of technologies from all branches of material production is quite understandable.

Currently, additive technologies also suffer from serious drawbacks: low production rate and high cost of consumables for some of the methods. Therefore, 3D printing is still used for piece or small batch production, whereas mass and serial production are more efficiently performed using conventional technologies such as injection moulding. However, it is noteworthy that a low production rate means a rate that is too low, particularly mass production. In the case of fabrication of a single intricate item, personal 3D printing ensures a much higher production rate than conventional techniques since the item can be manufactured directly at the workplace and there is no need to spend time looking for a special workshop, defining the scope of work, planning the design and manufacturing of tooling.

It is most appropriate to use 3D printing for unique products, especially those with intricate designs such as prototypes, parts and installations required as single copies, repair parts and tailor-made products (for example, medical appliances adjusted to a particular patient). Such items are widely used in scientific research, especially in chemistry and related disciplines, because experimental studies often require unique chemical reactors, mixers and miscellaneous laboratory accessories tailored for a particular chemical experiment.[15] A personal 3D printer can be installed in any chemical or biological laboratory, and researchers would be able to manufacture the necessary accessories themselves in a short time.

The technological sequence of 3D printing (Fig. 2) starts with the development of a 3D computer model using a suitable 3D modelling system. Then, the finished model is exported as a polygonal mesh to a file format meant for storing 3D models (most often, this is STL, which got its name from the word 'stereolithography') since this formal does not depend on the CAD program in which the model was designed and is appropriate for moving to the next stage called slicing. In the slicing procedure, the model is split by software tools into a set of layers to be used for constructing the model in the 3D printer chamber, taking into account the user's settings (layer thickness, printing velocity, and other process parameters).

Since additive manufacturing is based on the digital representation of an object, optimization of the design of a new product is significantly accelerated. After changes to the design have been made, the new version of the object can be immediately manufactured and tested,

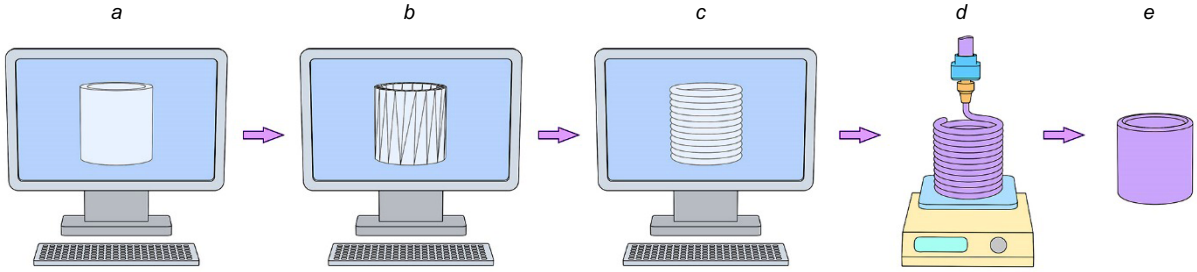


Figure 2. Technological sequence of 3D printing. (*a*) Design of the model using a computer-aided design system; (*b*) model export to a polygonal format, *e.g.*, STL; (*c*) adjustment of additive manufacturing parameters and slicing of the model; (*d*) 3D printing of the part; (*e*) finished part after postprocessing.

which is of great importance for research practice. Optimization can not only be 'topological' (concerning the object geometry) but can also be directed towards selection of the most appropriate material, since a very extensive range of construction materials suitable for solving most of the problems in everyday laboratory practice has now been offered for 3D printing.

This review addresses particular illustrative examples of application of 3D printing methods (first of all, widely available methods such as fused deposition modelling using thermoplastic materials and, to a lesser extent, stereolithography) in organic chemistry, biochemistry and biotechnology, analytical chemistry, pharmaceutics and chemical education. The benefits and drawbacks of 3D printing in the context of chemical laboratory applications are demonstrated. The applicability of the materials available for additive manufacturing and for solving practical problems is analyzed. Examples are given of the successful application of additive manufacturing methods in research projects in which 3D printing is an inherent part of experiments.

The 3D printing technologies generally accessible in scientific research and in education are discussed using specially selected representative examples. A detailed description of specific fields of additive technologies is beyond the scope of this review. To date, numerous review papers devoted to the application of 3D printing in particular fields of chemistry are available from the literature; these papers are cited in the relevant Sections of the review.

It is noteworthy that most of the available publications are concerned with a specific subject and cover the use of additive technologies in some particular fields. This review is characterized by wide coverage of the 3D printing application areas, which provides a general view of the opportunities offered by 3D printing not only for chemistry, but also for some related fields. This review is meant for a wide range of readers developing new approaches in the fields of chemical synthesis, biochemistry, materials science and chemical education.

2. Methods of 3D printing

The general principle that underlies all additive methods is that objects are fabricated one layer after another (layer-by-layer synthesis). 3D printing methods differ in the ways of layer formation and layer fusion (these two operations take place simultaneously), *i.e.*, in the set of physical principles that underlie the layer-by-layer synthesis. The choice of the 3D printing method is of prime importance, as it determines the applicable types of materials (and, hence, the strength and mass parameters), the surface quality of the finished product, the necessity and type of posttreatment and the microstructure of the material in the finished product For example, the necessity to manufacture a metal object immediately defines an appropriate group of additive manufacturing methods. Further specification of the type of metal, required dimensions, strength and surface roughness of the product allows for choosing a particular method.

In the early stages of development, additive manufacturing methods were mainly used for prototyping, *i.e.*, for designing prototypes and models of the future products. Therefore, in the early literature, the term 'rapid prototyping' was used synonymously for additive manufacturing. Currently, prototyping is only one of the application fields of 3D printing, as modern additive technologies have found wide use for manufacturing of the final functional items. This situation is referred to as 'rapid manufacturing' or 'direct digital manufacturing'.[6] The fabrication of plastic prototypes from general-purpose materials in chemical laboratory practice may be useful for optimizing the reactor and tooling designs before metals or expensive special plastics are used to manufacture the required items. Prototyping in the form of 'solid-state imaging' is used in chemical education, for example, for the construction of plastic molecular models. Some 3D printing techniques, for example, selective laser sintering of a metal powder, are scarcely used for prototyping due to the complexity of technology and the high cost of the resulting products and because, most often, there is no need for metal prototypes. These methods were initially meant for the production of final products.

Currently, according to the ISO/ASTM52900-15 standard, additive technologies are classified into seven groups (Fig. 3).[16,17]

1. Binder jetting (BJ) is a 3D printing technology (Fig. 3 *a*) in which the object is formed by selective binding of a powdered material. This method is also known as 3D printing (3DP),[18] that is, the term '3D printing' initially referred to this process in particular, but later, it became the general name. In the modern literature, the abbreviation 3DP is frequently used to mean printing by powder binding. The materials used for BJ technology include gypsum, sand, ceramics and metals.[19,20] During printing, the levelling roller makes a thin layer of the powder, and then the powder is bound, according to the layer profile, by means of a liquid binder deposited from an array of nozzles. The liquid binder can be additionally subjected to short-term curing. Then, the spreader makes the next layer of the powder, and the whole object is fabricated in this way. The BJ method is widely used to print three-dimensional devices, *e.g.*, sand cast moulds;[21] the technology allows for colouring the products, which is demanded in prototyping.[22] A benefit of the technology is that there is no need for supporting structures during printing of complex items, since the item is formed inside the powder bulk, which serves as the support for overhanging parts. The drawbacks of the technology are high surface roughness, the presence of polymer binder in the finished product and a narrow range of construction materials.

2. Directed energy deposition (Fig. 3 *b*). In this group of methods, a metal is fed as a powder stream carried by an inert gas, coaxial to a laser beam, to the focusing point of the laser beam.[23] At the focusing point, the metal is welded on the underlying material. A plasma or electron beam can also serve as the source of energy. This technology is used for metal materials; it is actively employed in mechanical engineering to manufacture new objects, including those with variable composition and properties,[24] to restore damaged metal surfaces,[25] and to apply protective coatings on working surfaces.[26] This group includes several methods: direct metal deposition (DMD), laser engineered net shaping (LENS), laser metal deposition (LMD) and so on. The additive technologies of this group are used, most often, in the traditional fields of mechanical engineering (aircraft building, automobile manufacturing, power engineering, *etc.*). Therefore to attain high surface quality and manufacturing

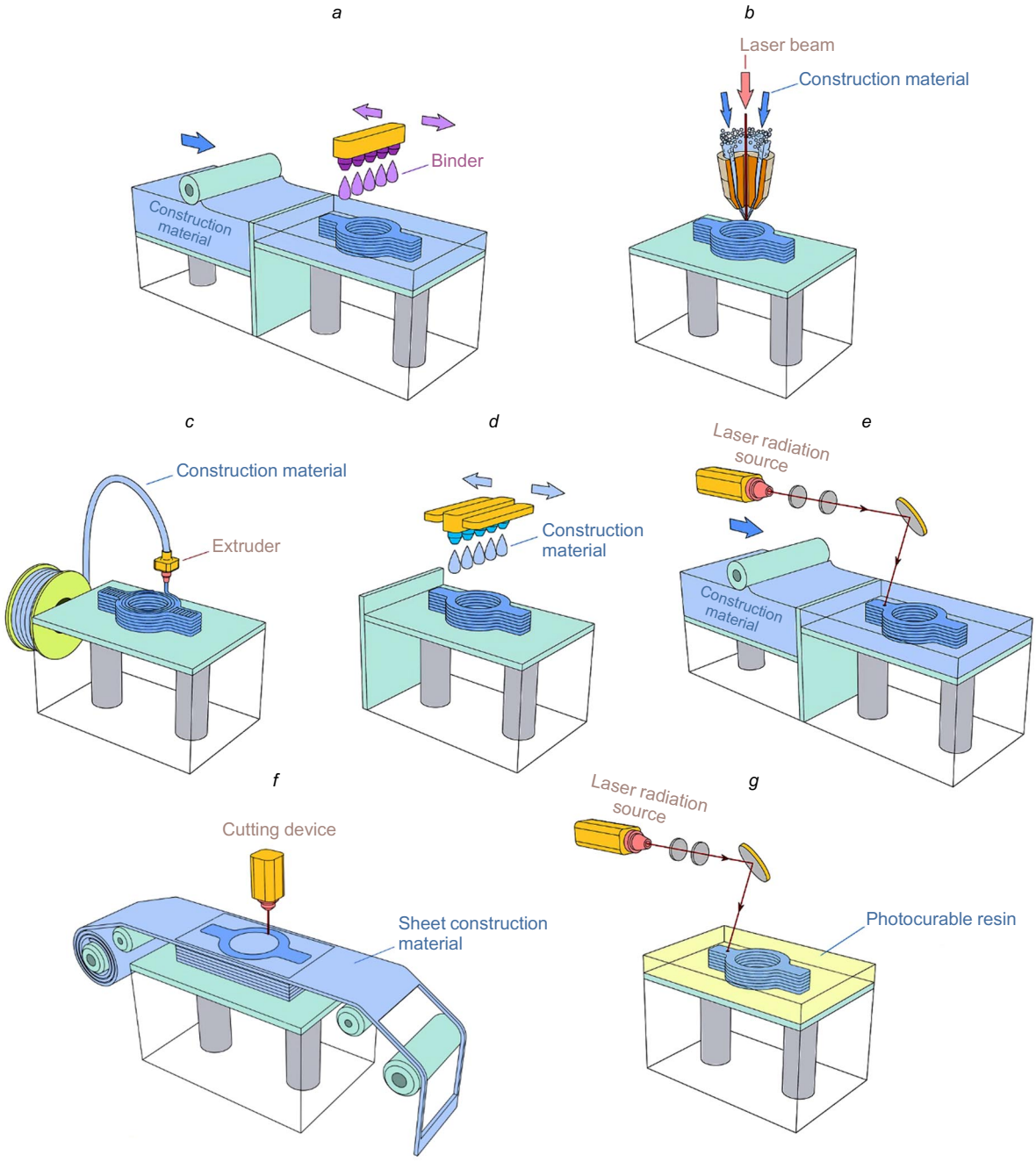


Figure 3. Main groups of additive manufacturing processes according to ASTM (American Society for Testing and Materials) classification.[16] (*a*) Binder jetting (BJ), (*b*) directed energy deposition (DED), (*c*) material extrusion (ME) exemplified by fused deposition modelling (FDM), also known as fused filament fabrication (FFF), (*d*) material jetting (MJ), (*e*) powder bed fusion, (*f*) sheet lamination (SL), and (*g*) vat photopolymerization (VP) exemplified by stereolithography (SLA). The Russian translation of the names of additive manufacturing processes is given in GOST R 57589-2017.[17]

accuracy, DED technologies are combined with traditional subtractive processing methods using computer numerically controlled (CNC) machines.[27]

3. Material extrusion (ME, Fig. 3 *c*). These technologies are based on extrusion of the material through the extruder nozzle. The extruder moves according to the geometry of each layer and continuously supplies the material through a thin orifice. Immediately after coming out of the nozzle, material retains its shape,[28] that is, each layer is automatically drawn on the build platform of the printer. After one layer is completed, the platform or the nozzle moves by a distance equal to the layer thickness, and the next layer is formed over the previous layer. The whole object is constructed in this way. This group comprises the fused deposition modelling (FDM) and direct-ink-writing (DIW) methods. According to the FDM method, the extruded material is a melt of a thermoplastic material, most often a polymer. This approach is also applicable for printing glass objects by extrusion of molted glass; however, 3D printing with glass is still at the pilot stage because of the high melting temperature of glass.[29–31]

Currently, the FDM method implemented as fused deposition of thermoplastic polymer filaments has

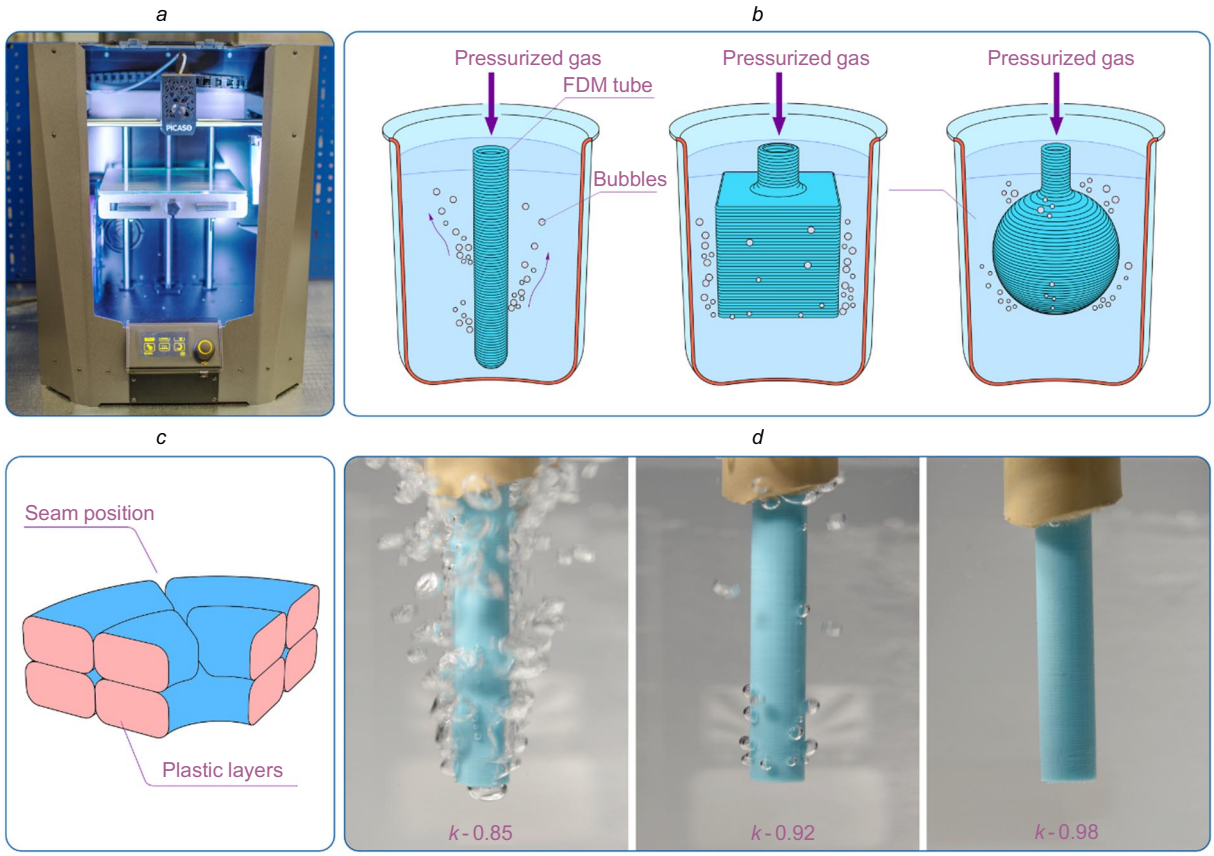


Figure 4. Appearance of a desktop FDM 3D-printer (*a*); schematic of testing of differently shaped FDM products for leak-tightness by compressed air pumping into the internal cavity of the product (*b*); illustration of the spatial arrangement of layers in the wall of the FDM-printed product (*c*); results of leak-tightness testing of cylindrical PLA test tubes produced by FDM printing with different extrusion multipliers (*k*) (*d*).[32]

become popular not only among professionals but also among amateurs and in the field of education; therefore, desktop FDM 3D printers (Fig. 4 *a*) can often be found in the workrooms of amateur engineers and artists. This wide popularity of FDM printing is facilitated by the possibility of cheap implementation of this technology in portable printers and the availability of a wide variety of inexpensive consumables (plastics) with various technical and decorative properties.

Personal FDM 3D printing is being actively implemented in scientific laboratories for fast manufacturing of equipment and accessories for experimental research. A specific feature of FDM printing, as opposed to powder sintering and stereolithography methods, is the clear-cut layered structure of the resulting products and the impossibility of high-quality production of small items (1 – 5 mm), since the plastic is extruded through a nozzle with a diameter of 0.1 – 0.5 mm, while the layer thickness varies in the range of 0.05 – 0.5 mm. In other words, FDM printers do not possess a high spatial resolution comparable, for example, with that of the SLA method. Furthermore, the use of very thin layers leads to an inadmissibly long printing time, since each layer is formed by a massive extruder, which moves at a moderate linear velocity.

The layer-by-layer extrusion of the plastic from the nozzle results in the formation of a porous wall structure of the resulting object (Fig. 4 *b*,*c*). This feature should be taken into account for using FDM products in chemistry and other fields where equipment must be leak-tight. The porosity of FDM products may be due to nonuniform fusion of the plastic layers (pores between the layers) and insufficient amount of the polymer melt filling the points of seams where the extruder switches to the next layer and the material supply is interrupted for a short period of time (the pores are within one layer). Therefore, to obtain leak-tight FDM products, for each particular material, it is necessary to thoroughly optimize the printing parameters (extrusion temperature, layer thickness, extrusion width, plastic feed rate), which should ensure strong adhesion of the layers into a single monolithic piece and filling of all possible small voids of the wall.[33 – 35]

The effect of various parameters of the additive manufacturing process on the leak-tightness of the laboratory reactors manufactured by FDM was evaluated using a relatively simple procedure consisting of the supply of compressed air into the cavity of a printed object located under a layer of water (Fig. 4 *b*).[32] If the object was not leak-proof, air bubbles appeared on its surface; this was a convenient tool for detecting the sites of defects of the reactor shell. This procedure was used to study reactors of various geometric shapes: cylindrical, conical, spherical, pyramidal and cubic. It was shown that in the case of flat-face geometry, defects were mainly concentrated at the edges. A high degree of porosity was found for conical products, as the layers were displaced relative to one another in this case. Cylindrical objects

proved to be most leak-tight since the plastic layers were located exactly above one another, which ensured a high degree of fusion of the layers. The variation in the material had little effect on the leak-tightness of the products since an appropriate choice of the temperature conditions ensures efficient fusion of the layers.[32] The most important parameter affecting the leak-tightness of the FDM products was the extrusion multiplier, which controls the plastic feed rate through the nozzle of the print head during printing. An increase in the extrusion multiplier leads to filling of wall voids with the material, thus enhancing the quality of the product (Fig. 4 *d*).

As the number of defects in the FDM products decreases, their mechanical strength and heat conductivity increase. The FDM method makes it possible to change the properties of the final product owing to the large number of adjustable parameters; for example, it is possible to vary the weight, strength, and heat conductivity of the printed objects by varying the infill density.[36]

In the DIW method, extrusion of a viscous material such as ceramic mass takes place without melting.[37] Materials possessing pseudoplastic behaviour (a decrease in the viscosity upon increasing shear strain) are well suited for this method. This feature allows free flow of the material from the nozzle, while the material shape is preserved on the 3D printer platform. The DIW method is widely used for bioprinting using various gels filled with living cells or materials for manufacturing artificial bone tissue scaffolds as the feedstock.[38] Extrusion methods offer the opportunity to use a virtually infinite range of feedstock materials for printing, which makes this group of technologies highly attractive for solving certain research problems. The extrusion methods proved to be most appropriate for printing products using numerous composite materials filled with a variety of particles, fibres or continuous reinforcing filaments.[39–41]

4. Material jetting (MJ, Fig. 3 *d*) is based on the formation of each layer of the object by jet deposition of the construction material by an array of nozzles in the 3D printer head, similar to jet printing on paper;[42] in other words, the material initially occurs in the liquid state. After deposition, the material layer can be cured by UV radiation emitted by the lamp mounted on the print head. This group includes the PolyJet technology developed by Stratasys,[43] MultiJet Printing (MJP) developed by 3D Systems[44] and Drop-on-Demand (DOD) method used in Solidscape printers.[45] In the PolyJet and MJM technologies, UV curable compositions are used as the feedstock, while commercial DOD technology is based on the use of wax, which is supplied to the print head as a melt. The wax models manufactured by DOD are subsequently used for metal casting, for example, in jewellery. Recently, the use of DOD for printing metal objects with molten metals has been reported.[46] The MJ group also includes the NanoParticle Jetting (NPJ) technology developed by the XJET company. According to NPJ technology, liquid ink for building objects contains metal or ceramic nanoparticles, *i.e.*, ink is a suspension. After 3D printing, the product is subjected to an additional heat-treatment stage, in which the particles are sintered, *i.e.*, using NPJ, it is possible to finally obtain a metal or ceramic product with a high spatial resolution typical of this group of technologies.

Material jetting technologies are distinguished by high accuracy of product construction and high quality of the product surface, as well as the possibility of printing transparent, coloured, and elastic objects (in the case of PolyJet and MJP). A specific feature of MJ technology is the ease of manufacturing objects from various materials during one continuous 3D printing process[47] and objects with a gradient (gradual) change in the properties along certain directions.[48] For example, it is possible to generate a gradual colour transition or gradual change in transparency, strength, elasticity and other properties. This is attained owing to the principle of jet deposition: during printing, it is possible to mix materials with different properties in different ratios. However, the equipment required for this technology is expensive, and as a rule, only certified consumables are allowed.

5. Powder bed fusion (Fig. 3 *e*) is based on selective sintering or fusion of a powder with a laser or electron beam.[49] The applicable construction materials are metals,[50] plastics,[51,52] ceramics,[53,54] composites,[55] glass[56] and other materials capable of existing as finely dispersed powders.[57] Manufacturing of objects using several materials simultaneously is possible.[58,59] Currently, this is the key group of additive manufacturing technologies for the production of metal objects (Fig. 5), including those exhibiting magnetic properties.[60,61] This group includes the following technologies: selective laser sintering (SLS), direct metal laser sintering (DMLS) of metal powders, selective laser melting (SLM), electron beam melting (EBM), and multi-jet fusion (MJF). In the SLS, DMLS, and SLM methods, sintering or fusion occurs under the action of a laser beam, while in the EBM method, fusion is induced by an electron beam in a vacuum (this approach is considered as a promising additive manufacturing technology for outer space); in the MJF method (relatively recent product of Hewlett-Packard[62,63]), fusion is affected by thermal energy.

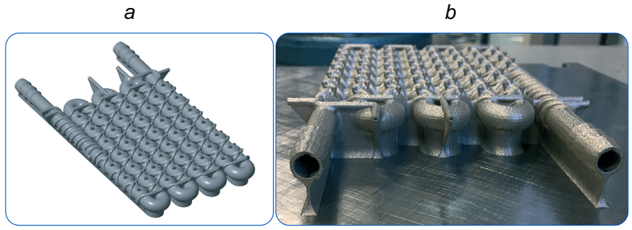


Figure 5. Three-dimensional CAD model of a flow chemical reactor (*a*); flow chemical reactor manufactured by SLM from 316L steel (*b*).[64]

Powder bed fusion printing starts with the formation of a layer of powder material by means of a levelling roller. Then selective fusion of the powder layer according to the digital model of the object takes place under the action of a particular energy source. Subsequently, a new powder layer is formed over the finished layer, fusion is induced once again, and so on until the object building is complete.

Like in binder jetting technology, powder bed fusion does not require additional supporting structures, as the printed product is formed within the powder bulk, except for the cases of printing metal objects. Currently, only polyamide powder is used in MJF technology; a specific feature of this method is that the product layer is formed upon jetting of a special binder and thermal fusion of

powder particles coated with this binder takes place in the next stage. The products obtained by powder methods have a rough surface, which is markedly inferior in this parameter to objects obtained by classical subtractive methods. However, for chemical applications, relatively low surface smoothness is usually not an obstacle to the use of a product.

In most cases, 3D printers operating on the selective sintering principle (especially for metal feedstock) are inaccessible for personal use, but represent expensive equipment for industrial use. However, in recent years, desktop 3D printers implementing layer-by-layer powder sintering technology have started to appear. Examples are Sinterit Lisa,[65] Sintratec Kit[66] and Formlabs Fuse 1 for selective laser sintering of a plastic powder. The price of such desktop 3D printers is acceptable for personal users, *i.e.*, fusion of plastic powder materials is gradually becoming a widely accessible personal 3D printing technology.

6. Sheet lamination (SL, Fig. 3*f*), includes laminated object manufacturing (LOM), selective deposition lamination (SDL) and ultrasonic additive manufacturing (UAM) technologies. UAM technology is also called ultrasonic consolidation and comprises the formation of an object by merging layers that have been cut out of a sheet material in one or another way (see Fig. 3*f*).[67] This process can be applied to a broad range of materials: paper, plastic, metals, textiles and composite materials. The SDL method implemented, for example, in MCor 3D printers for manufacturing paper objects is based on fusing sheets of the material together. In the case of polymer films, the layers can be fused together with a heated roller (LOM). Metal sheets are connected by ultrasonic treatment combined with high pressure (UAM); furthermore, this approach is applicable for joining sheets of different metals.[68] Ultrasonic additive manufacturing is combined with subtractive processing using CNC machines: in the first stage, several layers of metal foil are connected to one another by ultrasonic treatment, then a shape is cut by CNC milling, the next several metal layers are added, CNC milling is performed again and so on.

The sheet lamination printing is not accompanied by any phase transitions (melting, crystallization) of the main construction material, *i.e.*, no shrinkage takes place. The SL method is not always successful in manufacturing objects with internal cavities of complex topology or products with very small parts; however, the method is quite appropriate for obtaining medium-size and large objects,[69] and in the case of prototyping purposes, it is possible to print coloured objects (for example, coloured topographic models). The vertical spatial resolution of sheet lamination methods is limited by the thickness of the sheets of construction material. This technology is characterized by a significant amount of production waste since it includes a subtractive stage of cutting excess material.

7. Vat photopolymerization (VP) is a group of additive manufacturing methods based on selective curing of a liquid monomer under the action of UV radiation (Fig. 3*g*).[70] In rare cases, visible or infrared radiation is used.[71,72] Currently, this group includes SLA, digital light processing (DLP), liquid crystal display (LCD) and continuous liquid interface production (CLIP) methods. The last-mentioned technology is also known as continuous digital light processing (CDLP).

Stereolithography[73] in the classical design (SLA) is layer-by-layer curing of a liquid resin under the action of a laser beam, which performs two-dimensional scanning of each layer: a laser beam is focused in a thin layer of a liquid material and smoothly 'draws' the outline of the layer and the inner filling, moving from point to point. Owing to the two-dimensional scanning and monolithic fusion of the layers, stereolithography provides a very high quality object surface. Resins for photopolymerization consist of liquid monomers, photoinitiators, plasticizers and other additives that improve the quality of the final product.

Stereolithography is the first additive manufacturing method that is commercially used with success. The first studies dealing with the formation of 3D objects by laser curing of photosensitive materials appeared in the 1970s, while in the beginning of the 1980s, samples of products obtained by layer-by-layer curing of resins were reported in the scientific literature.[74,75] However, the modern history of SLA started in 1986, when C. Hull patented the method of laser stereolithography and used the term 'stereolithography' for the first time. In the same year he founded the 3D Systems company (USA), which is now one of the largest developers and vendors of additive manufacturing equipment and materials.[76]

Laser stereolithography is distinguished by very high spatial resolution in comparison with other additive manufacturing methods. For example, with appropriate choice of the resin, the Formlabs Form 2 desktop printer (Fig. 6*a*) can reproduce holes 0.5 – 1.0 mm in diameter, which makes even this readily accessible equipment suitable for the production of microreactors for fine chemical synthesis (Fig. 6*b*,*c*).

The record highest spatial resolution among the additive technologies belongs to two-photon stereolithography, which is suitable for the formation of micrometre-size objects to be used in optical and microelectronic systems, for surface microstructuring to endow the surface with the desired properties[78] and for producing cell scaffolds for medical applications.[79 – 81] Two-photon photopolymerization is initiated when the initiator molecule absorbs two quanta of electromagnetic laser radiation simultaneously. The probability of such absorption is high only in a very small area, that is, at the centre of

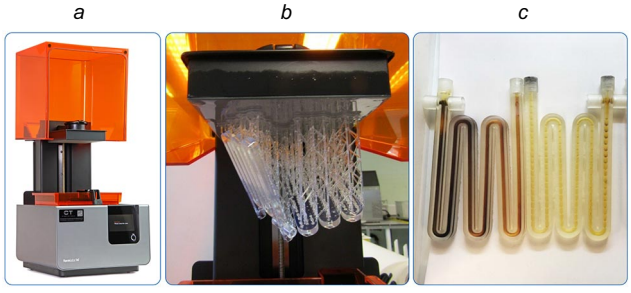


Figure 6. Appearance of a Formlabs Form 2 desktop 3D printer operating by laser stereolithography technology (*a*); chemical reactors manufactured by SLA on the build platform of the Formlabs Form 2 printer (*b*); finished flow microreactors manufactured by SLA for the synthesis of silver nanoparticles (*c*).[77]

the beam, which accounts for the high resolution of this method.[82]

The DLP, CLIP and LCD 3D printing methods are based on the projection technique of exposure of photocurable resins. In these methods, the whole layer (frame) is illuminated simultaneously, which considerably accelerates printing in comparison with the SLA method. For example, DLP 3D printers make use of a digital DLP projector, which projects the pattern of each layer during printing on the material being cured. In LCD 3D printing, the layer is exposed by means of an array of light-emitting diodes, while the areas that should not be cured are shielded from UV radiation by an LCD matrix. The DLP and LCD technologies include a rather long stage of formation of a fresh photoresin layer after curing of the previous layer has been completed: to provide curing of the next layer, the resin must fill the space between the object and the bottom of the bath. For the formation of a fresh layer of the resin, the object is somewhat lifted above the bottom of the bath and then positioned again for the exposure stage. According to CLIP technology, the long-term stage of formation of a fresh resin layer is avoided because the object does not touch the bottom of the bath, but is continuously drawn out of the bath, with the fresh resin being continuously fed into the space between the object and the bottom. This is achieved by oxygen inhibition of the photopolymerization near the bottom of the bath. For this purpose, oxygen is supplied into this area through a permeable membrane. In other words, CLIP is a continuous technology that markedly accelerates printing compared with other additive manufacturing methods.[83]

Currently, photopolymerization methods are among the most popular 3D printing processes. SLA, DLP and LCD 3D printers are widely used both in research laboratories and by personal users.

Not all of the additive manufacturing technologies can be made less expensive and personally usable. In particular, the high cost and complexity of metal powder sintering technologies are due to the need to use expensive finely dispersed powders with a definite size of spherical particles to ensure the required 'fluidity' of the material during printing. The application of powders requires additional equipment for purging the finished products to remove the residual powder and for preparing the remaining material for repeated use. Furthermore, during laser sintering of metal powders, it is necessary to maintain an inert atmosphere (argon or nitrogen) in the build chamber of the printer, *i.e.*, the chamber must be airtight and equipped with a gas transport system with a powder filtration mechanism, while powder sintering by an electron beam requires high vacuum in the chamber. Additionally, rather powerful and expensive lasers should be used for metal processing. However, the methods of selective laser sintering of plastic powders are gradually entering the inventory of personal 3D printing options.

Directed energy deposition methods are used only to solve production and service tasks in mechanical engineering. Binder jetting, material jetting and sheet lamination are also still far from widely accessible.

The methods that have become most widely accessible for personal use are material extrusion methods, first of all FDM, and vat photopolymerization methods (SLA, DLP and LCD). The DIW (direct-ink-writing) method is also suitable for wide use, but it is used to solve more special problems, such as manufacturing ceramic products, fabrication of scaffolds for regenerative medicine, and working-out bioprinting technologies. These methods will be considered in more detail in the context of application in chemistry and related disciplines.

All additive manufacturing methods make it possible to design an object considering only the function for which the object is meant. In other words, the designer can fully concentrate on attaining the highest performance and convenience of operation of the printed object, taking into account the fact that additive technologies allow any shape for the material. This fundamentally distinguishes additive methods from conventional production methods. When using conventional methods, one should always take into account the limitations of production technology and adjust the design of the future object to production methods, which in some cases markedly deteriorates the convenience of using the finished object. The versatility of 3D printing techniques and the possibility of implementing 3D printing in any laboratory make these methods an efficient tool for solving scientific problems.

3. Polymer materials for 3D printing

The vat photopolymerization and especially extrusion 3D printing methods are characterized by a high diversity of applicable materials. While choosing the 3D printing material, one should take into account not only the characteristics of the material but also the particular additive manufacturing method. Indeed, the mechanical strength of FDM products for some types of impact may be markedly lower than the strength of geometrically identical objects manufactured by casting or by subtractive methods because of the relatively large number of defects present in FDM products.[84–87] This is also true for other characteristics of materials: heat conductivity, transparency, elasticity, *etc*. In some cases, 3D printed products are inferior in physicomechanical characteristics to objects manufactured by conventional methods. Therefore, 3D printing should be used in cases where this deterioration of properties is insignificant. Additive manufacturing products may have anisotropic mechanical properties that are not inherent in the initial material because of the layered structure of the finished item; additionally, distortion of the geometric shape may take place due to material shrinkage (Fig. 7 *a*). This anisotropy is especially pronounced for FDM products, since in this case, not only the object has a layered structure, but also

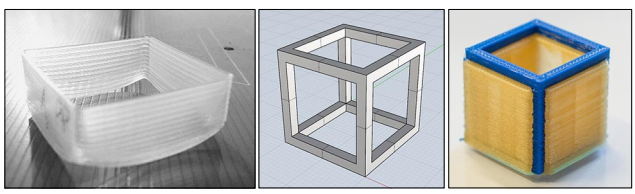


Figure 7. Deformation due to shrinkage of an FDM-printed polypropylene item in the case of inappropriate printing conditions (*a*);[96] model of an object the FDM manufacturing of which requires a support (*b*); FDM-printed object manufactured using a PVA support (light-coloured material; the photo was taken by the authors) (*c*).[97]

each layer is formed by tight deposition of polymer filaments coming from the print head nozzle.[88, 89]

The use of 3D printing in chemistry and in related areas imposes additional requirements on the materials. In particular, the use in fine organic synthesis requires, most often, high chemical stability of the equipment material that would be in direct contact with the reaction mixture.[90] Chemical stability is meant not only retention of the geometric shape and strength of the object upon contact with the medium, but also the absence of low-molecular-weight compounds that could be washed out during the chemical reaction. When organic synthesis is carried out at elevated temperature, the polymer material should possess sufficient thermal stability.

In the case of the application of microfluidic systems, additive manufacturing methods and materials should provide high spatial resolution for the formation of microchannel and cavity structures. In this case, the choice is limited, almost in all cases, to photopolymerization methods;[91] however, most of the available materials for this group of methods do not possess high chemical stability; therefore, the application of microfluidic systems manufactured by photopolymerization (SLA, DLP or LCD) is often limited to experiments in water or in mild solvents; this is quite appropriate for biochemical and medical research and applications.

3.1. Thermoplastic polymers as materials for fused deposition modelling

FDM technology based on the formation of an object from a material melt allows the use of any thermoplastic polymers. In most cases, the feed mechanism of FDM printers is meant for the use of feedstock as filaments with a diameter of 1.75 or 2.85 mm wound on a spool. There are also FDM systems for the use of pelletized plastics with a screw mechanism of feeding the pellets to the melting zone.[92]

Thermoplastic polymers can reversibly pass into a viscous-flow state with increasing temperature. A polymer material should be heated in the print head to a temperature slightly above the temperature of transition into the viscous-flow state, since after coming out of the nozzle, the material should solidify as soon as possible to preserve the shape of the product. Often, to accelerate solidification, additional air cooling is used, especially for the production of small parts. Amorphous polymers, which do not possess a definite viscous-flow point, are most convenient for FDM technology. As the temperature increases, the viscosity of the polymer melt gradually decreases; therefore, control of the heater temperature in the print head becomes a convenient tool for optimizing the physicomechanical characteristics and the outer surface quality of the finished item.

Manufacturing objects of a complex shape with parts hanging over the platform of the printer requires the presence of a supporting structure (Fig. 7 *b*,*c*) because without such a support the quality of printing of overhanging parts would be unsatisfactory.[93] The support can be built from the main material of the object (in this case, it is separated mechanically) or from another material soluble in water or in a special solvent. In the latter case, separation of the support is much more convenient and does not damage the surface of the object. For printing the support from a soluble material, the printer should be equipped with two extruders. The frequently used support materials include polyvinyl alcohol (PVA) or high impact polystyrene (HIPS), in combination with polylactic acid (PLA) or acrylonitrile butadiene styrene (ABS) copolymer serving as the main materials, respectively.[94, 95] Polyvinyl alcohol, unlike PLA, is readily soluble in water, whereas HIPS (unlike ABS) is soluble in D-limonene. A soluble support material should be adhesive to the main material and soluble in solvents that do not dissolve the main material; therefore, in some cases, the choice of the support material is quite a challenge. For many FDM printing materials, there is still no suitable support material; in this case, the only option is to print the support using the main FDM material.

Solidification of a polymer melt leads to shrinkage, which is a key drawback of FDM. Various materials are characterized by different degrees of shrinkage. If the printing conditions are inappropriate, this can lead to significant distortion of the product (Fig. 7 *a*). To minimize the shrinkage, it is necessary, as a rule, to reduce the temperature difference between the manufacturing object and the surrounding space in the build chamber of the printer. Hence, high-quality printing with such materials requires a printer with a heated build chamber and slow cooling of the printed product after completion of printing. The shrinkage can also be reduced by filling the polymer with solid components such as soot, glass fibre, carbon fibre, natural fibres, *etc*.[98] Materials characterized by high shrinkage are polypropylene, polycarbonate, polyoxymethylene and nylon and high-temperature plastics such as polyphenylsulfone, polyetherimide and poly(ether ether ketone). The performance characteristics of FDM products considerably depend on not only printing conditions, but also the manufacturer of the initial plastic and the FDM printer design.[99]

Below, we consider in more detail the main available materials for FDM 3D printing and materials for the manufacture of objects with enhanced or special characteristics.

Polylactic acid (PLA), prepared from plant raw materials and capable of degrading in the environment, is used most widely for FDM printing.[100] This material is convenient for FDM printing since it has a moderate melting temperature (190 – 220 °C) and low solidification shrinkage (*i.e.*, it is suitable for printing large objects) and emits no smell during printing. It is very easy to attain high adhesion of PLA to the printer platform, which provides a stable additive manufacturing process. Polylactic acid has a high strength;[101, 102] however, the strength of FDM products made of any material depends on the degree of filling of the inner space.[103, 104] Since PLA is readily soluble in most organic solvents, it cannot be used for manufacturing items that are meant for contacting a harsh chemical environment.[90] In addition, PLA is not very convenient for mechanical treatment and has moderate thermal stability.

Polylactic acid for FDM printing is produced by most manufacturers of consumables for personal FDM printers in a wide range of colours. Uncoloured PLA has the lowest degree of crystallinity and the highest mechanical strength compared to coloured materials.[107] This material can be used in any FDM printer, even a low-level printer, since due to insignificant shrinkage, objects of reasonable quality can be produced without using closed-chamber printers, but inexpensive open-source devices are quite

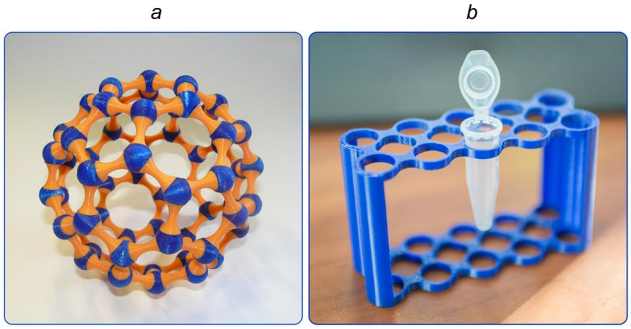


Figure 8. FDM printed objects manufactured from PLA using a desktop personal 3D printer. (*a*) Molecular model of fullerene C_{60} (the photo was taken by the authors),[105] (*b*) test tube rack for handling microcentrifuge tubes in a chemical laboratory (the photo was taken by the authors).[106]

suitable.[108] Therefore, PLA has found a wide use among makers and in the field of education (Fig. 8 *a*).[109] In laboratory practice, PLA is used for the manufacture of any tooling that does not contact organic solvents (Fig. 8 *b*) and chemical reactors for conducting experiments in aqueous or alcohol media;[110] it is a promising material for regenerative medicine[111] and pharmaceutics.[112]

The technical implementation of extrusion methods is very convenient for the application of composite materials, that is, thermoplastic polymers (in the case of FDM) filled by various fibres or particles.[113–115] Fillers can not only improve the properties that are already present in pristine materials but also endow materials with absolutely new properties: electrical conductivity, catalytic activity, non-flammability, *etc*.[116] A large number of PLA-based composite materials suitable for FDM printing have been developed.[117] Filling of the polylactic acid matrix with particles or fibres is performed either by mixing the polymer melt with a filler or by mixing a polymer solution with a filler followed by evaporation of the solvent. Currently, due to the surge in popularity of FDM printing, desktop personal extruders have appeared for the manufacture of moderate amounts of plastic filaments for 3D printing. These installations allow laboratory manufacturing of plastic filaments from secondary raw materials and composite materials with any fillers.[118] Polylactic acid-based composites have been prepared and characterized for fillers such as carbon fibres,[119–121] glass fibre,[122] wood and other natural fibres,[123–125] metal particles,[126–128] ceramics,[129] graphene,[130] carbon nanotubes,[131] microdiamonds[132] and so on. It was shown that PLA-based composites containing fibrous fillers often possess improved mechanical and thermophysical characteristics compared with the pristine polymers.[132,133] The addition of carbon materials and metal particles may be used to obtain electrically conducting composites,[134–136] which are suitable for the FDM manufacture of electrical components such as small antennas;[137] however, the addition of some metal alloys may lead to a considerable impairment of the strength characteristics of PLA-based composites.[138]

One should distinguish between short fibre-reinforced thermoplastics (SFRT) and continuous fibre-reinforced thermoplastics (CFRT).[139] In most cases, mentioning composite materials for FDM printing means ready-to-use plastics reinforced with short microscale fibres, which are distributed more or less uniformly throughout the polymer matrix.[140] The addition of short fibres decreases the shrinkage of the printed objects and has little effect on their strength. The most pronounced increase in the strength is attained by reinforcement with a continuous fibre, which is supplied from a spool by a special feed assembly and is fused into layers of the printed object during manufacturing.[141–143] The fibre and the plastic melt are fed through the same nozzle; this process is called co-extrusion. Since the fibre is continuous, the reinforcing effect is much more pronounced compared with short fibres and largely depends on the pattern of fibre deposition.[144] An important factor affecting the reinforcement of the printed products with a continuous carbon fibre is the efficiency of adhesion between the fibre and the polymer matrix. For example, the flexural strength of pristine PLA products was 53 MPa, that of continuous fibre-reinforced samples was 59 MPa, and that of samples reinforced with continuous fibres pretreated for improving the adhesion between the fibre and the matrix was 156 MPa.[145] This reinforcement method for FDM products has not yet become popular, but desktop-type personal 3D printers suitable for coextrusion of any common plastic (including PLA) with carbon fibre have already been commercialized.

The support material used for PLA printing is water-soluble polyvinyl alcohol, a biodegradable elastic material with a melting temperature of ~200 °C. The mechanical strength of PVA is relatively low; therefore, it is not normally used as the main construction material for manufacturing technical products. However, PVA is actively used for biomedical research related to regenerative medicine and new drug delivery systems. For example, PVA tablets containing paracetamol or caffeine were produced by the FDM technique.[146] After entering the body, these tablets dissolve and gradually release the drug. Polyvinyl alcohol serves as the base for the fabrication of scaffolds (for cell culturing in regenerative medicine) in combination with other biodegradable materials such as gelatine or alginic acid derivatives.[147–149]

Another widely used FDM printing material is ABS plastic, which is produced (unlike PLA) from oil processing products. ABS is a copolymer of acrylonitrile, butadiene and styrene, the ratio of which varies depending on the brand of the plastic. ABS plastic is printed at a higher temperature (230–250 °C), has a higher thermal stability and is much more convenient for mechanical treatment than PLA. However, ABS is characterized by greater solidification shrinkage, which often results in delamination and deformation of FDM products; therefore, high-quality printing of this material using inexpensive personal printers requires a more thorough selection of conditions.[150] In particular, it was shown that the key parameter affecting the deformation of ABS products is the temperature of the printer platform where the object is located, with the least deformation being observed when the platform temperature during manufacturing is maintained at approximately 100 °C.[151] In some cases, printing with ABS is accompanied by a slight smell. This plastic is not susceptible to fast biodegradation, but it still gradually degrades on exposure to UV radiation. The chemical stability of ABS plastics is relatively low; therefore, in a chemical laboratory, this material, like PLA, is suitable only for the production of objects that would not

be in direct contact with reactive organic solvents.[152] The degree of crystallinity of ABS does not change after it has passed through the FDM print head, whereas the PLA degree of crystallinity increases in this case; meanwhile, the mechanical strength of FDM-printed ABS objects is lower than that of analogous ABS objects manufactured by injection moulding.[153] However, particular strength parameters of FDM products made of ABS may reach values characteristic of moulded ABS products, *e.g.*, Young's modulus or tensile strength, but not all of the parameters simultaneously.[99]

The ABS copolymer is often used as the matrix to produce composite materials. In particular, the addition of amorphous carbon, carbon nanotubes or nanofibres to the ABS matrix increases the hardness, electrical conductivity and thermal conductivity of the material.[154, 155] If the content of the carbon filler exceeds 4 mass %, passing of electrical current through the material is accompanied by a noticeable heat evolution. A further increase in the content of carbon nanotubes leads to a significant increase in the melt viscosity, which makes the material unsuitable for extrusion methods.[156] The possibility of manufacturing functional electronic devices and in-line analyzers for the volume fraction of a gas in a flow, using electrically conducting ABS-based composites was demonstrated.[157] An increase in the mass fraction of carbon nanotubes to 7% increases the tensile strength of the composite by 288% in comparison with that of pristine ABS plastic.[158] A substantial increase in the tensile strength (by 58%) and Rockwell hardness (by 495%) was observed when ABS plastic was filled with CuO particles.[159] The incorporation of cellulose-modified nanosized silica particles into the ABS matrix almost completely eliminated the shrinkage of thin-walled FDM products.[160]

The supporting structures for manufacturing ABS products are printed using high-impact polystyrene, which represents a styrene – polybutadiene copolymer (polystyrene chains are attached to the polybutadiene double bonds to form a graft copolymer). This material is readily soluble in D-limonene, a terpene hydrocarbon that is present in citrus peel oil and is produced upon citrus fruit processing. Therefore, when the object together with the support is immersed in limonene, HIPS is gradually dissolved, while the ABS object remains free from the supporting structure. HIPS can also act as the support for PVA. For example, this method was used to manufacture microchannel systems from polydimethylsiloxane (PDMS): the complex geometry of the channels was implemented using water-soluble PVA with a HIPS support; after the process, HIPS was dissolved in limonene and the PVA channels were filled with PDMS; at the final stage, PVA in the channels was dissolved upon treatment with water.[161] High-impact polystyrene can also be used as a separate construction material;[162] in this case, thorough selection of the temperature and speed parameters of the FDM printing provides for high dimensional accuracy of the products.[163]

In recent years, poly(ethylene terephthalate) glycol (PETG) has started to be used for FDM printing. This material is characterized by higher chemical and thermal stability and is more convenient for mechanical treatment than PLA. The shrinkage of PETG on solidification is lower than that of ABS, while the mechanical strength is higher;[164, 165] PETG is characterized by high stability to variable mechanical load (cyclic strain) and is superior in these characteristics to PLA or nylon. In the case of PETG, the mechanical properties can also be changed by filling the polymer matrix with carbon or glass fibres.[166, 167]

FDM technology is suitable for printing elastomers, *e.g.*, thermoplastic polyurethane (TPU), and thermoplastic ester ether elastomer (TEEE) such as Primalloy.[168] These materials can be used for the fabrication of gaskets, flexible parts of chemical installations, sensors, *etc.*[169 – 171] A number of biocompatible polyurethanes suitable for 3D printing could find medical applications.[172, 173] The adhesion between the layers of an elastic FDM-printed product is relatively high, so that no splitting of layers takes place upon reversible elastic deformation.

Among general-purpose plastics, polypropylene (PP) is most significant for the chemical applications of 3D printing (Fig. 9), since it is most chemically stable; however, the thermal stability of this polymer is moderate (the degradation of PP starts at a temperature somewhat above 300 °C).[90, 152] The main drawback of PP as a material for FDM printing is high shrinkage on solidification (see Fig. 7 *a*), which decreases the dimensional accuracy of the resulting objects and necessitates additional measures to compensate for this shrinkage: either introduction of corrections to the object size during modelling or mechanical posttreatment of the finished product.[174] The tendency for high shrinkage and moderate adhesion to most materials results in possible detachment of the object from the build platform of the printer during additive manufacturing. For more reliable attachment, the build platform of the printer is coated by polypropylene sticky tape, a polypropylene sheet or an ultrahigh-molecular-weight polyethylene sheet. Separation of this material from the finished item also requires some mechanical treatment.[175] The shrinkage of polypropylene is due to its crystalline nature: when the melt solidifies, macromolecules in some parts of the material move to attain a better packing, which changes the size of the product. In the case of amorphous polymers, shrinkage is usually less pronounced since the disordered arrangement of macromolecules inherent in the melt is retained in the solid state. However, for polymers with a high content of crystalline phase, stronger adhesion of the layers is possible because the crystalline phase is not softened with increasing temperature, as is the case for



Figure 9. Laboratory chemical microreactors with integrated capillaries and magnetic stirrers for monitoring chemical reactions by mass spectrometry made of polypropylene using a personal FDM 3D printer.[191]

amorphous polymers, but melts, thus providing a better integration of FDM layers.

The mechanical properties of PP can be considerably improved by introducing reinforcing fillers.[176,177] For example, whereas the flexural modulus for pristine PP is 1800 MPa, the addition of 30% glass fibre increases the flexural modulus to 5500 MPa. The FDM-printed objects have a 30% lower ultimate tensile strength than injection-moulded PP samples. It is assumed that this decrease in the strength is not related to insufficient adhesion between the layers but is caused by the presence of numerous voids in FDM products, *i.e.*, lower solidity of the samples.[96] The reinforcing effect of the fillers is retained for FDM products, *i.e.*, after the material has passed through the extruder of the printer.[178] The addition of a filler also decreases PP shrinkage and improves adhesion to the build platform.[179–183]

Electrically conducting composites comprising the PP matrix and finely dispersed carbon (soot) have been reported. These conductors proved to be quite functional in electronic systems and can be used for 3D packaging of electronic devices (as opposed to planar packaging based on printed circuit boards) and for integrating current-carrying components into a chemical installation, which may be useful for electrochemistry.[184,185]

Other important features of polypropylene as an FDM printing feedstock are its wide availability and low cost. In particular, it was shown that recycled polypropylene obtained by processing plastic waste, first of all packaging, is well suited for 3D printing, while dyes and other additives contained in the material decrease shrinkage. The use of polypropylene filled by cellulose-based materials, also produced by processing industrial waste, enables FDM printing completely based on recycled materials.[186] Currently, additive technologies account for a small share of the total material production output; therefore, the environmental friendliness of 3D printing is not a relevant task; however, the situation may change in the future, and additive manufacturing using new environmentally safe materials, including recycled materials, would become a topical issue.[187–190]

One more representative of thermoplastic polyolefins used, in some cases, for FDM printing is polyethylene (PE). In the context of additive manufacturing, PE suffers from the same drawbacks as PP, in particular, high shrinkage and the necessity to take special measures to ensure adhesion between the material and the build platform of the printer. These features are even more pronounced for high-density polyethylene (HDPE) than for PP, since HDPE possesses a high degree of crystallinity.[192] However, by thorough selection of parameters for the FDM process using polyethylene, it is possible to print medium-sized objects of a reasonable quality.[193,194] For example, it was found that a sufficient level of PE adhesion to the build platform and the subsequent detachment of the printed product without damage are possible when the platform is coated by a sheet made of styrene–ethylene–butylene–styrene block copolymer (SEBS). Despite the wide popularity of PE as a general-purpose plastic, the use of PE in FDM 3D printing is still limited to experimental works. Nevertheless, it was shown that with the wide use of personal 3D printing as a method of distributed production, an environmental benefit may be gained from the use of recycled polyethylene. PE processing should also be performed in a distributed way using personal extruders producing filaments for 3D printers in geographical locations with low population density.[195] This hypothesis, of course, remains debatable, but the appearance of such studies shows that additive technologies are regarded as a possible base for a new economic and technological paradigm.

The use of polypropylene and polyethylene in the laboratory practice of FDM printing is justified only in the case where high chemical stability of the material is actually needed. Otherwise, in view of the complexity of FDM printing with these plastics, it is more appropriate to use other materials such as PLA, PLA+, PETG and composites based on them.

To produce objects with enhanced mechanical strength by FDM printing, so-called engineering materials are used. Some of these materials also have other characteristics superior to those of general-purpose plastics: enhanced thermal stability, chemical stability and low friction coefficient. Unfilled materials of this group most often exhibit considerable shrinkage.

Among polymers of this group, polyamides (PA), in particular polyamide-6 and polyamide-12, are used most often for FDM printing both in the pristine state and as composites with carbon fibres, glass fibres, *etc*.[196–199] Polyamides possess high impact strength, low friction coefficient and high chemical stability, which allows using these plastics for manufacturing machine parts to be operated under load and in contact with lubricants. Some brands of polyamides are highly hygroscopic; therefore, if the polymer is not dried before FDM printing, bubbles deteriorating the surface quality of printed products may appear. Therefore, it is necessary to dry the material before manufacturing.[200]

A combination of high hardness, high wear resistance, high impact strength and low friction coefficient is also inherent in polyoxymethylene (POM), or polyformaldehyde, formed upon polymerization of formaldehyde. This material is fairly resistant to organic solvents and less prone to creep; it has a higher hardness and lower friction coefficient than nylon. However, the shrinkage of POM (2.2%) is greater than the shrinkage of nylon-6 (1.2%).[201,202] The FDM printing of large POM objects without geometry distortion is a challenge; therefore, this material has not yet become common for additive manufacturing, despite some successful attempts to optimize personal FDM printers towards printing with this particular plastic.[202] A vivid example of the application of POM is the fabrication of a POM-based (as a mixture with polyamide) magnetic composite for 3D printing containing neodymium–iron–boron (NdFeB) particles. This material was shown to be applicable for printing functional magnets of an arbitrary shape tailored for a particular device (compact blood pump), which is a considerable advantage over the use of commercial magnets.[203] Direct additive manufacturing of magnets is also important for chemical laboratory practice, in which magnetic stirring systems are actively used.

An important representative of engineering plastics suitable for FDM printing is polycarbonate (PC), which is widely used as a structural material in construction, decoration work and manufacturing of consumer goods owing to its high strength, transparency and low cost. FDM-printed polycarbonate products are characterized by markedly lower strength than moulded bulk products. For example, the decrease in the ultimate tensile strength

for FDM products made of PC compared to moulded bulk samples is 30% to 60% (depending on the stress orientation relative to the layers).[204] Thus, the reference values of strength characteristics of materials reported for injection moulded samples do not provide even a rough estimate for the physicomechanical characteristics of FDM products, since the choice of material, printing parameters, infill of the product, and arrangement of layers relative to the applied external forces — all these factors significantly affect the resulting strength parameters of FDM products. Recently, a method was implemented for polycarbonate production from plant feedstock, which makes PC the first engineering bioplastic.[205, 206] Biopolycarbonate has noticeably better physicomechanical characteristics: higher stability to UV radiation and higher thermal stability than polycarbonate produced from fossil raw materials. This makes biopolycarbonate suitable for manufacturing sterilizable medical appliances. Furthermore, additive manufacturing using biopolycarbonate is accompanied by a lower emission of hazardous gases than that with conventionally produced PC.[207] The chemical stability of PC to many organic solvents is modest, which restricts its application for manufacturing objects that would be exposed to the environment.

Polyvinylidene fluoride (PVDF), resulting from polymerization of 1,1-difluoroethylene (vinylidene fluoride), also known as fluoroplastic-2, is a promising material for the chemical applications of FDM. Unlike fluoroplastic-4 (polytetrafluoroethylene), in which all hydrogen atoms are replaced by fluorine, PVDF can be processed as a thermoplastic material (the melting temperature is ~180 °C). Polyvinylidene fluoride is characterized by high mechanical strength, high wear resistance, low friction coefficient, chemical and biological inertness and the absence of foreign impurities. This polymer is used for the production of equipment in the chemical and pharmaceutical industry and in medicine, it is a material of surgical threads, and it can be processed by extrusion methods. The production of filaments with a diameter of 1.75 or 2.85 mm for 3D printing from pelletized PVDF is quite technically practicable and can be accomplished even with a desktop personal extruder. For FDM printing with polyvinylidene fluoride, the extrusion temperature should not exceed 240 °C; otherwise, the material poorly retains its shape and loses dimensional accuracy. Additionally, it is not recommended to use printing speeds above 30 mm s^{-1}, since this makes the cooling conditions non-optimal and results in considerable distortion of the object geometry. With appropriate selection of the parameters for FDM printing using PVDF, it is possible to manufacture 3D-printed parts almost without shrinkage even on an inexpensive personal printer.[208] Despite the chemical inertness, PVDF can serve as the matrix for the design of composite materials. For example, electrically conducting PVDF composites with carbon nanotubes and piezoelectric composites filled with barium titanate particles were obtained.[209, 210] The conductivity of FDM products made of composites with carbon nanotubes is higher in some directions than the conductivity of moulded products manufactured from the same material. The reason is that nanotubes are aligned along the direction of extrusion as they pass through the 3D printer nozzle, whereas in moulded materials, the filler particles are arranged randomly.[209]

In recent years, some personal FDM 3D printers have been equipped with high temperature print heads able to maintain extrusion temperatures of up to 400 °C. These printers are compatible with high-performance structural plastics, which are sometimes called superstructural materials. These materials include poly(ether ether ketone) (PEEK) (Fig. 10), poly(ether ketone ketone) (PEKK), polyphenylsulfone (PPSU), polyetherimide (PEI), *etc.* The first publications dealing with additive manufacturing by the FDM method using this group of materials appeared relatively recently.[211]

In recent years, high-quality FDM printing with high-performance plastics has been implemented for professional additive manufacturing systems, and now these materials start to appear in the personal 3D printing segment. However, by no means, all personal 3D printers can use these plastics, which is due to obvious reasons: first, personal 3D printers are not normally used to solve production tasks at a professional level; second, high-quality printing with these materials requires a more sophisticated design of the printer, which would thus become more expensive. Nevertheless, personal 3D printers are now regarded as a means for manufacturing finished functional products; therefore, the capabilities of such printers gradually start to include printing with high-performance materials.

These plastics have exceptional performance characteristics among other plastics: high mechanical strength, thermal stability, chemical and radiation stability, biological inertness, nonflammability and high dimensional accuracy under the action of an external load.[213] In some cases, materials of this group can serve as substitutes for metals. A key feature of these materials is the ability to operate at continuously elevated temperatures (> 150 °C) without deterioration of properties; therefore, printing with these materials in the laboratory, without the need to purchase expensive professional equipment, would be fairly useful. Note that high-temperature plastics are expensive, but this shortcoming is not a fundamental obstacle to using them, since in the laboratory, they serve to manufacture relatively small parts and assemblies, requiring high stability to external action.

Products made of PEEK [the melting temperature of which is approximately 343 °C (Ref. 214)] can operate at temperatures up to 260 °C (depending on the brand) without geometry distortion, while short-term operation is possible even at 300 °C with simultaneous exposure to

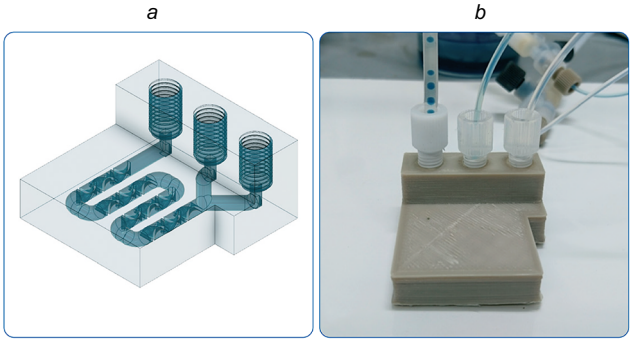


Figure 10. Chemical microreactor manufactured from PEEK by FDM, suitable for continuous flow synthesis at high temperature of the reaction mixture.[212] (*a*) reactor model, (*b*) finished product with input/output channels.

harsh chemicals. In terms of stability to organic solvents and thermal stability, PEEK is superior to polypropylene and, more so, to other general-purpose plastics. The tensile strength of PEEK is in the 75 – 118 MPa range; for comparison, this value for nonreinforced ABS plastic is 26 – 57 MPa.[215,216] Poly(ether ether ketone) is used to produce various parts of analytical instruments, fittings, valves and other accessories for chemical laboratory installations, chemical microreactors, micropumps, *etc*.[217] Similar to other materials, the mechanical strength of FDM products made of PEEK crucially depends on the orientation of the layers relative to the direction of the applied load. For example, with the optimally selected orientation of the layers, printing temperature of 400 °C, 100% infill of the printed item, and printing speed of 20 mm s^{-1}, samples with mechanical strength not inferior to that of moulded samples were manufactured.[218] The number of microdefects on the surface of an FDM product considerably depends on the printing speed.[219] In the field of medical applications of PEEK, extensive studies are in progress: owing to its high biological compatibility, it can be used to manufacture dental prostheses and implants and serve for orthopedic restoration and tissue engineering with the aid of FDM technology.[220 – 223]

Polyphenylsulfone and polyetherimides differ little from PEEK in their performance characteristics (Table 1). These materials are also highly chemically stable; in particular, they are not prone to hydrolysis at elevated temperature, which allows for repeated autoclave sterilization of the manufactured products.[224,225] Polyetherimides for FDM printing are produced under the brand names Ultem, most often, Ultem 9085 and Ultem 1010. Polyphenylsulfone and polyetherimides can be used as substitutes for metals in systems for the supply of hot water and aqueous solutions and for medical appliances subjected to repeated sterilization. Ultem 9085 and 1010 are widely used in transport mechanical engineering, and research into the applicability of FDM-printed polyetherimides for the manufacture of space equipment components is in progress.[226] It is noteworthy that Ultem 9085 is a mixture of polyetherimide and polycarbonate rather than pure PEI.[227] The admixture of PC to PEI somewhat deteriorates the thermal stability but enhances the rheological properties during FDM 3D printing.[228]

Successful printing using high-temperature plastics requires not only high temperature of the extrusion system and heating of the build platform but also maintenance of high temperature of the atmosphere (> 100 °C) in the build chamber to avoid considerable distortions of the object geometry. An increase in the temperature in the chamber not only reduces product shrinkage and warping but also enhances strength, since the material exists in the viscous state for a longer period of time, which promotes more efficient fusion of the layers.[229]

Thus, three groups of FDM printing materials have now formed, namely, general-purpose plastics, engineering plastics and high-performance materials (Fig. 11). The transfer from general-purpose materials to high-performance materials is accompanied by a fundamental

Table 1. Some physicomechanical characteristics of plastics used for FDM printing and conditions of additive manufacturing using these materials.

Material	Yield strength [a] /MPa (Ref. 230)	Operating temperature [b] /°C (Ref. 230)	Printing temperature /°C	Resistance to organic solvents (Ref. 90)	Special conditions during printing [c]
			General-purpose plastics		
PLA	46.0 – 49.0	60	190 – 230	Low	–
ABS	42.0 – 55.0	88	210 – 250	Low	A, B, C
PETG	28.3 – 58.6	65	230 – 250	Low	B, C
HIPS	26.0 – 28.0	74	230 – 245	Low	A, B, C
PP	34.1 – 36.5	80	220 – 250	High	A, B, C
			Engineering plastics		
PA	50.0 – 66.0	120	230 – 270	Medium	A, B, C
PC	58.6 – 70.0	152	260 – 310	Low	A, B, C
POM	55.0 – 62.5	110	210 – 230	High	A, B, C
PVDF	46.0 – 54.0	110	245 – 265	High	A, B, C
			High-performance plastics		
PEEK	65.0 – 98.0	160	375 – 410	High	A, B, C, D
Ultem 9085	84.0 – 88.0	152	350 – 380	Low	A, B, C, D
Ultem 1010	105.0 – 110.0	190	370 – 390	Low	A, B, C, D
PPSU	62.0 – 74.0	195	360 – 390	Medium	A, B, C, D

[a] The yield strengths are given for the initial material (not having passed through the extruder); the strength of the FDM product substantially depends on the spatial orientation of layers relative to the direction of load applied.

[b] Temperatures of deformation under load are given. *i.e*., the maximum temperature at which the plastic does not change the shape under continuous mechanical loading (1.8 MPa).

[c] A is the closed chamber of the printer, B is the heated platform, C are special methods for increasing the adhesion between the material and the platform (*e.g*., printing on a sheet made of a material with similar structure, on a perforated sheet, treatment of the platform with a special formulation increasing the plastic adhesion), D is the maintenance of a constant elevated temperature in the closed chamber of the printer.

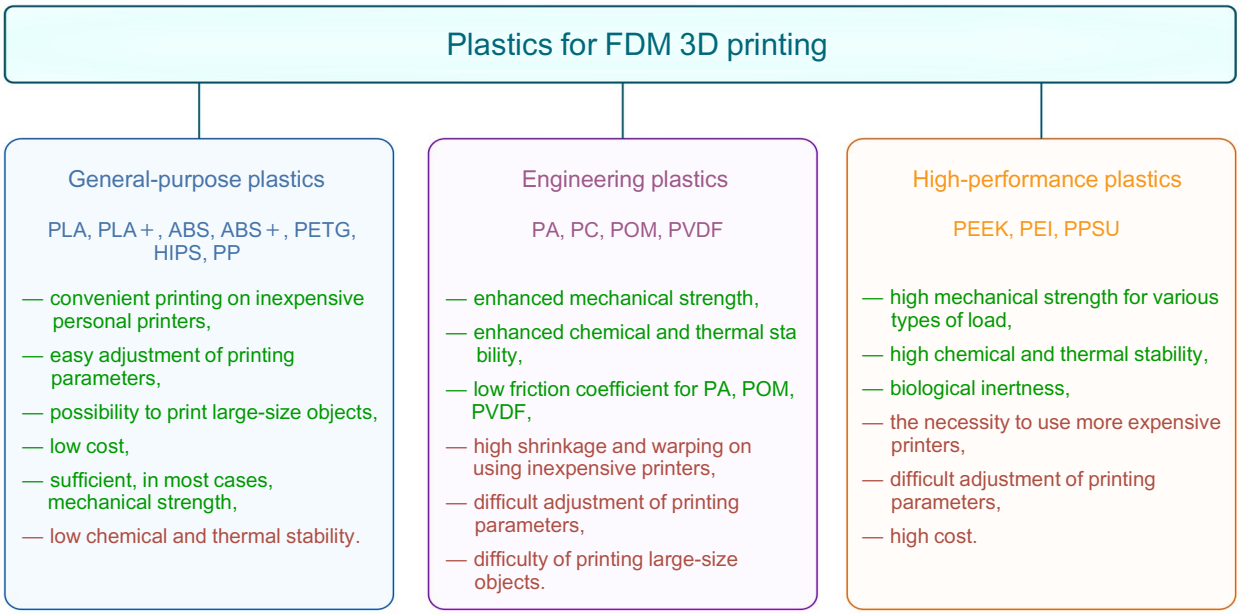


Figure 11. Groups of plastic materials for FDM 3D printing.

improvement in the performance characteristics of the obtained products and considerable complications of additive manufacturing conditions (see Table 1).

When FDM-printed products are meant for chemical applications, it is recommended to investigate their stability to the action of the medium that will be in contact with the printed product. In this case, the standard reference data on the chemical stability of plastics may be misleading, since FDM products have a layered and porous structure, which markedly affects the pattern of destruction of the product in a particular medium. To evaluate the chemical stability of FDM products, a simple procedure was proposed. According to this procedure, the product as a small cylindrical cell is placed into a solvent, and a metal bead is used as an indicator load to detect the time of destruction of the test sample (Fig. 12 *a*,*b*).[90] In the absence of a load, the material can seem to retain its shape, while the mechanical strength has actually been lost. FDM products made of the same material can follow different patterns of destruction depending on the solvent. Four types of destruction of FDM products can be distinguished (Fig. 12 *c*):

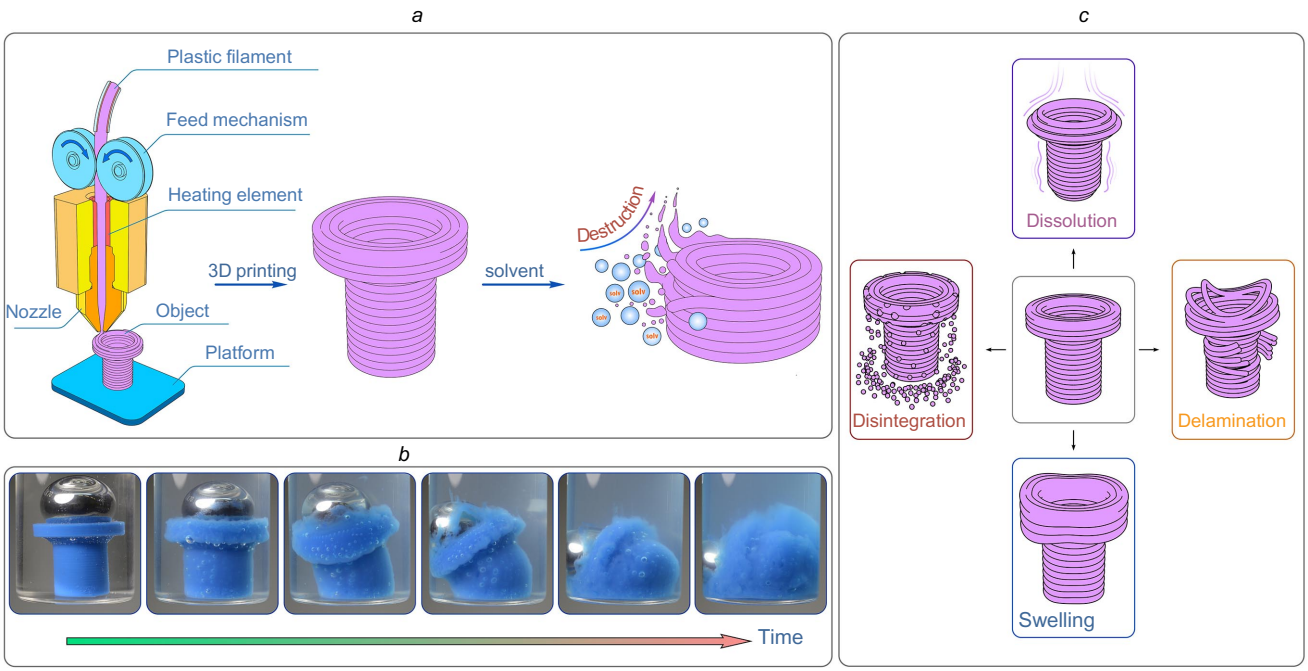


Figure 12. Testing of the chemical stability of plastics for FDM printing.[90] (*a*) General chart of the testing procedure; (*b*) example of testing the chemical stability of an ABS plastic object in dichloromethane using a metal bead as an indicator load; (*c*) types of destruction of FDM-printed objects upon exposure to organic solvents.

dissolution — gradual complete transfer of the item material to the solution; disintegration — gradual degradation of the item into small particles caused by dissolution of the polymer matrix (this type of destruction is typical of items made of composite materials); delamination — splitting of the item into layers with the formation of cracks and large gaps between the layers without visible signs of dissolution; and swelling — absorption of a considerable amount of the solvent by the material with increasing size of the item and loss of mechanical strength. The proposed procedure was used to test FDM products made of a broad range of polymer materials. It was shown that PP, nylon and POM provide sufficient chemical stability for chemical applications of FDM products.[90] In particular, FDM-printed polypropylene test tubes can be used on an equal basis with glassware at appropriate temperature conditions in fine organic synthesis (Suzuki–Miyaura coupling and Heck reaction). Thus, FDM printing using polypropylene would also be suitable for manufacturing more complex chemical reactors, in particular, for multistep synthesis.[32]

All materials shown in Fig. 11 have found wide use in some fields. Along with the above-considered plastics for FDM printing, there are special materials intended for specific types of applications in FDM technology. An example of such a material is wax, which is used to print models that are subsequently used as consumable patterns for casting. After printing, a refractory (*e.g.*, ceramic) shell is formed around the wax model; upon heating of the shell, the wax melts away through a gating system of channels to leave a ready mould for metal casting. Thus, FDM printing can greatly facilitate and accelerate the production of metal castings. However, the low spatial resolution and clear-cut layered structure of FDM products restrict the use of extrusion-based fusion for precision casting.

One more low-melting material for FDM printing is polycaprolactone (PCL) with melting temperature in the range of 60–65 °C. Owing to the capability of 3D printing to make bulk porous structures, this biodegradable and biocompatible plastic and its composites are used in regenerative medicine to produce bone tissue scaffolds[231–234] and endoprostheses such as stents.[235,236] Due to the low melting temperature of PCL, it is possible to introduce various biologically active substances (antibacterial agents, compounds improving the biological compatibility and so on) into the polymer without the risk that they would decompose during additive manufacturing.[237]

The BASF corporation developed an interesting composite material, Ultrafuse 316L, which represents a polymer matrix filled with 316L stainless-steel particles, with a metal content of 80 mass %. Unlike usual metal-filled materials where the metal filler serves for decorative purposes, Ultrafuse 316L and similar materials are meant for manufacturing metal products using a personal FDM printer.[238,239] The whole production process of a metal product consists of three stages. The first stage is FDM printing of the future product (the extrusion temperature is 230–250 °C). Then, the obtained model was subjected to chemical treatment with concentrated nitric acid at 120 °C to remove the polymer matrix binding the metal particles. This gives a highly porous, but now a metal object. At the final stage, the product is thermally treated (>1300 °C, 3 h, argon atmosphere) for complete sintering of metal particles. Apart from the complexity of the whole production sequence, a drawback of this process is a very high shrinkage of the material at the last sintering stage, *i.e.*, fabrication of metal items with a high dimensional accuracy by this method may become a sophisticated task. Due to these drawbacks, the use of FDM printing as an initial stage of production of metal objects is now not popular: this approach is too expensive and too complicated for amateur use, while for systematic solving of professional problems, laser sintering of metal powders is more appropriate.

The performance and processing characteristics of materials are improved not only by using finely dispersed particles or fibres as fillers but also by using polymer blends. A widely used polymer composition is an ABS and polycarbonate blend. The addition of PC results in increasing thermal stability and hardness of the material and improves the mechanical characteristics at lower temperatures.[240–242] A specially designed extruder was employed to fabricate FDM filaments with a homogeneous PC–ABS blend as the core and polyethylene shell as the outer layer.[243] It was shown that at a PE mass fraction of approximately 50%, it is possible to print objects with a high dimensional accuracy and with enhanced strength characteristics compared with those of the PC–ABS blend without polyethylene. The addition of 10 mass %–20 mass % thermoplastic polyurethane to ABS increases the adhesion between the layers, while the increase in the TPU content to 30% improves the adhesion of the material to the platform of the printer.[244] The addition of up to 15 mass % recycled high-density polyethylene to ABS plastic insignificantly deteriorates the quality of products compared to purely ABS products. Thus, if economically appropriate, the use of HDPE additives can provide the involvement of polyethylene waste in additive manufacturing.[245]

A considerable advantage of additive methods as a whole and, in particular, extrusion methods is the possibility of using several materials in one product with a continuous 3D printing process, *i.e.*, multimaterial printing. In personal FDM printers, it is most often possible to print using two materials; in most cases, this possibility is implemented for printing products with a soluble support. However, multimaterial printing can be a tool for controlling the mechanical properties of an object in the case where the model is a layered structure in which some layers are manufactured from one material and the other layers are manufactured from another material differing from the first one in mechanical properties.[246] In particular, it was shown that the mechanical properties of a product can be controlled using alternating layers of three materials: ABS, PLA and HIPS.[247] The mechanical properties of the product depend on which material is located in the middle of the layered structure. In this context, note an important feature and distinction of additive methods from conventional production methods: in conventional methods, the object is fabricated from a specified invariable construction material, whereas additive methods are able to create not only the geometry of the printed product but also the material by combining the initial constituent materials as components of a new 'metamaterial'. This approach forms the concept of material multifunctionality, which consists of the integration of various properties in one material taking advantage of specific features of additive manufacturing.[248,249] For example, a neat unfilled material can have a high

mechanical strength but possess no electrical conductivity. Filling with carbon nanoparticles increases the conductivity but decreases the strength. A multifunctional material may represent a layered structure with alternating high-strength and conducting layers; hence, the composition would combine both high strength and electrical conductivity. Metamaterials are in demand in chemical synthesis. In particular, the external layers of the chemical reactor shell can be manufactured from a strong inert material with a dense packing of the layers, which ensures leak-tightness of the vessel, whereas internal layers can be composed of a porous composite material containing particles of a catalytically active filler.

This is not to say that the idea of multifunctional materials is fundamentally new; however, additive methods have endowed this idea with new prospects, offering wide opportunities for combining various materials in one product.[250]

3.2. Materials for robocasting

One more method technically resembling FDM is robocasting, known as liquid deposition modelling (LDM), which is a type of direct-ink-writing (DIW). Direct-ink-writing is used to manufacture products from materials that exist as gels, pastes or viscous liquids under ambient conditions, *i.e.*, no melting of the material takes place in the print head. After printing, the product is solidified as a result of either solvent evaporation or chemical reactions that take place in the material during thermal treatment (Fig. 13). Any material that can be converted to a viscous liquid is suitable for additive manufacturing by DIW. An additional requirement for materials is that they should retain their shape when exiting the nozzle; that is, the shape should be preserved until the material solidifies. Polymers are also applicable for DIW technology if it is possible to select a solvent that would soften the polymer to the required state.[251] The spatial resolution of DIW is moderate; therefore, this technique is not used as a rule to manufacture precise mechanical engineering products, but serves for the production of relatively large objects of a simple shape or for arrangement of the material into an ordered porous structure. It is noteworthy that robocasting is, in principle, suitable for miniaturization, and there

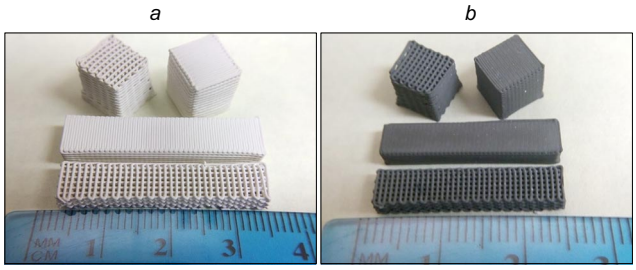


Figure 13. Porous and monolithic structures manufactured by robocasting from silicon nitride Si_3N_4, which is used for the fabrication of implants in orthopaedic restoration.[253] (*a*) Primary non-solidified products, (*b*) finished products after sintering; one can see considerable shrinkage of samples without change in the topology.

are examples of the production of submillimetre-scale objects by this method.[252] A specific feature of the DIW method is the need to optimize the composition of the material and the printing parameters to attain a satisfactory correspondence between the digital model and the actually obtained sample. Whereas in other 3D printing methods, the user receives the ready material, which cannot be changed, in the case of DIW, the material is prepared by the user considering a definite research task.

The DIW method is widely used in experimental regenerative medicine for the fabrication of scaffolds possessing a porous structure for the adsorption and subsequent growth of living cells. For example, soft tissue scaffolds are often printed using hydrogels, *i.e.*, polymers that have absorbed a large amount of water and are hence capable of being extruded through the nozzle.[254, 255] However, seeding of cells pre-printed scaffolds results in a disordered structure of the tissue; therefore, the technique called bioprinting is being actively developed for this application. Owing to the absence of significant heating during additive manufacturing by DIW, the extruded hydrogel can contain living cells and biologically active compounds; such a mixture is called bioink.[256, 257] A key parameter is the viscosity of bioink, since it determines the ability of the material to preserve

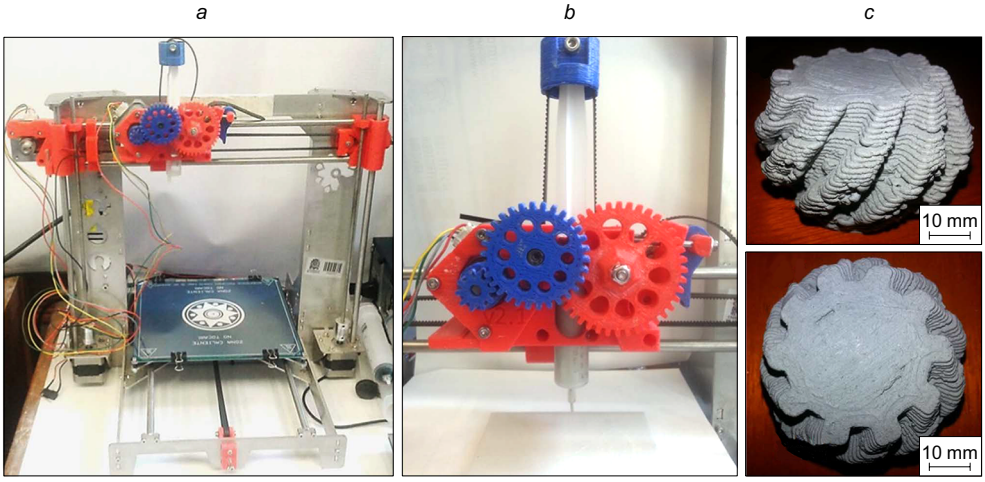


Figure 14. Inexpensive desktop 3D printer for printing clay products by robocasting.[264] (*a*) General view of the printer; (*b*) extruder for the clay mass; (*c*) example of an item obtained using this printer.

the shape and affects the structuring of cells within the hydrogel.[258,259]

However, another promising trend in the application of DIW is 3D printing of ceramic products,[260–263] which can be done using even a simple 3D printer with a conventional plastic syringe as the extruder (Fig. 14).[264] In this case, a ceramic paste serves as the feedstock to produce the primary product. After printing, the primary product is thermally treated, which results in sintering of ceramic particles. Ceramic materials possess high thermal and chemical stability and are widely used in chemical laboratory practice.

Scaling robocasting makes it possible to produce construction 3D printers, which can serve to construct the walls of buildings and decorative structures by extrusion of a specially prepared construction mix or concrete grout, which confirms once again the versatility of extrusion methods. Currently, 3D printing construction is a very rapidly developing trend mainly related to the construction of relatively small buildings and small architectures for area improvement.

An important advantage of robocasting over other additive manufacturing methods is the possibility to use materials containing any finely dispersed fillers over broad concentration ranges:[265,266] metal particles,[267,268] amorphous carbon,[269] carbon nanotubes,[270,271] graphene,[272–275] fibres[276] *etc*. This gives rise to an almost infinite number of composites with specified properties.

3.3. Materials for photopolymerization methods

In laser stereolithography and analogous DLP, LCD and CLIP stereolithography techniques, the formation of objects is based on chemical polymerization processes taking place in the liquid feedtock under the action of ultraviolet (most often) or visible light. These reactions are called photopolymerization and give rise to a solid polymer material formed from liquid monomers. It can be said that 3D printers operating according to this technology accomplish not only layer-by-layer assembly, as in other additive methods, but literally the chemical synthesis of the product. In this case, the final material of the finished product is formed during printing and not supplied in the ready state, such as in FDM or SLS methods. Therefore, the user cannot even roughly evaluate the performance characteristics of the future product proceeding from the properties of the starting material, which is supplied as a liquid photopolymer resin in bottles. Currently, liquid-phase photopolymerization methods have entered the personal 3D printing segment, owing to the appearance of numerous manufacturers of desktop systems for SLA, LCD and DLP printing.

The initial liquid photopolymer compositions mainly consist of epoxy resins with the addition of acrylates or vinyl ethers, photoinitiators, plasticizers, dyes, stabilizers and other additives depending on the purpose of the composition (printing of medical objects, jewellery products, *etc*.) and required properties of the final product. Epoxy resins and acrylates are monomers for photopolymerization and represent construction materials for future products. Epoxy resins undergo ring opening polymerization by a cationic mechanism, which is accompanied by insignificant shrinkage (2%–3% by volume), but it may proceed at a relatively low rate. The cationic mechanism of curing epoxy resins does not resemble the mechanism of curing epoxy resins with amines. In the case of the cationic mechanism of curing, the resulting polymer has a large number of cross-links and, therefore, is highly brittle. To accelerate photopolymerization and increase the strength of products, acrylates or vinyl ethers, which are polymerized by the radical mechanism, are added to the composition (vinyl ethers can also polymerize by an ionic mechanism). The use of acrylates or vinyl ethers alone is possible, but photopolymerization of these compounds results in a considerable distortion of the geometry of objects.

The curing process of a photopolymer composition starts with capture of a quantum of radiation by a photoinitiator molecule, which passes to the active state. There are two types of radical initiators for photopolymerization. The first type are unimolecular initiators, single compounds that decompose into radicals upon irradiation; initiators of the second type are two-component systems, in which one component absorbs radiation and detaches a proton from the second component (synergist), thus giving a biradical system, which initiates polymerization.[277] Cationic polymerization initiators are compounds that decompose to active intermediates (cations, radical cations or radicals) upon exposure to radiation; a series of reactions of the active intermediates afford molecules of superacids, which initiate polymerization. Each initiator is characterized by a definite radiation wavelength that converts it to the active form. The initiators used for UV-curable compositions normally operate at wavelengths ranging from 300 to 415 nm.[278] If the composition is a mixture of monomers that are polymerized by different mechanisms, a mixture of radical and cationic initiators is used.

The activated initiator reacts with the monomer molecule, thus activating it towards the reaction with the next monomer molecule. As a result, polymer chain growth starts and propagates in the monomer bulk. After completion of polymerization due to exhaustion of the monomer, a polymer structure with a large number of cross-links between the chains is produced, *i.e*., the resulting cross-linked polymer is not thermoplastic. It is noteworthy that combined polymerization of epoxy resins and acrylates yields interpenetrating polymer networks rather than copolymers.[70]

A key parameter of additive manufacturing using photopolymerization methods is the exposure time, *i.e*., the time for which the photopolymer composition is irradiated. The exposure time affects the printing speed and the degree of curing of the resin and is specified depending on the properties of the composition, characteristics of radiation and layer thickness. Even if the exposure time is properly chosen, additional exposure of the finished product in a special UV chamber is often required for complete solidification of the material. These parameters of photopolymerization finally influence the physicomechanical characteristics of the printed product.

The exact composition of commercial photopolymer compositions is, in most cases, unknown; therefore, for solving research and engineering problems, the performance characteristics of the final products should be tested by the users themselves. The chemical stability of products obtained by photopolymerization methods to organic solvents is moderate; they tolerate long-term exposure to aqueous and alcohol solutions and short-term exposure to harsh chlorinated solvents;[90] however, in view of the high diversity of available photopolymer

compositions, the chemical stability of the products can vary over a broad range.

Distinctive features of the printed products obtained by photopolymerization are the high quality of the surface and almost complete absence of a layered texture (as opposed to FDM method) and high consolidation attained owing to the efficient and seamless fusion of layers during the polymerization process. For this reason, for example, SLA products have highly isotropic mechanical properties: the strength of the samples virtually does not depend on the orientation of the layers relative to the direction of the applied external load.[224] This also results in leak-tightness of all products intended for holding liquids or gases; this favourably distinguishes the photopolymerization methods from FDM, which is often associated with the need to thoroughly adjust the printing parameters to obtain leak-proof products.

Highly thermally stable materials can also be found among photopolymers. For example, a composition for the production of objects stable up to 415 °C was recently proposed; hence, this polymer can be considered an efficient construction material.[279]

Some recently proposed photopolymer compositions have been certified for medical applications. In particular, in orthodontic practice, transparent aligners — plastic orthodontic appliances for improving dental occlusion — are produced by laser and DLP stereolithography methods.[280, 281]

Photopolymerization methods allow the use of composite materials, which are obtained by the addition of various fillers to the initial composition. Filling of the photopolymer with SiO_2 particles results in a considerable increase in the tensile strength of the products and accelerates curing.[282]

Photopolymerization can also serve as the first stage in the production of items from materials that are not directly formed upon photopolymerization. In particular, this was done using a composite photopolymer containing graphene oxide. After pyrolysis, resulting in polymer destruction and reduction of graphene oxide, the material was completely converted to graphene and became electrically conducting.[283] One more interesting example is manufacturing glass items by pyrolysis of a silica-filled photopolymer precursor. Glass obtained in this way possesses transparency and high thermal stability.[284] In view of the high technical complexity of obtaining glass items by other additive methods, this approach can be considered to be quite promising provided that no high dimensional accuracy is required for the product geometry.

Specially developed photopolymer compositions make it possible to obtain unique materials. Framework structures were produced by laser stereolithography using a polymer material with siloxane, silazane or carbosilane backbone and photopolymerizable side groups. The subsequent pyrolysis of these products at 1000 °C converted the polymer to ceramics with full retention of the topology and with uniform shrinkage.[285]

It can be noted that photopolymerization methods make it possible to tailor the properties of materials for a particular scientific or engineering application no less efficiently than extrusion methods.[286] Owing to the high spatial resolution, photopolymerization methods may serve as additional tools in any chemical laboratory and are used when the spatial resolution of extrusion methods is insufficient, for example, for the production of microfluidic systems.

4. Application of 3D printing in chemistry and related fields

Quite a few publications of the last several years are dealt with application of 3D printing in chemical research.[287, 288] Why did additive technologies prove to be so relevant particularly to chemical science? This is because chemical experiments are associated with the use of numerous equipment items for manual preparation and purification of compounds without the use of complex automatic equipment. In everyday laboratory practice, an experimentalist manually assembles a setup for chemical synthesis and selects all the necessary accessories (adapters, valves, fasteners, various mounting elements, *etc.*), uses auxiliary laboratory equipment for ordering, storage and handling of chemicals (supports, stands, clamps, *etc.*). In other words, even in research work, chemistry has all features of material production that require many production tools. Moreover, these tools are meant for particularly mechanical or manual holding, moving, stirring, filtering or drying of reaction mixtures; they contain no electronic components or are operated by conventional electronic components (electric motors, light-emitting diodes, pumps, external heaters). Often, the equipment of a chemical laboratory should be optimized for a particular experiment; that is why most chemical research institutes have their own mechanical and glass blowing workshops. The production capacities of these workshops are often moderate and are suitable for manufacturing medium-size objects, *i.e.*, it is impossible, for example, to fabricate microchannel reactors or items of complex geometry. In addition, because of the necessity to compose a work specification and the long time needed for production, it is impossible to quickly obtain the required equipment by outsourcing to external workshops.

Problems of this type can be efficiently solved by personal 3D printing, which allows manufacturing items of a complex shape directly in the laboratory within a short time. This substantially accelerates the multiple repeated design optimization stages and allows for the use of unusual materials, including multifunctional materials absent from typical inventories of external workshops. An advantage of digital manufacturing in a chemical laboratory is the possibility of creating small amounts of own unique materials while working with plastics.

Digital manufacturing in a chemical laboratory does not require a specially arranged workplace or special conditions for using personal 3D printers: the process generates no waste, produces almost no noise and no toxic emission and 3D printers require little maintenance. The deployment of digital manufacturing in a chemical laboratory may be complicated by the insufficient skills of most chemists in technical 3D modelling based on computer-aided design systems. However, this is not a great obstacle, since printing of the objects needed in a chemical laboratory does not require a comprehensive knowledge of 3D design systems at the expert level. Indeed, there is no need to design objects pertaining to precision mechanical engineering (geared transmissions, complex assembly modules, *etc.*). Any chemist can learn how to operate a 3D printer.

The use of additive technologies in various fields of chemical science has specific features. The fields of application of 3D printing can be divided into chemical synthesis, analytical chemistry, biochemistry and biotechnology, pharmaceutics and chemical education. A large application area of 3D printing pertains to medicine, including prosthetics, regenerative tissue engineering and medical equipment. For example, 3D printing makes it possible to commence the production of complex medical appliances over a short period of time in the case of urgent and emergency situations.[289]

In the next Sections, we consider some representative examples of application of 3D printing to illustrate the opportunities offered by this method for the laboratory practice. Today, additive technologies are being vigorously developed; therefore, the number of scientific publications devoted to this subject rapidly grows. The purpose of this review, which does not claim to completely cover the published data, is to analyze the strategies of laboratory application of 3D printing, illustrated by most vivid examples of research works.

4.1. Additive technologies in chemical synthesis

Currently, investigations of the scope of applicability of 3D printing in chemical synthesis are mainly related to the development of new laboratory reactors for organic synthesis and studying their efficiency for various types of chemical processes.[290–292] One more recent field of investigation is concerned with the applicability of additive technologies for the production of new types of catalytically active materials for fine organic synthesis.[293]

3D printing is well suited for manufacturing any laboratory ware for conducting reactions of fine organic synthesis (Fig. 15).[294] When using FDM-printed products, one should bear in mind that the surfaces have porous and rough textures, which may promote the adsorption of catalysts or reaction products. Additionally, it is necessary to ensure leak-tightness of the reactors by optimizing 3D printing conditions and by thorough testing prior to chemical synthesis. Due to the low cost of plastics, this laboratory ware can be intended for single use to carry out reactions catalyzed by transition metal complexes. Thus, it is possible to avoid washing the reactor to remove the catalytically active compounds, which may be active even when present in trace amounts.[295] Provided that the construction material is inexpensive (*e.g.*, polypropylene), the use of disposable 3D-printed chemical reactors can be quite economically rational if the organic synthesis gives valuable products.

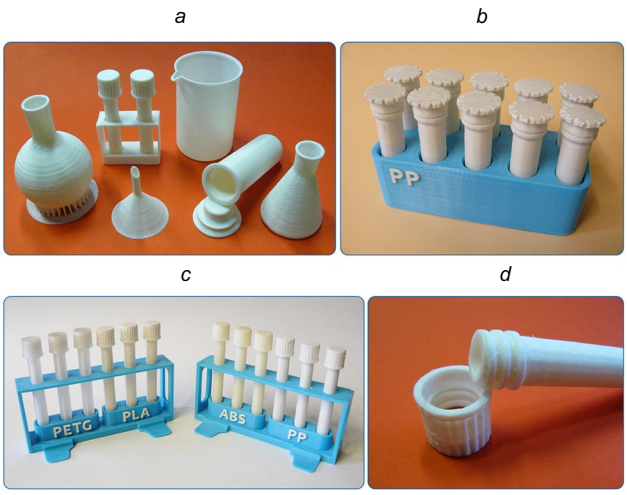


Figure 15. Examples of FDM-printed laboratory ware.[294] (*a*) Round and conical flasks, a funnel, a beaker, test tubes of various sizes; (*b*) polypropylene tubes; (*c*) chemical test tubes made of various materials; (*d*) functional threaded connection of a test tube and a lid.

The interest in the invention of new designs of chemical reactors is naturally associated with the versatility of 3D printing for the fabrication of objects of any shape, the possibility of using various materials and the possibility of integrating various functions in one chemical reactor without the need for prolonged and complex production process.

For example, a multichamber reactor for multistep organic synthesis was printed using the FDM method from polypropylene as the thermoplastic polymer most stable to chemicals (Fig. 16 *a*).[296] The organic synthesis implemented using this reactor consists of three steps. The first step is the Diels–Alder reaction catalyzed by Lewis acids (in this case, powdered K-10 montmorillonite was chosen as the catalyst), which ends in the formation of a product containing a carbonyl group. In the second step, the cycloaddition product reacts with aniline to give an imine containing the C=N group. The last step is catalytic hydrogenation of the imine yielding a secondary amine. Hydrogenation is catalyzed by carbon-supported palladium. Each step is supposed to proceed in a separate chamber of the reactor. The chambers are connected by passages, and the liquid reactants move between the chambers upon manual rotation of the device. The catalytically active compounds were embedded into one of the walls of the reactor chambers for catalytic reactions using 3D printing. For this purpose, powdered catalysts were distributed in the polymer matrix to form a material suitable for deposition with the printer head equipped with syringe extruders (in Fig. 16 *a*, the K-10 montmorillonite is shown in light yellow and palladium supported on carbon is shown in black). The reactants and magnetic stirrer bars were placed into the first reactor chamber during printing. The additional vessel present at the reactor outlet was filled during manufacturing, with a silica gel slurry. This served for purification of the product after the synthesis. After completion of 3D printing, the reactor represented a one-piece device accommodating reactants, stirrer bars, catalysts and the adsorbent for product purification. Only the product can be taken out of the reactor. It was shown that polypropylene, which serves as the reactor material, and the inert polymer matrix of the catalysts do not affect the course of chemical reactions, and the product yield in each step was slightly lower than that in the organic synthesis carried out in laboratory glassware.

The possibility of using 3D printer not only to construct the reactor, but also to insert specified amounts of reactants and to embed catalytically active materials into the reactor resulted in the development of a completely automated system for organic synthesis based on the desktop personal FDM 3D printer.[301] The operation of this automated system was demonstrated in relation to the multistep synthesis of ibuprofen, a widely used anti-inflammatory drug. The head of the printer was supplemented by an assembly of metal capillaries, which were connected by fluoroplastic tubes to five syringe pumps

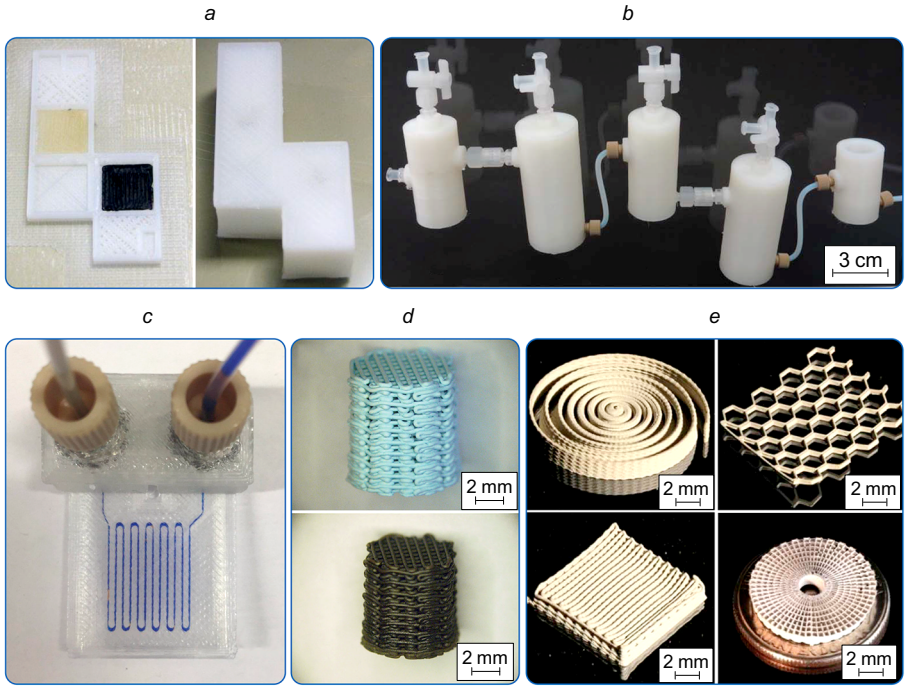


Figure 16. Examples of using 3D printing in organic synthesis. (*a*) FDM-printed polypropylene laboratory reactor meant for multistep organic synthesis. The left picture is the reactor in the beginning of manufacture with embedded catalytically active materials (the light yellow and black areas), and the right picture is the finished product containing the reactants inside.[296] (*b*) Modular system for fine organic synthesis FDM-printed with polypropylene. The modules are connected by standard connection fittings.[297] (*c*) FDM-printed polypropylene microchannel reactor for continuous flow chemical reactions. The channel width is 200 μm. For better visualization, the channel is filled with ink.[298] (*d*) Structured catalytically active material containing copper particles dispersed in an alumina matrix. This catalytic cartridge is meant for fine organic synthesis reactions. The top picture shows the material after DIW printing and drying, and the bottom picture (black) shows the material after sintering.[299] (*e*) Structured catalyst manufactured by DIW and containing gold and silver particles.[300]

that supplied liquid reactants for the synthesis. First, a polypropylene reactor was printed on a 3D printer. After printing was complete, liquid chemicals needed according to the synthetic procedure were fed into the reactor through metal capillaries. Positioning of each capillary above the inlet of the reactor, which was fastened on the build platform of the printer, was performed by moving the print head by means of specially developed software, which also controlled the syringe pumps. Since the addition of reagents occurred several times during the synthesis, the reaction remained open throughout the process; therefore, the synthesis could not be carried out under an inert atmosphere, and atmospheric moisture could not be prevented from entering the reaction mixture. The chosen printer brand implied the possibility of moving the platform along one of the horizontal coordinate axes. Owing to this design feature, stirring of the reaction mixture was accomplished by oscillations of the platform, similar to the laboratory shaker. The amplitude and frequency of platform oscillations were controlled by the user *via* the control software. During the synthesis, which lasted for many hours, the reactor material showed no signs of degradation. The use of 3D printers as parts of robotic systems of chemical synthesis can be an inexpensive way to automate this type of process and can serve as an alternative to more expensive and complex automation systems in organic synthesis, which have recently caused increased interest.[302, 303]

The possibility of adding reagents into the reactor during 3D printing was used to develop an efficient procedure for hydrothermal synthesis of coordination polymers (metal-organic frameworks).[304] Hydrothermal synthesis is a process in which compounds are prepared in a closed space at a temperature exceeding the boiling point of water and at elevated pressure. Usually, this type of synthesis is carried out in metal autoclaves or in fluoroplastic reactors, which have additional metal fittings for better sealing. It was shown that FDM-printed polypropylene reactors with a wall thickness of 4 mm can be successfully used for hydrothermal synthesis at temperatures of up to 140 °C for 72 h. During manufacturing, printing was paused for the addition of chemicals. After completion of printing, the reactor represented a fully sealed capsule with liquid reactants inside. This eliminates the need to assemble the reactor and to take additional measures to ensure leak-tightness. In view of the low cost of polypropylene, this approach can be useful for screening studies for optimization of synthesis conditions. The yield of the product (MIL-96 coordination polymer based on aluminium cations and trimesic acid) obtained in the polypropylene reactor at 130 °C in 18 h was 60%, whereas the product yield in the conventional synthetic procedure was 65%, *i.e.*, the efficiency of FDM reactors is, in this case, quite comparable with the efficiency of conventional autoclaves.

An important advantage of 3D printing for manufacturing chemical reactors is the possibility of fast optimization of the geometric parameters of the reactor to achieve the highest performance in a particular chemical process. A change in the volume of the chamber for

mixing the reactants in a chemical reactor printed by the DIW method from quick-curing organosilicon sealant may change the yield of the product of organic synthesis by more than 10%.[305] The design of the reactor allowed monitoring of the reaction by UV spectroscopy on a real-time basis.

3D printing is a fully digital manufacturing (except for preparation of the printer to print and post-treatment of the product: removal of supports, drilling-out of improperly formed holes, *etc.*); therefore, this production technology can be considered to be a part of general, fully digital, description of chemical synthesis.[297] According to this concept, each step of a complex chemical synthesis is described by a unified system of descriptors that determine the duration and conditions of the step. On the basis of this description, a set of modules — future chemical reactors — is formed in such a way that the whole multistep chemical synthesis can be performed. To embody each module as a chemical reactor, the 3D model is constructed by selection from a library of standard elements (bottom head, top head, connections). The next stage is 3D printing of all reactors, which are assembled as a modular system for the preparation of the desired product. This approach minimizes the intervention of the user in the construction of a successfully operating synthetic system, since the final ready-to-use structure of this system, is generated automatically on the basis of a digital description of the whole process. Successful application of this approach requires correct description of all steps of chemical processes in the first stage of development. The potential of the digital preparation of chemical synthesis was demonstrated by the authors of the concept in relation to the syntheses of a number of biologically active compounds, including the muscle relaxant baclofen;[297] the modular system for baclofen synthesis is shown in Fig. 16 *b*. The implementation of this modular system afforded baclofen as the final crystalline product in 44% yield. In the authors' opinion, the digital description of the whole synthesis covering the key steps and manufacturing of the reactors could be used to rapidly start the synthesis of pharmaceuticals when needed in those cases where implementation of full-scale industrial production or a laboratory with high-skilled personnel is uneconomic.[297] Certainly, this is a much more versatile approach for automation of chemical synthesis than the use of a 3D printer as a robotic chemical unit described above.

The efficiency of modular implementation of a laboratory unit for chemical synthesis fabricated by FDM printing on the basis of formal description of all steps of a chemical process was demonstrated by preparation of not only pharmaceuticals but also products of fine organic synthesis relevant to everyday laboratory practice such as catalyst precursors and reagents for biomolecular research.[306] The purchase of a large assortment of such compounds for future use in a single laboratory is inappropriate, in view of the very high commercial price and moderate shelf life of these compounds. Therefore, it appears reasonable to synthesize some compounds when needed directly in the laboratory. For example, it was shown that using a modular system made of polypropylene, it is possible to prepare the Pd_2dba_3 complex, a precursor of catalytically active Pd(0) species.[306] Test experiments demonstrated that the properties of compounds synthesized in the FDM-printed modular system do not differ from the properties of the same compounds received from commercial sources and that the synthesis can be performed much faster than the conventional synthesis in glassware, which thus saves time for experimentalists. Modular systems are markedly more convenient for conducting parallel syntheses and can reduce the cost of the product 100-fold compared to the cost of commercial products.[306] Acceleration of the synthesis in a modular system is due to the use of stricter and more reproducible protocols describing the synthesis and to greater self-sustainability of the modular system compared to conventional laboratory units. Modular systems for synthesis are relevant when freshly prepared compounds are required.

Additive technologies were shown to be efficient for the manufacture of reactors for continuous flow chemistry.[307] Unlike batch reactors, continuous flow chemical reactors represent channels in which liquid compounds react with one another while moving along the channel. Flow reactors are used for continuous flow synthesis; in some cases, this markedly increases the productivity of the process, which is especially useful for industrial production. In particular, the high efficiency of FDM-printed microchannel flow reactors was demonstrated for the synthesis of biologically active amino alcohols.[308] The synthesis of amino alcohols comprised two steps. In the first step, the catalytic nitroaldol condensation of nitroalkane with aldehyde took place, resulting in the formation of nitro alcohol. The copper(II) complex, the catalytic form of which was generated *in situ*, was chosen as the catalyst for this reaction. In the second step, catalytic hydrogenation of the nitro group (catalyzed by palladium supported on carbon) took place to give amino alcohol as the final reaction product. The FDM-printed reactor was used only for the first step. Nitroaldol condensation can be carried out in ethanol at low temperature; therefore, the materials used to manufacture the flow reactor for the tests included not only relatively chemically stable nylon but also PLA and HIPS, which have a moderate stability to most organic solvents except for alcohols.

The flow reactor had as a zigzag channel enclosed in a box with two connected capillaries through which the reactants were injected with a syringe pump and one capillary for withdrawal of the intermediate nitro alcohol. A set of reactors differing in the cross-section geometry (circle or square) and in the inner volume of the channel were tested for condensation. The cross-sectional shape proved to be fairly important: the conversion attained in the square channel was twice as high as the conversion obtained in the circular channel, with the residence times of the reaction mixture in the reactor being equal. This result may be attributable to different efficiencies of stirring of reactants in differently shaped channels.[308] It is noteworthy that the conversion was always higher in FDM reactors than in the coiled tube reactor manufactured from the standard fluoroplastic capillary. Meanwhile, the material of the reactor had little influence on the yield of the intermediate product.

In relation to the two-step synthesis of norephedrine, it was shown that flow reactors of this type can be embedded into more complex systems for continuous flow chemical synthesis without manual isolation of the intermediate products. In the combined system, the mixture containing the intermediate moved from the FDM-

printed flow reactor into a filtration chamber in which the catalyst was separated from the reaction mixture. After that, the reaction mixture was delivered to the catalytic hydrogenation module in which the final product formed in a yield of up to 90% and with high stereoselectivity. These flow reactors can be connected to one another to arrange any sequence of synthetic steps or to perform fast scaling-up of the chemical process.

Flow reactors can be used not only for separate functioning, but also as parts of commercial systems for the arrangement of a continuous flow chemical synthesis. An example of this integration is provided by successful use of the FDM-printed polypropylene reactor as a part of the Uniqsis FlowSyn system.[309] The FDM reactor was a column with a size designed to fit into the heating unit of the Uniqsis FlowSyn system. The channel 2 mm in diameter inside the column had a coiled shape, which increased the residence time of the reaction mixture in the heated zone. The reactor was connected to a capillary for injection of reagents and a capillary for removal of the product by standard fittings made of PEEK. Reactor heating, temperature control and injection of chemicals at a specified volumetric flow rate were provided by the automated Uniqsis FlowSyn system. It was shown that by using the FDM reactor in combination with Uniqsis FlowSyn, it is possible to synthesize complex bicyclic and tetracyclic compounds that form the basis of important pharmaceutical drugs.

Quite a few papers are devoted to 3D printing of milli- and microfluidic systems for chemical applications.[310 – 315] Microfluidic systems are small-sized (a few centimetres) devices containing a system of microchannels (0.5 mm to several tens of nanometres wide, depending on the type and purpose of the device), valves and other functional microparts, which control the flow of liquid microvolumes. Microfluidic systems differ from the equipment for handling small amounts of liquids in that they are manufactured using microfabrication methods.[316] The liquid microflow dynamics differs considerably from the liquid dynamics in larger chemical systems. In particular, a laminar flow regime can predominate in microflows, which is highly important for mass and heat exchange processes. The use of microvolumes makes it possible to arrange uniform conditions throughout the reaction mixture, which leads to increasing yield and selectivity of chemical synthesis and provides a high degree of reproducibility. Microfluidic systems are used as sensors and devices for microbiological studies, chemical synthesis and other fields. Microfluidic systems are traditionally manufactured by lithography, micromilling, injection moulding and hot embossing.[317] All of these methods are time-consuming and require special production equipment which in most cases can be used only for microfabrication and high skill of the user.

Unlike conventional microfabrication techniques, 3D printing can be used to manufacture microfluidic systems of any shape in a short time, with little special skills required, while remaining a versatile production method. Currently, three additive technologies are widely used to manufacture microfluidic devices, namely, FDM, stereolithography and photocurable material jetting (*e.g.*, PolyJet). According to a systematic methodical study,[318] the minimum microchannel width for FDM is in most cases $\sim$500 μm (with additional optimization of the printing process, it is possible to fabricate channels with a width of down to 200 μm), whereas the DLP-SLA method can provide a channel width of $\sim$150 μm in the case of appropriate choice of the photocurable resin.[318] The channel width in the products obtained by FDM printing is usually smaller than the design size due to some spreading of the polymer melt during printing. The PolyJet method occupies an intermediate position and is suitable for printing microfluidic devices with $\sim$200 μm channels. When DLP-SLA is used, the microchannels have the most distinct shape with walls strictly perpendicular to the base in the case of rectangular cross-section. In this respect, stereolithography approaches conventional microfabrication methods in terms of product quality. In addition, the DLP stereolithography method gives rise to the lowest surface roughness (R_a = 0.35 μm), whereas FDM printing, as expected, gives surfaces with the highest roughness (R_a = 11.0 μm).[318] High surface roughness in the FDM-printed microreactors leads to increasing fluid flow turbulence and more vigorous stirring of mixture components, while in SLA microreactors, the flow can remain laminar; therefore, if precise control over flow processes is required, microreactors should be produced by stereolithography. FDM printing is suitable in cases where relatively fast component mixing is needed. However, DLP implementation of stereolithography has the drawback of undesirable light exposure of photopolymer parts within the microchannel, which can result in microchannel blockage; therefore, thorough optimization of the light curing conditions is required for each type of resin and each microfluidic system design.

It is noteworthy that the SLA and PolyJet methods can ensure the transparency of microreactor walls; this is often useful for visual monitoring of the reactions, whereas in the case of FDM printing, a partial transparency of the products can be attained only in thin films of material (Fig. 16 *c*), while increasing wall thickness quickly results in complete loss of transparency because of light scattering on inner wall defects inherent in extrusion fused deposition. In view of the high cost of 3D printers operating by material jetting technology, SLA and FDM can be considered to be the most promising methods for the production of microfluidic devices in the laboratory. The choice between these methods is determined by the availability of materials suitable for a particular experiment.

Microfluidic systems can be efficient chemical reactors for both single-step and multistep processes of fine organic synthesis. In particular, FDM-printed polypropylene microreactors with a channel diameter of 0.8 mm were used for the synthesis of imines by the reaction of benzylamine with benzaldehyde.[319] Each reactant was injected into the reactor through the standard fluoroplastic capillary with a syringe pump (there are known designs of specialized pumps for microfluidic devices also fabricated by 3D printing[320]). The reactant flows were combined in one channel in which synthesis of the product took place. The microreactor outlet was connected to an IR spectrometer, which detected the formation of the imine derivative. Complete conversion of reactants to the product was attained at the optimal volumetric flow rate through the microreactor channel; an increase in the volumetric flow rate decreased the conversion. The imine formation and hydrogenation steps can be combined in one microreactor. For this purpose,

an additional hole for injecting the reducing agent was located in an intermediate point of the microchannel. Thus, imine was formed in the first part of the channel and subsequently mixed with the reducing agent at the intermediate injection point; in the second part of the channel, reduction took place to give a secondary amine.

FDM-printed polypropylene microreactors demonstrated high efficiency in modular microfluidic systems for multistep processes, for example, in glycosylation reactions, that is, replacement of a hydrogen atom of an organic molecule by a sugar residue.[298] Glycosylation is a highly important biochemical process. Two microchannel flow reactors were combined into a single system. In the first reactor, the glycoside donor molecule was formed *via* replacement of one hydrogen atom of pyranose (monosaccharide) by an organic group. Glycosylation, that is, replacement of the hydrogen atom of the alcohol molecule by the pyranose residue, took place in the second flow reactor. The product yield in this two-step process reached 69%. It was shown that reactors with circular channel cross-sections are not leak-proof, because of the stepwise deposition of layers, which was in full agreement with the results obtained previously for spherical FDM vessels.[32] High leak-tightness of reactors is attained in the case of rectangular channels.

A promising approach to the design of microfluidic systems is assembly from separate standardized modules manufactured with high accuracy by stereolithography.[321] Each module has a microchannel and fittings for connection to other modules. When the modules are connected, microchannels mate to each other, thus forming a common system. This approach allows one to assemble microfluidic systems of any three-dimensional configuration, similar to the assembly of Lego parts. In addition, some detectors for analysis of the liquid that flows along the microchannels can be fabricated in the same way as standard modules, which allows integration of detectors into the microreactor and provides automated real-time monitoring of the process. Apart from the high versatility, the modular approach markedly simplifies the operation of microfluidic systems. During operation, microchannels can be plugged by particles of the precipitate or solid impurities. In the case of modular design, it is sufficient to identify and replace a disabled module and not repair the whole system, as would be the case for a monolithic object.

The modular design of a microfluidic system may be considered an analogue of an electronic circuit containing liquid capacitors for collection of a liquid, liquid diodes for 'rectifying' the pulsed liquid flow into a continuous flow and liquid transistors performing 'amplification' of the liquid flow by increasing pressure. It was shown[322] that these elements can be manufactured by material jetting, namely, using MJM method. Unlike stereolithography methods, which are suitable for printing with only one material using accessible printer designs, in the case of the MJM, it is possible to use a soluble support, which conceptually enables printing of miniature parts with internal cavities of a complex topology.

The above examples of using additive technologies in chemical laboratory practice can be assigned to traditional applications aimed at the production of technical equipment: reactors and accessory tools. Meanwhile, 3D printing can be conceived as a universal method for the arrangement of matter into an ordered structure, with such structures including not only technical equipment but also any material object that requires structuring of the material for functioning. For example, an exciting application of 3D printing is the fabrication of structured catalysts in the form of cartridges for a particular reactor and chemical process.[323–326] In this case, catalytic mass or catalyst precursor serves as the printing material.

Structured heterogeneous catalysts containing catalytically active copper particles distributed in an alumina matrix were manufactured by DIW (Fig. 16 *d*).[299] These catalysts can be used for implementing continuous flow catalytic processes since immobilization increases the stability of the catalyst to leach out of active particles and rules out contamination of the reaction product by particles of the catalyst mass, which is especially important for the pharmaceutical industry. For 3D printing of the catalytic cartridge, it is necessary to prepare ink, *i.e.*, a flowing material that can be extruded with the print head of a printer. In this case, ink was made of alumina, an aqueous solution of copper(II) nitrate, hydroxypropyl methylcellulose (HPMC) as a viscosity adjuster and some other auxiliary components. The rheological properties of the ink can be optimized by varying the content of the polymeric viscosity adjuster and by evaporating the water contained in the suspension. The suspension was loaded into a syringe extruder and extruded layer-by-layer through a nozzle with a diameter of 0.41 mm; this gave the primary ('green') form of catalytic cartridge, which was sintered in a furnace for 2 h at 1400 °C. The sintering gave a mechanically strong and highly porous ceramic mass. The activity of the catalyst obtained in this way was tested in the Ullmann reaction — a coupling process resulting in the formation of a carbon–heteroatom bond. The reactions carried out for short time periods (2–4 h) afforded a series of compounds with N–aryl bonds in high yields (up to 94%). The known catalytic systems based on copper(II) oxide provide a comparable yield of the product only in 8 (and more) hours even at higher copper content. Furthermore, the printed catalyst was used ten times without a considerable decrease in the product yield (the yield of one of the products was 91% in the first run and 86% in the tenth run).

The DIW method was also used to produce structured catalysts consisting of a porous metal (Fig. 16 *e*).[300] As in the previous example, 3D printing was performed using viscous ink containing metal particles, in this case, gold and silver particles in a 70 : 30 ratio. Immediately after 3D printing, the resulting structure consisted of separate metal particles bound by a polymer binder. For particle sintering and formation of a homogeneous metal alloy, the product was subjected to thermal treatment at 850 °C for 12 h. In this stage, microporosity was generated upon decomposition of the polymer binder. Next, the alloy was treated with concentrated nitric acid to dissolve silver particles, which resulted in the formation of nanosized pores. The final product was composed of gold and possessed hierarchical porosity: macroporosity was generated during 3D printing and was determined by the initial digital model of the cartridge, while micro- and nanoporosity were formed upon the removal of the polymer binder and silver particles, respectively. Nanoporous gold possesses catalytic activity, for example, in the oxidation of organic compounds.[327, 328] The presence of macropores provides for efficient mass transfer in the catalytic cartridges during chemical reactions, as the

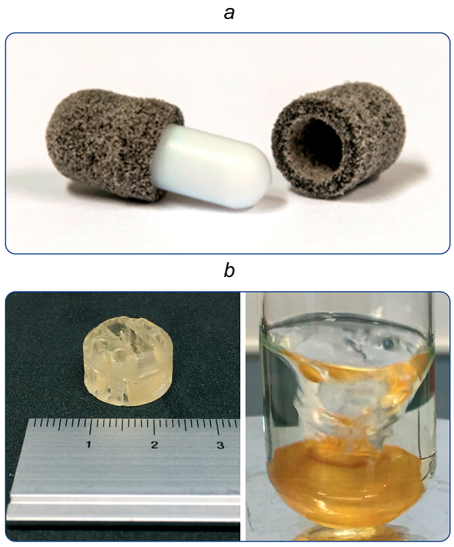


Figure 17. Magnetic stirring bars manufactured with catalytically active materials. (*a*) Shell for a magnetic stirring bar containing palladium nanoparticles in a polypropylene matrix;[329] (*b*) holder for a magnetic stirring bar manufactured by laser stereolithography and containing *para*-toluenesulfonic acid for catalysis of the Mannich reaction; the stirring bar is shown separately and during organic synthesis.[330]

reaction mixture rapidly moves along wider channels to reach the active sites in the nanosized pores.

One more approach to the production of 3D printed catalysts is the fabrication of magnetic stir bars containing catalytically active compounds or particles. For example, a shell for the stirring bar with palladium particles distributed in the polypropylene matrix to catalyze the Suzuki – Miyaura cross-coupling reaction was fabricated by selective laser sintering (SLS) (Fig. 17 *a*).[329] The SLS method is convenient for the formation of catalytically active structures since the printing feedstock is a finely dispersed plastic powder in which it is easy to introduce any other powdered components. In this case, a commercially available silica-supported palladium catalyst (Pd/SiO_2) was used. The stirring bar shell manufactured by SLS had a relatively high porosity, which provided rather efficient contact between the catalyst and the reaction mixture. Since the catalyst particles were attached to the surface of the rotating stirring bar, the reaction mixture occurring in direct contact with the active sites was continuously renewed. The product of coupling aryl halides and phenylboronic acid was formed in a markedly higher yield (99.5%) with the printed catalyst than with the standard powdered catalyst (92.0%). Upon reuse, the activity of the 3D printed catalyst decreased more slowly than that of the conventional catalyst.[329] An advantage of the palladium catalyst immobilized on the magnetic stirring bar is convenient catalyst removal from the reaction mixture with a magnetic rod without filtration. It is worth noting that despite the solid state of the catalyst, cross-coupling took place in solution rather than on the surface of solid particles and was catalyzed by the molecular form of palladium complexes.[331]

Stereolithography can also be used for the fabrication of catalytically active materials of stirring devices. In this case, the catalytically active components can be added to the initial liquid photopolymer composition. This approach was used to fabricate a magnetic stirring bar holder containing 5% *para*-toluenesulfonic acid as the organocatalyst for the Mannich reaction (Fig. 17 *b*).[330] The holder was a cylinder with a groove for the magnetic bar and vertical columns on the sidewall providing more intense stirring of the reaction mixture. The reaction of cyclohexanone, aniline and benzaldehyde using this stirring device gave the product in 91% yield.

4.2. Additive technologies in analytical chemistry

The use of personal 3D printing in analytical chemistry develops along the following avenues: (1) fabrication of special chemical reactors, including microfluidic reactors, for separation of mixtures and monitoring of specimens; and fabrication of reactors and tools for efficient sampling during studies of dynamic processes in reaction mixtures or in biological substrates; (2) fabrication of new accessory equipment for analytical instruments (mass spectrometers, chromatographs, microscopes, *etc.*) tailored for a particular experiment; (3) development of new materials or new ways of arrangement of materials for analytical research.[332 – 335] The greatest number of examples of using additive technologies in analytical chemistry corresponds to the first two areas.

It is often convenient to conduct analytical studies as series of experiments. This not only accelerates the studies but also considerably facilitates comparison of the results, as several samples can be analyzed under the same conditions or similar samples can be analyzed under different conditions. For example, a multichannel device with eight horizontal channels equipped with standard threaded connections for syringes was proposed for studying the effect of biologically active compounds on living cell cultures (Fig. 18 *a*). Each channel had a side branch chamber contacting the environment. The chamber was separated from the channel by a permeable

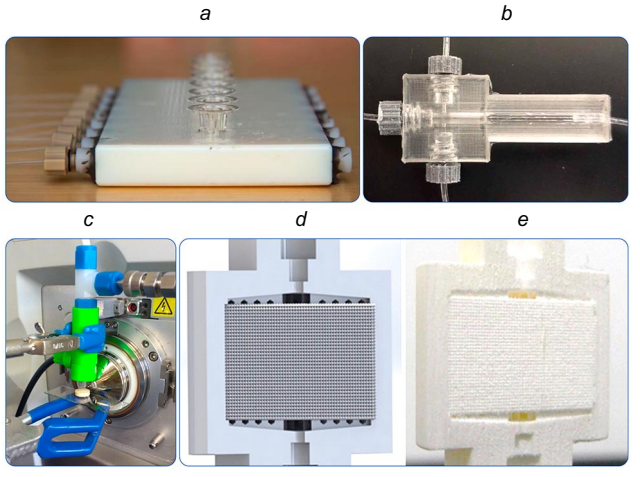


Figure 18. Examples of using 3D printing in analytical chemistry. (*a*) Multichannel system for studying the effect of biologically active compounds on living cells;[336] (*b*) FDM-printed microfluidic mixer made of polylactic acid;[337] (*c*) low-temperature plasma ionization system for mass spectrometry;[338] (*d*, *e*) chromatographic column manufactured by MJP as an integral unit with an adsorbent bed (on the left is the 3D model and on the right is the finished device).[339]

polycarbonate membrane and served for insertion of cell cultures. Solutions of biologically active compounds were pumped by syringes through the channels, gradually penetrated the membranes, and acted on the cells. The device was tested by studying the dynamics of action of antibiotics, levofloxacin and linezolid, on the pulmonary artery endothelial cells of mammals. It was shown that this design makes it possible to monitor both the concentration of the drug in solution and cell viability. Multichannel systems of this type can be optimized for a variety of biochemical and medical studies.

For the visual monitoring of processes, it is convenient to use transparent mixing vessels, reactors and connection fittings. The FDM method was proposed for manufacturing microfluidic systems sufficiently transparent for visual monitoring of processes during analytical experiments (Fig. 18 *b*). Transparency makes it possible to observe mixing of components, monitor the formation and movement trajectories of particles and drops *in situ*, and analyze the kinetics of chemical processes. Transparent reaction vessels can be used in combination with optical microscopes, which further extends the scope of visual monitoring.

FDM printing with transparent materials usually gives products with no or little transparency. This is due to the presence of numerous small defects in the walls of FDM products, which is caused by the pattern of deposition during printing. Light is scattered at the boundaries of defects upon transfer from one medium to another, and the chemical reactor wall loses transparency. To increase the transparency, thin walls were used and a special procedure for printing of the first layer was developed. To attain high light transmission, the first layer was printed on a glass surface with a large extrusion width.[337] The extrusion width determines the degree of spreading of the plastic as it comes out of the nozzle. A large extrusion width in combination with a moderate height of the layer increases the consolidation and transparency. Using this method, the authors manufactured transparent leak-proof microfluidic devices with square cross-sections (400×400 μm), able to hold an internal pressure of up to 5.5 MPa.[337] Transparently was attained without any posttreatment of finished objects. The microchannel systems thus formed were tested in experiments on microdrop tracking; the wall transparency proved to be sufficient for droplet tracking by means of specialized software. Additionally, the manufactured devices were used to perform test experiments on melting profiles of DNA molecules. In these experiments, fluorescent markers active only in the presence of double-stranded DNA were added to a DNA solution.[337] Upon heating, DNA denatured and cleaved into separate nucleotide chains, which coiled. The temperature profile of DNA transfer from the double helix to the coil makes it possible to determine the DNA length, nucleotide composition and other parameters. FDM-printed reactors with transparent walls showed a high performance in this method of analysis, comparable with the performance of commercial products.

One more method for endowing FDM-printed products with transparency is based on a useful feature of extrusion fused deposition, *i.e.*, the possibility to pause the printing. In this case, the print head moves away from the incomplete product; this opens up the possibility for additional manipulations: inserting magnets, electrodes, membranes, heating elements, various electronic components, chemicals and other materials. After completion of the required operations, printing can be resumed from the same position where it was paused, *i.e.*, the integrity of the object is not disrupted. As a result, the additional components become embedded into the plastic product. Other additive manufacturing methods offer little possibility of this type. This procedure was used to manufacture microchannel PLA systems with an embedded window for visual inspection of processes in the liquid.[340] Printing was paused, a glass slide was inserted to cover the channel, and printing was resumed. Of course, the design should envisage the insertion of the glass plate. The plastic and glass are not fused together, and there are gaps in the joints between these materials, which enables leakage of the solution from the channel. By optimizing certain printing parameters, it is possible to minimize the size of such gaps or eliminate them; however, even the presence of these defects does not cause leakage from the device.

Transparent microchannel systems can be manufactured by combinations of 3D printing with conventional production technologies such as casting. In this case, a master model is 3D printed and used for fabrication of a casting mould or template, which is filled by the casting material. Then a microchannel system is cast from transparent silicone. However, these processes suffer from a drawback of FDM printing, namely, high surface roughness, which is inherited by the master model and even persists in cast products. In other words, although the casting material is transparent and the cast product wall is monolithic and has no light-scattering defects, the resulting object may have moderate transparency because of the rough surface.[340] In this case, it may be more appropriate to use other 3D printing techniques that produce smooth surfaces, *e.g.*, stereolithography and material jetting methods such as PolyJet.[341]

3D printing is an efficient tool for miniaturization of analytical equipment. This is always needed for analytical chemistry, since with increasing total population and population density and with more active migration of people, mobile analytical systems for solving medical problems and for environmental monitoring issues become more in-demand.[342–344] Microfluidic systems are often the key components of compact and portable devices for analysis. Laboratory separation and analysis of mixtures of proteins, amino acids and cells in compact devices is carried out using free flow electrophoresis.[345] According to this method, a solution containing proteins moves along a channel, with an electric field being applied normally to the plane of movement, which results in separation of protein molecules. A microchannel system FDM-printed with ABS plastic using a desktop personal 3D printer was proposed for free flow microelectrophoresis.[346]

Succsessful attempts to miniaturize this type of analysis have also been made earlier; however, this required the use of either rather expensive equipment or multistage production processes. FDM printing is free from these drawbacks and allows fabrication of microchannel systems for electrophoresis in one stage without considerable material expenses. Despite the fact that ABS plastics and other general-purpose plastics (PLA, PETG), which are now used in FDM printing, do not possess high chemical stability, they are still quite suit-

able for the purposes of electrophoresis of biological components, since the analysis is carried out in water and without high temperatures. The microchannel device was equipped with threaded ports for connecting the capillaries for injection and withdrawal of components using standard connecting fittings; moreover, the thread was also produced with an FDM printer.[346] After printing, the device was placed into an acetone bath. Solvent baths are often used for posttreatment of FDM products. The solvent should dissolve the material of the device. For treatment in the bath, the object is hung or mounted at some distance from the solvent layer on the bottom of the bath. Upon heating, the space of the bath is filled with solvent vapour, which gradually affects the outer layers of the printed product. This treatment considerably increases the light transmission and leak-tightness of microchannel systems made of transparent ABS plastic; this enables convenient visual observation of processes that take place in the channels. It was shown that FDM-printed microchannel systems are quite suitable for the electrophoretic separation of proteins. The separated protein molecules are most often detected by optical methods based on fluorescence; therefore, the transparency of the material of the separation system is highly important. FDM 3D printing always produces a rough surface. Even after treatment in the acetone bath, the surface microroughness is retained, which results in a considerably more pronounced light scattering by the material of FDM systems in comparison with glass systems. Therefore, the limit of detection of proteins is markedly higher for FDM-printed reactors than for glass reactors.[346] Thus, in each particular case of additive manufacturing of these separation systems, experiments should be carried out to determine the lower limit of detection if optical methods are used, and the method sensitivity should correspond to the task at hand because some analytical problems do not require high detection accuracy.

Microchannel systems of this type can be used for point-of-collection (POC) diagnostic systems for fast diagnosis of diseases, field determination of toxic compounds or fast analysis of contents of particular compounds in the human body.[347, 348] A specific feature of POC diagnostic systems is that these systems combine operations that are performed, in laboratory analysis, using different instruments operating on different physical principles, *i.e.*, separation of mixtures, preconcentration to obtain a detectable signal, detection and quantification of components — all of these operations should be implemented in a mobile diagnostic system.

Therefore, POC diagnostic systems, which represent miniature automated laboratories, are multicomponent devices capable of implementing different types of analysis as a coherent sequence. Photopolymerization techniques (stereolithography, PolyJet, MJP), which possess high spatial resolution and are often used to manufacture microfluidic systems, have an important drawback: a very narrow range of applicable materials. Materials for SLA differ in colour and strength after photopolymerization; multimaterial printing by SLA and related methods is still at the stage of pilot experiments. In the context of fabrication of multifunctional devices, such as POC diagnostic systems, extrusion fused deposition methods appear more promising. The FDM method allows multimaterial printing even when inexpensive printers are used; furthermore, a variety of materials are suitable for printing, including transparent, elastic, high-strength, porous, thermally stable, chemically stable and electrically conductive materials filled with catalytically active particles or biologically active compounds. FDM printing can be performed for materials from any manufacturer, and it is possible to fabricate user materials with unique properties. For example, a microfluidic analytical system (with main channel cross-section of 0.8×0.5 mm) for determining the content of pharmaceutical agents in liquid biological specimens was manufactured by multimaterial FDM printing.[349] The device was fabricated using four materials: transparent ABS plastic, electrically conductive PLA plastic and elastic porous plastics, Lay-Felt and Lay-Gel, meant for making membranes. The Lay-Felt and Lay-Gel plastics contain water-soluble components, which are washed away to leave a nanoporous structure (pore size of $\sim$12 nm for Lay-Felt and $\sim$1 nm for Lay-Gel).[349] Multimaterial printing was performed with a personal FDM printer capable of simultaneously using five materials. The analysis implemented in this device was based on electrophoretic separation of components and tested by detection of ampicillin. The sample used for POC analysis was not prepared, *i.e.*, it contained a mixture of biological components, and the large-pore membrane (Lay-Felt) served as the filter, which separated protein molecules and cells but transmitted low-molecular-weight pharmaceuticals. The second membrane with small pores (Lay-Gel) retained the pharmaceutical molecules in the main separation channel, but other components with lower molecular weights, which were not the purpose of analysis, passed the membrane, *i.e.*, the test compounds were trapped in the channel. The components trapped in the main channel were separated by electrophoresis and analyzed. These systems were shown to be highly selective and efficient for the detection of pharmaceutical products.[349]

Thus, multimaterial FDM printing can be used to obtain multifunctional analytical devices over one printing session, *i.e.*, without the manual assembly. Considering the very low production rate of 3D printing compared to mass production methods such as injection moulding, the use of 3D printing for the manufacture of this type of device is appropriate if a small number of analytical systems optimized to detect particular components are required.

Despite the relatively low spatial resolution, FDM printing can serve for producing miniature units of analytical systems, which showed a high efficiency quite comparable with the efficiency of conventional analytical equipment even in important areas such as studying the biochemistry of the brain.[350] Important information about the activity of the brain under certain conditions can be gained by monitoring the content of compounds involved in the energy exchange of neurons, such as glucose, lactic acid (and lactates), in the extracellular space. These compounds must be monitored during vital activity of the body, accompanied by intense energy consumption by the brain. One of the ways of monitoring is implanting biochemical sensors into the mammalian brain.[350] However, this approach has some drawbacks, in particular, the fact that electrodes are gradually coated by biological materials. Another approach is continuous microdialysis of extracellular fluid components. For microdialysis, a capillary probe with a semipermeable

membrane as the wall is inserted into a tissue. A perfusion fluid is continuously fed into the capillary through a narrower channel; the composition of the perfusion fluid should desirably be as close as possible to the composition of the extracellular fluid except for the components that are to be analyzed. Due to the difference between component concentrations inside and outside the probe, the analyte components penetrate into the capillary and are carried away by the flow of perfusion fluid for the subsequent analysis (dialysis is exactly the exchange of molecules between the perfusion fluid and the extracellular space). To obtain analytical signals from glucose and lactic acid molecules, they are oxidized under the action of enzymes, glucose oxidase and lactate oxidase, respectively. Glucose is oxidized to glucono-δ-lactone and hydrogen peroxide, while lactic acid gives pyruvic acid and hydrogen peroxide.[350] In order to monitor the glucose and lactate concentrations on a real time basis, flow reactors were fabricated by FDM printing, and the microdialysate containing the test components was passed through these reactors. The reactors were made of ABS plastic as U-shaped tubes filled with macroporous structures of overlapping cuboids to increase the contact area between the microdialysate and the reactor surface. The enzymes for glucose and lactate oxidation were deposited on the surface of porous structures. The formed hydrogen peroxide reacted with a specially developed set of organic molecules, which was thus converted to a fluorescent product, which was quantified by a fluorescence spectrophotometer. The test compounds were oxidized in separate reactors since each enzyme selectively acts on its own substrate; therefore, it was possible to estimate both the content of glucose and the content of lactic acid in the extracellular space of the rat brain.[350] The analytical system obtained in this way had a high sensitivity and was efficient for biochemical analysis related to investigation of functioning of the nervous system of mammals.

Thus, microchannel systems for laboratory research can be manufactured using inexpensive desktop 3D printers; furthermore, the product quality depends to a higher extent on the material and printing parameters than on the cost of the printer. When the printing parameters are adjusted appropriately, even an inexpensive personal FDM printer provides a reasonable quality of the products.[337]

A promising trend of using 3D printing in analytical chemistry is the development of accessory tools that expand the scope of instrumentation or make the use of instruments in particular experiments more convenient.

For example, spray ionization of samples is often used in mass spectrometry. A facile and versatile method for spray generation at atmospheric pressure is paper spray, while the ionization method using this spray is called paper spray ionization (PSI).[351,352] According to this method, the sample is deposited on the surface of a paper triangle, with one of its vertices pointing towards the inlet of the ionization chamber of a mass spectrometer. After the paper triangle bearing the sample has been wet with an appropriate solvent and a voltage has been applied, spray generation takes place with an electrospray ionization mechanism. Paper spray is mainly used to determine the content of pharmaceutical products in biological samples; this method is fairly convenient for this purpose since it allows long-term storage and transfer of dried samples deposited on paper. An important feature of PSI is the possibility of continuous supply of the solvent through the paper substrate. In this case, the piece of paper acts as the sorbent. In essence, this implementation of the method combines paper chromatography and mass spectrometry, thus opening the possibility to separate mixtures and separately analyze each of the components. In addition, chemical reactions can be conducted in solution on the paper substrate and can be simultaneously monitored by mass spectrometry. A compact PLA cartridge manufactured by FDM printing was proposed for continuous supply of the solvent.[353] Since the PSI method is most often employed for the analysis of biological samples in aqueous ethanol, polylactic acid is quite relevant as the construction material; however, if necessary, a rather wide range of chemically stable materials can be proposed for FDM printing. The cartridge is an open vessel comprising two compartments, one for the solvent and one for the paper triangle. The paper triangle was connected to the vessel by thin paper strips for the supply of solvent. This design allows the solvent supply through the paper substrate to be continued for tens of minutes without using pumps. Using this cartridge, a mixture of organic pigments was successfully separated, and the components were then analyzed by mass spectrometry.[353]

A similar FDM-printed device made of ABS plastic has been proposed.[354] In this case, the design of the cartridge was very simple: a solution of the test compound was charged into a small cylindrical vessel and gradually moved towards the inlet of a mass spectrometer along a 500 μm wide channel. A 'needle' manually cut out of paper was fastened at the end of the channel, and spray emission took place from the needle tip. This device was not intended for continuous supply of the solvent, but provided a stable spray formation for 10 min.

Mass spectrometry is a useful method not only for determining the qualitative and quantitative composition of mixtures but also for fundamental studies of the mechanisms of chemical reactions. In this type of study, mass spectrometry is used for real-time monitoring of the composition of the reaction mixture during a chemical reaction. The monitoring of chemical reactions makes it possible to study the structures of intermediates and the variation of concentrations of reaction products with time, *i.e.*, it provides data on the reaction kinetics. 3D printing can be used to manufacture very convenient tooling for such experiments. In particular, an FDM-printed polypropylene microreactor was used to conduct a chemical reaction with simultaneous supply of the reaction mixture through a metal capillary to the inlet of a mass spectrometer for electrospray ionization (see Fig. 9).[191] The microreactor was a cylindrical chamber equipped with two inlet holes for the injection of reactants and an outlet capillary. During the manufacture of the reactor, printing was paused to insert a magnetic stirring bar and embed a capillary inside the chamber. Hence, the finished reactor was a one-piece object. Owing to the use of polypropylene, it was possible to carry out experiments with any organic solvents. Prior to the experiment, the reactor was inserted into a jig, which was also FDM-printed. The jig was equipped with threaded connections for injection of reagents, while at the bottom of the jig, there was a compact fan with

attached magnets, which rotated and thus activated the stirring bar within the microreactor, *i.e.*, it was possible to conduct the reaction with vigorous stirring. This system was successfully used for online monitoring of the Diels – Alder reaction.[191]

A larger-size FDM-printed polypropylene reactor for ESI-MS online monitoring has been described.[355] The device was equipped with three channels for the injection of reagents, which moved in the reactor along a zigzag channel, and with one outlet for the reaction mixture, which was connected to the inlet of a mass spectrometer. This system was employed to monitor a complex formation reaction.

Low-temperature plasma (LTP) ionization is a universal ionization method for mass spectrometry. This method is applicable for samples in any physical state (liquid, solid or gaseous); it does not require solvents and possesses a high potential for miniaturization; for example, an LTP mass spectrometer can be fabricated as a portable device and carried in a backpack to be used for field analyses.[356] In LTP mass spectrometry, sample ionization is accomplished by a cold plasma jet (temperature of 30 – 60 °C) generated by gas discharge in helium, nitrogen, air or another gas. Owing to mild ionization conditions, even biological samples can be used without damage. Highly functional accessory equipment was 3D-printed for compact and convenient control over the plasma stream (Fig. 18 *c*), which made it possible to analyze organic compounds. Polycarbonate parts caused the least pronounced interfering signals in the mass spectrum in comparison with PLA or ABS plastics.[338]

A 3D printer operating by a material extrusion method (FDM or DIW) can be easily adjusted not only for manufacturing parts pertaining to chemical mechanical engineering but also for arrangement of the adsorbent in chromatographic processes.[357]

An open-design FDM 3D printer was used to manufacture a system for deposition of a silica gel layer on thin layer chromatography (TLC) plates.[358] Thin layer chromatography is a facile and fast laboratory method for the separation of mixtures. The TLC version with a fixed sorbent layer attached to the substrate is most popular. While conducting TLC, one can easily vary the solvent (mobile phase) for the separation of mixtures; however, the type of sorbent is determined by the type of commercially available plate. Silica gel and modified silica gel are frequently used TLC sorbents. For silica gel deposition on a plate, the standard print head of the printer designed for extrusion of plastics was replaced by a polypropylene syringe, with the piston being activated by an additional stepper motor, *i.e.*, an FDM printer was converted to a DIW printer. A silica gel suspension in water (pulp) was loaded into the syringe and then squeezed out of the metal tip of the syringe (with a diameter of 1.2 mm) onto a glass substrate. In this way, any tracks specified by the user in the G-code, as in the usual 3D printing, could be printed with the silica gels slurry. The thickness of the silica gel layer was 0.2 mm. A 10×10 cm plate was completely covered by silica gel within $\sim$4 min. After completion of printing, plates were heated directly on the platform of the printer up to 110 °C and dried for 5 min. Using this method, it is possible to print several separate channels of the adsorbent on the same substrate, which is very convenient for comparing several mixtures or various eluents for the same mixture, *i.e.*, this enables serial chromatographic analysis.[358] In addition, this approach to fabricating TLC plates opens up prospects for using any adsorbents and any geometric shapes of the adsorption layer. The printed plates were tested with success for separation of a mixture of dyes.

Many additive manufacturing products have a layered structure, which in some cases can be used for adsorption. Such an approach to adsorbent layer formation was proposed in a study[359] where planar chromatography systems were fabricated by the PolyJet method. The channels printed on the plates contained additional ordered microchannels, which is a useful feature of PolyJet printing. The layer systems formed in this way were tested with success to separate mixtures of dyes and mixtures of proteins.

3D printing techniques are able not only to spread a ready adsorbent but also to generate a strictly ordered porous structure from a CAD model.[360] For example, the MJP method possessing a high spatial resolution was utilized to manufacture a whole chromatographic column consisting of connecting tubes, devices for distribution of a liquid flow throughout the sorbent bed and the proper sorbent bed (Fig. 18 *d*,*e*).[339] Three geometric designs of sorbent beds were formed: a monolith with straight channels; a monolith with zigzag channels; and octahedra with common vertices. Chromatographic columns designed in this way were suitable not only for analytical but also for preparative chromatography with any configuration of the porous adsorbent. These porous adsorbents may find use in filtration systems and for the design of catalytic cartridges. However, MJP printers are still expensive.

It is also worth mentioning that there are some examples of 3D printing of chromatographic columns, which were subsequently packed with conventional adsorbents, in the same way as serially produced columns, and printing of other components of liquid-phase analysis units.[361 – 364] This application of additive technologies is similar to their use to manufacture chemical reactors for analytical chemistry (see above). According to the trend towards miniaturization of analytical equipment, columns for capillary liquid chromatography suitable for compact chromatographs were produced by selective laser sintering of metal powder (316L stainless steel and a titanium/aluminium/vanadium alloy) on a desktop SLM-50 unit.[365] Owing to the capabilities of 3D printing, a column with an inner diameter of 0.9 mm was fabricated as a spiral embedded into a metal cartridge, which was conveniently placed in a chromatograph by means of standard fittings. For temperature control during the chromatographic process, the cartridge with the column can be located between the heating plates of Peltier elements.[365]

Compact columns produced by stereolithography were proposed for gas chromatographic applications.[366] As in the previous example, a 450 mm long column with a diameter of 1 mm was made as a spiral within a one-piece cartridge equipped with fittings for connection to a common chromatographic system. This column connected to the gas transport system of a chromatograph could withstand an internal pressure of up to 5 bar without any leakage at the threaded connections. It is noteworthy that when a plastic serves as a material for chromatographic columns, it is necessary to ensure that

this plastic does not give off volatile compounds upon heating during the analysis. The possibility of 3D printing of objects of any geometric shape proved to be fairly in-demand for the fabrication of separation membranes.[367] Ion exchange membranes were obtained by photopolymerization of a composition based on diurethane dimethacrylate and poly(ethylene glycol) diacrylate (PEGDA). It was shown that membranes with a surface that is not flat but has a regular pattern have a much lower ionic resilience for the same volume of the membrane.[368] The difference between membrane resistances is especially pronounced with increasing membrane thickness. Additive technologies make it possible to deliberately produce membranes with a patterned surface of any complexity.

High-performance characteristics were found for membranes made of organosilicon polymers (silicones). For the production of silicone membranes of a complex shape, 3D printing may act as an intermediate 'shape-forming' stage for the fabrication of a casting mould, which is filled by silicone. Curing of the silicone gives the finished membrane. This procedure was used to fabricate polydimethylsiloxane (PDMS) membranes of a complex shape.[369]

It is beyond doubt that personal 3D printing is a useful and accessible tool for analytical chemistry. The use of 3D printing is most efficient for manufacturing specialized accessory tools for analytical instruments to conduct unique experiments. The production of such tools by third-party manufacturers may require considerable material expenses, whereas personal 3D printing enables the production of this equipment right in the laboratory. High efficiency was also found for various AM reactors for analytical studies, and special design of chromatographic columns may considerably facilitate packing of the adsorbent and insertion of the column into a chromatograph.

4.3. Additive technologies in biochemistry and biotechnology

A specific feature of application of 3D printing in biochemistry and biotechnology is the possibility to use any materials including general-purpose plastics (PLA, ABS, PETG), since in most cases, biochemical applications imply the use of water or aqueous ethanol as the medium. In addition, DIW is more frequently used in biochemical applications since it allows operation without heating, which is important for preserving the structure and vital activity of biological objects.

The use of additive technologies in biochemistry and biotechnology can be conventionally divided into several areas: the fabrication of research reactors and accessory tools; production of ordered substrates for cultivation of animal and plant cells; and design of special analytical systems for working with biological samples, in particular, systems for detection of bacterial cells.[370–373]

For example, an efficient procedure was proposed for attaching enzymes to the inner surfaces of channels of FDM-printed nylon microreactors for biocatalytic processes.[374] Biocatalytic processes are used to produce pharmaceutical products; they possess some advantages over conventional fine organic synthesis: components of enzymatic reactions have, most often, low toxicity for humans; high selectivity of enzymes results in the formation of only the target product and a minimum amount of byproducts; biocatalysis implies the use of water or aqueous ethanol solvents and rules out participation of transition metal complexes, *i.e.*, biocatalytic processes are more environmentally benign, which corresponds to the modern green chemistry paradigm.[375] The immobilization of enzymes on solid supports makes the use of biocatalysis much more convenient than homogeneous catalysis. Catalysis by immobilized enzymes combines the benefits of homogeneous and heterogeneous catalysis: on the one hand, enzymes have high selectivity (typical of homogeneous catalysis), and on the other hand, biocatalyst immobilization on the surface results in easy separation of the catalyst from the reaction product (typical of heterogeneous catalysis).[376] Immobilization of aminotransferase (an enzyme that catalyzes the transfer of amino groups between amino and keto acids) was performed using an FDM-printed reactor, which represented a zigzag channel located inside a box with threaded connections for attaching capillaries. Polyamide 6 (poly-ε-caproamide), which serves as the reactor material, has relatively high chemical stability and mechanical strength and does not release undesirable low-molecular-weight compounds under the action of reaction mixture components. Prior to aminotransferase immobilization in the flow reactor channel, the channel surface was treated successively with hydrochloric acid and glutaraldehyde. The chemical treatment resulted in surface functionalization for better attachment of enzyme molecules. The catalytic activity of these bioreactors was tested in the continuous flow conversion of α-methylbenzylamine to acetophenone. The activity of immobilized enzymes was found to be almost the same as that of free enzymes. The continuous flow conditions proved to be more efficient than batch conditions.

An extensive application area of 3D printing is so-called bioprinting, which allows easy formation of structures of living cells and biomaterials for scientific or medical purposes.[377,378] Like traditional 3D printing, bioprinting is performed on the basis of a digital model of the future biological structure. Systematic research into bioprinting started in the first half and in the middle of the 2000s.[379] Bioprinting is considered an important component of personalized medicine, since in the future, it may enable direct digital fabrication of organs from patient cells. Unlike scaffold-based tissue engineering in which fabrication of scaffolds, immobilization of cell cultures and subsequent cell growth are separate stages, bioprinting by means of a special bioprinter furnishes the whole biological structure in one operation. However, in the case of bioprinting, the created biological tissue should undergo a 'maturing' stage, in which the physiological and mechanical properties of the tissue reach normal values. Currently, 3D-bioprinted biological structures are used for testing and searching for new drugs,[380–382] studying the toxic effects of various compounds [383,384] and modelling of the course of diseases;[385] however, the key goal of the development of bioprinting is the creation of transplantable organs from patient cells.

A promising material for 3D bioprinting is tissue spheroids, *i.e.*, spherical microparticles consisting of cells of a particular tissue and a matrix. The spherical shape improves the rheological properties of particles and makes them convenient for bioprinting. In bioprinting, as in other additive methods, a tissue construct is formed layer-by-layer in accordance with the G-code. An impor-

tant feature of tissue spheroids is the ability to coalesce as they contact each other to give a homogeneous cell tissue.[386]

A special bioreactor capable of controlling the flows of physiological fluids in tissue constructs was proposed for optimization of maturing conditions of the tissue constructs prepared by bioprinting and to study the influence of various compounds on the resulting tissues.[387] The bioreactor was manufactured by stereolithography using a photopolymer composition suitable for contact with biological tissues. The bioreactor was meant to work with tissue constructs printed from tissue spheroids. An array of thin metal needles was located at the centre of the bioreactor chamber, and tissue spheroids were threaded on the needle array during bioprinting,[388, 389] *i.e.*, the tissue was printed directly in the bioreactor chamber. After completion of printing, the tissue construct was loaded on the needles, and the subsequent operation of the bioreactor could be performed independently of the bioprinter. In particular, the bioreactor was connected to the liquid inlet/outlet system and placed into an incubator for tissue perfusion in the required liquid medium. This design of the bioreactor makes it possible to find the optimal perfusion conditions for each type of biological tissue, to ensure the best conditions for tissue maturation. The perfusion fluid can contain various biologically active compounds, which are used to study their effect on a particular living tissue; this can markedly accelerate drug development and testing.

A detailed consideration of bioprinting and bioprinter designs is beyond the scope of this review, as a substantive consideration of these issues would also imply a comprehensive analysis of the biomedical context of the application of bioprinting products.

A type of bioprinting is 3D printing using bioink containing bacterial cells. Bacterial cells are efficient producers of some valuable organic compounds, for example, polyhydroxyalkanoates (PHAs), biopolymers with relatively high physicomechanical characteristics, which may become a promising biodegradable substitute for plastics. These biopolymers are formed from renewable natural raw materials and meet all requirements for green chemistry. In Nature, PHA serves as an energy and carbon source for bacterial cells.[392, 393] A specific feature of potential future application of 3D printing with bacterial bioink is that a substance should be produced in a preliminarily formed geometry: first, an object would be printed from a bacterial precursor and then it would be converted to the product as a result of cell activity. This eliminates the stage of isolation and purification of the biomaterial and, in some cases, may be economically appropriate. The vital activity of bacterial cells should not be disrupted during 3D printing. For optimization of bioprinting conditions with bacterial ink, a 3D printer obtained by modification of an inexpensive desktop FDM printer was proposed.[394] In this design, liquid bioink containing sodium alginate and an *E.coli* culture is fed with a syringe pump through a tube to the printer head (represented by a pipette tip). Printing takes place at room temperature. Calcium chloride is applied on the build platform of the printer and initiates cross-linking of alginate molecules to give a relatively rigid structure as an aerogel, which is sufficiently strong for supporting the product being printed for a long period of time. Using this simple device, it was shown that after completion of printing, the bacterial cells retained viability and metabolic functions for two days. This time is quite sufficient for the cells to produce useful products.[394] In addition, the possibility of printing structures composed of layers that contain different bacterial cells was demonstrated, with clear spatial separation of the cells being retained 24 h after printing. The alginate gel can be dissolved without damage to the useful material produced by the bacteria. Bioprinting systems of this type can be used not only to produce the final product, but also to automate optimization of the cultivation of bacterial cultures: the bioink composition, printing support and thickness and shape of the printed gel can be quickly changed without noticeable technical complications.

Classical 3D printing methods are also employed in cell technologies. For example, a microinjector produced by DLP stereolithography (Fig. 19 *a*) makes it possible to mix living cells with auxiliary components and form equally sized spherical particles with similar highly organized structures from this composition.[390] Existing methods give cell spheroids of different sizes. For example, traditional procedures of cell cultivation in a Petri dish result in a planar arrangement of cells, which does not always correctly reproduce the physiological properties of a three-dimensional living tissue. The proposed microinjector design furnishes spheroids of equal size with the possibility of mass production. A microinjector is a monolithic object requiring no assembly or posttreatment after printing. The diameter of the channel in which spheroids are injected is 0.2 mm. This spheroid size provides cell viability, as it corresponds to the distance of oxygen diffusion in living tissues. The components of future spheroids are fed into the microinjector *via* coaxial channels by syringe pumps. A cell suspension in the extracellular matrix is supplied to the inner channel, while a solution of sodium alginate is supplied to the outer channel. The jet coming out of the injector after coextrusion has a cell suspension at the centre and alginate as the outer layer. The jet splits into separate spherical drops, which retain a core – shell structure. This microinjector was used to obtain spheroids containing human neuronal stem cells, which gradually converted to neurons inside the microspheres. This gave a three-dimensional neural microtissue inside the capsule, with the outer alginate layer serving as the protective shell. These spheroids can be used for studying the neuro-

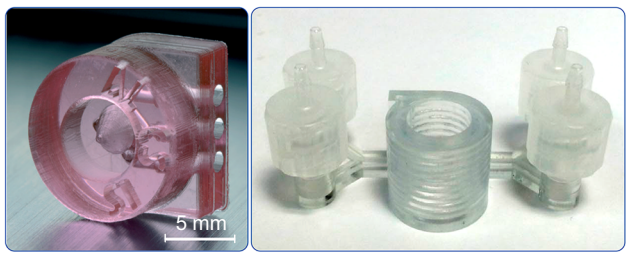


Figure 19. Examples of 3D-printed laboratory equipment and materials for biochemical and biotechnological applications: (*a*) microfluidic mixer for the production of hydrogel microcapsules for cultivation of human neuronal stem cells;[390] (*b*) microfluidic system for detection of pathogenic bacteria.[391]

toxicity of various compounds and as a base for the formation of more complex three-dimensional tissue structures for regenerative medicine.[390] The proposed technique is simple and can be implemented in any laboratory. The microinjector efficiency is due, first of all, to the high spatial resolution of stereolithography, which allows fast fabrication of microchannel structures of this type.

Semicontinuous and continuous cultivation are widely used in biotechnology to grow cells (both bacterial cultures and animal tissue cells). These approaches imply the addition of fresh culture medium during cell growth and removal of an equal volume of liquid from the reactor. The removal of some of the medium from the reactor decreases the concentration of cell activity products and thus increases the life cycle of cells. The withdrawal of cells from the reactor during removal of the medium can be prevented using various filtration systems at the bioreactor outlet. SLA-printed flask lids were proposed for bacterial cultivation with continuous stirring for homogenization of the biological medium.[395] The lid design included two connections, one for injection of the liquid components of the culture medium using a syringe pump and the other for removal of the medium to maintain a constant volume in the reactor and for sampling. This design makes it possible to implement the biotechnological process in a usual flask with stirring on a rotary shaker and provides continuous injection of components into the bioreactor and removal of the liquid medium without interruption of stirring, which increases the process performance and relevance for modelling industrial processes of similar types. The cytotoxicity of the material used to manufacture the lid was studied[395] for both mammalian cells and bacterial cells; it was found that no toxic compounds were washed out of the SLA components during the biotechnological process.

An interesting strategy of application of 3D-printed bioreactors in regenerative medicine is cultivation of living tissues *in vivo*, *i.e.*, the bioreactors are implanted directly into patient's body. This approach was demonstrated in relation to reconstruction of a severely damaged sheep mandibular bone.[396] First, a 3D model of bone damage was constructed using the results of computed tomography or magnetic resonance imaging. FDM printing from poly(methyl methacrylate) based on the model furnished a bioreactor with the inner cavity geometry exactly corresponding to the geometry of the lost part of the bone. The open part of the reactor was filled with a porous material that ensured the growth and support of bone tissue cells. Then, the reactor was implanted against the periosteum of the rib cage of the patient (sheep) in such a way that the open face of the reactor adjoined the periosteum. The periosteum is an external layer covering the bone, in which active formation of bone tissue can take place. After several weeks, the reactor cavity was filled with the bone tissue with required geometry. The reactor was dismounted and the resulting part of the bone was implanted into the site of the mandibular defect.[396] This approach simultaneously solves two problems: fabrication of a graft from the patient's own tissue (autologous graft), which leads to its integration into the surrounding tissues without complications, and formation of a graft of the desired geometry personalized for a particular patient.

One of the most vigorously developing applications of 3D printing in regenerative medicine is the fabrication of scaffolds both for transplantation and for biochemical research.[397] The procedure of formation of a scaffold-based transplant includes several stages: first, a 3D model of the future transplant is constructed using MRI data, then 3D printing of this model is performed by one or another additive manufacturing technique using a material depending on the particular transplanted tissue; this gives a scaffold. In the next stage, the scaffold is filled by cells taken from the patient; the resulting piece is subjected to maturing to give a tissue construct suitable for transplantation. As in the case of bioprinting with tissue spheroids, a scaffold-based tissue construct consists of the patient's living cells, which facilitates transplant integration, minimizes the probability of rejection and, as a consequence, eliminates the need to take unsafe immunosuppressive drugs.[398] The scaffold geometry and chemical composition should be favourable for multiplication of tissue cells, migration to provide cell–cell interactions, and cell differentiation to a particular biological tissue (since the scaffolds are seeded with stem cells). The key element of the geometrical design is the scaffold porosity and the possibility of contacts between the pores. The character of scaffold porosity is highly important for successful cell cultivation.[399] For example, a procedure for obtaining a controlled pore volume was developed for FDM-printed scaffolds.[400] The high porosity of scaffolds provides efficient transport of nutrients and signalling molecules between cells and enables growth of the vessel network (vascularization), which is a necessary condition for successful tissue implantation.[401] The vascularization and innervation of scaffold-based tissue constructs is a key problem in this type of tissue engineering.[402] There are procedures used to enhance the porosity of the tissue scaffold, such as etching and foaming. However, such procedures give a random distribution of pores and provide no control over the pore size. 3D printing gives way to generate pores of a necessary size located at optimal distances. With the assumption that a blood vessel would pass through each pore, the distance between the pores should not exceed the maximum distance of oxygen diffusion in the transplanted tissue to avoid the appearance of necrotic areas.[403] Excessively small pores hamper the growth of the vessel network, while too large pores induce the growth of tissue along the pore walls and do not promote the formation of a three-dimensional structure of the tissue. As a rule, effective vascularization of the tissue construct requires that the scaffold pores be of 100–250 μm size. The scaffold material should be biocompatible (*i.e.*, possess no toxicity and cause no adverse clinical response in the body) and bioresorbable (*i.e.*, be able to degrade in the body without the formation of toxic products). The rate of scaffold biodegradation in the body also depends on the porosity and should be equal to the growth rate of the implant tissue. Scaffolds can be made of both natural polymers (collagen, silk, keratin, actin, fibrinogen, cellulose) and synthetic polymers (polyesters, polylactones, *etc.*).[404] Poly(lactic-co-glycolic acid) (PLGA) is a popular material for 3D printing of soft tissue scaffolds using extrusion methods.[405] Bone tissue scaffolds are produced using both biodegradable polymers supplemented by components inherent in bone tissue and nonbiodegradable materials.[406]

Organized substrates for cell culturing can be used not only as tissue engineering scaffolds but also to solve other problems of biotechnology. A highly productive source of biomass, in particular for the production of biofuel, plant protein and other valuable biological products, is benthic algae. Benthic algae are adapted for life in the immobilized (immobile) state as biofilms on various surfaces on the bottom of running water bodies. These organisms are distinguished by fast growth, unpretentiousness and relative ease of biomass harvesting. In addition, immobilized algae can be used to purify water reservoirs from toxic pollutants, both organic compounds and metal compounds. To induce biofilm formation, algae spores are attached to a substrate, and the outcome of this stage under continuous water flow conditions depends on the substrate surface roughness. The substrate surface microrelief also affects the type of near-surface water flow (laminar or turbulent), which in turn influences the ability of algae to take up nutrients from the environment and, ultimately, affects the intensity of biomass growth. 3D printing is a versatile tool for the fabrication of substrates of any topology and with controlled surface roughness; this offers broad opportunities for optimizing the cultivation conditions of benthic algae. It was shown[407] that the surfaces of solid substrates obtained by the PolyJet method from a photocurable composition are actively populated by algae (mainly filamentous *Spirogyra communis*) and produce more developed biofilms than the surfaces of ceramic substrates used for comparison. Artificial substrates were tested both in a laboratory bioreactor with running water and in a natural water body. Smooth surfaces of the substrates correspond to the least active production of biofilms, whereas the introduction of deliberately specified surface roughness during 3D modelling results in a pronounced growth of the algae biomass. High efficiency was found for substrates with a developed surface, for example, in the form of a gyroid. In this case, all parts of the substrate were populated with algal cells, including the external surfaces and internal channels, *i.e.*, the substrate material can be compactly arranged without the loss of cultivation productivity. Substrates of a complex topology can be used to simultaneously cultivate photophilic (on the outer surface) and sciophilic (inside channels and cavities) organisms. Additionally, a specially designed geometry may provide different intensities of water flow inside the substrate channels ranging from the normal current velocity to completely stagnant areas, which can also be a tool for substrate optimization towards cultivation of various types of algae.[407]

It should be noted that for generation of a rough surface by photopolymerization methods (SLA, PolyJet, MultiJet printing), it is necessary to specify the roughness optimal for attachment of algae spores (500 – 1000 μm) in the 3D model, since these methods produce rather smooth surfaces. In this case, the FDM method may prove to be more effective, since by using this method, it is easy to produce a rough surface and to vary the degree of roughness during preparation of the model for printing (either by specifying different heights of printing layers or by adjusting the infill pattern, which is a network structure). Among the whole diversity of materials suitable for FDM printing, it is possible to find materials with sufficient biological stability able to retain service properties over numerous cultivation – biomass harvesting cycles, such as polypropylene or ABS plastics.

In addition to 'traditional' scaffolds, nanostructured substrates for cell cultivation are also being studied. In particular, a material was proposed consisting of 2.3 μm polystyrene particles surface-functionalized with short DNA chains (oligonucleotides).[408] As the DNA chains are linked according to their complementarity, the polymer microspheres are attached to one another, also not in a random way. Functionalization of microspheres by various nucleotides gives rise to the possibility of controlling the microstructure of the material formed upon multiple binding of the microspheres to one another. The gel-like material thus formed is a promising substrate for cell cultivation. The microspheres can be functionalized to enable controlled release of growth factors, morphogens and other cell development regulators. 3D printing can be used to impart an optimal geometric shape for cultivation of the material. During printing, the material is injected into the printer head with a syringe pump *via* a system of tubes, and the printed structure is formed upon extrusion. Analogous materials were obtained from hydrogel particles and tested for cultivation of mammalian cells. The inclusion of cells into the gel was accomplished by coextrusion during 3D printing. It was shown[408] that, if the substrate is a gel composed of particles linked by oligonucleotides, cells cultured in this matrix form three-dimensional spherical colonies and exhibit higher activity than the cells cultured on a clean polystyrene surface; moreover, no cell colonies are formed in the latter case.

One more application area of 3D printing in biochemistry and biotechnology is fabrication of analytical devices for detection of biological objects. An example of the utility of the high resolution of stereolithography in the analytical microbiology is a proposed microchannel system for the detection of pathogenic bacteria in food products (Fig. 19 *b*).[391] The general procedure for the detection of pathogenic bacteria in foodstuffs is cultivation of bacteria present in the test samples followed by detection of cells by some method. However, cultivation-based methods are too slow for today's turnover in the food industry; therefore, faster microbiological control methods, without the cultivation stage, are actively developed. A promising method of fast microbiological investigation is based on the binding of magnetic nanoparticles to bacterial cells and the subsequent separation of the resulting complexes by inertial focusing. To enable the bacterial cells to bind to magnetic particles (Fe_3O_4), molecules of antibodies are grafted to the magnetic particle surface. The nanoparticles are approximately ten times smaller than the bacterial cells. The bacterial complexes with magnetic particles and free magnetic particles are separated from the food product sample by application of an external magnetic field.

This mixture is then separated by inertial focusing, which is a method to separate particles according to their mass. The essence of this method is as follows: when a liquid moves in a gently curved channel, two oppositely directed vortices of the liquid (Dean vortices) are generated in the direction normal to the major flow, and the intensity of vortices is dependent on the radius of curvature of the channel.[409] A microchannel separation device as a spiral channel with a constant radius of curvature and a trapezoidal cross-section was manufac-

tured by laser stereolithography.[391] The invariable radius of curvature of the channel ensures the constant intensity of Dean vortices (as opposed to spiral channels, the coils of which are located in one plane and have different radii), while the trapezoidal cross-section promotes more efficient separation of particles by mass due to vortex motion: heavier particles of bacterial cell complexes with magnetic nanoparticles are concentrated near the inside wall of the channel (closer to the centre), whereas free magnetic particles are concentrated at the outside wall. At the outlet of the spiral channel, the liquid flow containing particle-bound bacteria and the flow carrying only free particles are separated. The fabrication of a leak-proof microchannel (the trapezoid height is 1 mm) representing a three-dimensional spiral with an intricate cross-section by traditional manufacturing techniques is a complicated, labour-consuming, multistage procedure, whereas 3D printing makes it possible to fabricate such devices over a short period of time without mechanical processing or assembly. The efficiency of this microchannel device was demonstrated by separation of *E. coli* cells from milk with subsequent detection of the cells by UV spectroscopy. The sensitivity of such microbiological assay is $\sim$100 CFU per mL.[391] The method demonstrated high selectivity, *i.e.*, the possibility of determining the content of a particular species of microorganisms, to pathogenic bacteria — a Salmonella species (*Salmonella typhimurium*) and a Staphilococcus species (*Staphylococcus aureus*).

Owing to high resolution, stereolithography methods can be used to fabricate equipment for studying living cells at the microscale. An analytical microchamber (inner size of $20 \times 20 \times 20$ μm; sidewall thickness of 8 μm; roof thickness of 3 μm) was manufactured by multiphoton lithography. Only several cells can be encapsulated into the chamber, which allows studying cell metabolism processes by scanning electrochemical microscopy (SECM).[410] SECM is a probe method; the probe was represented by an ultramicroelectrode, which moved above the test surface and detected redox active compounds. This method is nondestructive and is suitable for working with living biological cells at the microscale without disrupting their vital functions. It should be noted that the possibility of fabrication of microcontainers capable of trapping single bacterial cells by multiphoton lithography was demonstrated back in 2007.[411,412] The need to manufacture these analytical cells is due to the high rate of bacterial growth, which makes conditions of electrochemical measurements poorly controllable; therefore, a container is needed for spatial isolation of cells. The container can trap several cells for studying the mechanisms of cell – cell interactions. The walls of the microcontainer were made of a protein capable of forming a cross-linked structure under the action of light. Owing to the chosen material, the container walls contained pores and were permeable for small molecules — products of bacterial cell metabolism, which enabled the detection of these compounds using an ultramicroelectrode in the close vicinity of container walls.[410] Even with these microdimensions, the permeability of the container walls can be changed by controlling the printing parameters that determine the degree of cross-linking of the protein materials and, hence, the material porosity.

4.4. Additive technologies in pharmaceutics

One more area in which 3D printing is used for organization of matter rather than for the fabrication of functional products is pharmaceutics.

Today, active studies are in progress on the use of 3D printing for the preparation of new dosage forms and drug delivery systems that provide more controlled drug release in the human body than the traditional dosage forms.[413,414] In other words, the challenge is to literally print an effective tablet using the unlimited capabilities of additive technologies in the creation of diverse items from any material. The dosage form affects the kinetics of release of the active ingredient. Drug release can be prolonged, *i.e.*, the drug is released gradually and slowly, at a constant rate; delayed, *i.e.*, drug release does not occur immediately after drug administration, but starts after some time period; and pulsed, *i.e.*, the drug is released in several pulses separated in time.[415] A comparison of dosage forms of the same size manufactured by different methods — powder pressing, injection moulding and the additive FDM method — showed that the pressed tablets tend to rapidly release the drug, since they are rapidly disintegrated in aqueous medium; in the case of moulded tablets, prolonged release is most typical, since the moulded tablets have the highest material density and no microporosity; and FDM-printed tablets exhibit an intermediate drug release rate, since, on the one hand, they are microporous due to the layered structure and, on the other hand, they disintegrate at a lower rate than the pressed tablets.[416] The dissolution rate of FDM tablets can be controlled over a broad range depending on the printing settings: an increase in the porosity promotes more intense release, whereas printing of monolithic forms retards the process. Thus, 3D printing is a tool for a highly flexible personalization of dosage form dynamics.

The first studies dealing with the capabilities of 3D printing in the production of drug delivery systems appeared in the mid-1990s.[417] In 2015, the US Food and Drug Administration (FDA) approved the first drug (in particular, levetiracetam, an antiepileptic drug for oral administration), the tablets of which were manufactured by 3D printing using binder jetting method. Due to the absence of pressing, 3D printing afforded a highly porous dosage form, which was completely dispersed upon contact with water within 4 s; this was several times faster than the dispersion of tablets obtained by conventional methods. This FDA decision gave an impetus for the implementation of additive technologies in pharmaceutics.[418]

The benefits of 3D printing for the production of drug delivery systems are, first of all, the possibility of obtaining complex structures, production only on request, and personalization of the dosage form taking into account the treatment regimen of a particular patient.[419]

The absence of restrictions on the geometric complexity of printed products allows any arrangement of drugs and excipients. A tablet can contain several drugs distributed as ordered zones, can have a shell structure and can have any shape. The main goal of definite arrangement of the substance in a dosage form is to attain a controlled drug release in the body.

At present, FDM 3D printing is used most frequently; therefore, studies on the design of new dosage forms by

exactly this method are actively carried out. The FDM printing of dosage forms consists of two key stages: loading of the active ingredient into the printing material and the proper printing of the dosage form. Thus, materials for pharmaceutical FDM 3D printing are combinations of polymer matrix and a biologically active substance [if the pharmaceutical is a part of the composition, it is often called an active pharmaceutical ingredient (API)].

The polymer matrix being filled with the active ingredient for FDM printing should have a melting temperature not exceeding the decomposition points of the loaded pharmaceutical agents. Obvious requirements are polymer solubility in the body, lack of toxicity and hypoallergenic properties. The introduction of small amounts of the active ingredient may have no pronounced effect on the applicability of the filled polymer material for FDM printing; however, in the case of a large amount of a drug, the mechanical properties of the material are markedly deteriorated, and additional fillers should be added as plasticizers to retain the possibility of 3D printing.[428] Most often, poly(vinyl alcohol),[420] hydroxypropyl cellulose,[421] hydroxypropyl methylcellulose,[422] polycaprolactone[423] and some other polymers are used as matrices for this purpose.[424, 425]

One of the methods for introducing the agent into the FDM material is loading from a solution. For example, keeping PVA in a saturated ethanol solution of prednisolone for 24 h at a temperature of 30 °C followed by drying affords a material containing ~2 mass % active ingredient.[426] A similar approach to 4- and 5-aminosalicylic acids and PVA provides a <1 mass % content of the active substance in the material.[427] A benefit of this method is that prepared filaments are used for FDM printing, *i.e.*, there is no need to subsequently extrude the material; however, obtaining a high content of the active ingredient loaded from solution is problematic.

However, another versatile method for insertion of an active ingredient into a thermoplastic material is hot-melt extrusion (HME), which is widely used in the pharmaceutical industry and for polymer processing; in particular, it is employed to obtain the thermoplastic filament for FDM printing.[429, 430] In this case, the polymer is fed into the hopper of the extrusion system as granules or powder, and the drug is added. The mixture is transported from the hopper to the screw extruder barrel. In the barrel, the material melts and is mixed and homogenized. The twin screw extruders, in which the mixture is squeezed into the gap between the two rotating screws, are most efficient. Under the action of high pressure and friction and an additional heat supply (if necessary), the mixture melts and is efficiently homogenized. Thus, hot-melt extrusion ensures a homogeneous distribution of the drug in the polymer matrix bulk. Unlike loading from solution, in the case of HME, no solvents are used, which rules out contamination of the finished product with toxic compounds; hence, extrusion can be classified as a green processing technology. Drug loding into a polymer matrix increases the solubility and bioavailability of poorly soluble drugs, since the polymer matrix keeps the drug molecules in the discrete state attained during extrusion and prevents them from agglomerating and crystallizating.[431] Melt extrusion can be combined with FDM 3D printing in a combined production system; furthermore, such a system can be compactly mounted on a single laboratory bench, since there is a wide choice of both desktop melt extrusion units and desktop FDM printers.[432] Melt extrusion may give high drug loadings of materials. For example, FDM printing filaments containing up to 50% paracetamol were obtained on the basis of hydroxypropyl methylcellulose (water-soluble amorphous polymer).[433] The following drawbacks can be noted for HME: during melting, API decomposition or recrystallization may take place. To eliminate these events, plasticizers are added to the material, reducing the melting temperature of the mixture and hence shortening the residence time of the material in the extruder barrel.[434]

Examples of complex dosage forms produced by FDM printing are the layered and core – shell forms (Fig. 20); in some cases, 3D printed tablets are called printlets.[428] The drugs used in this example were paracetamol and caffeine (which are employed together in antipyretic and analgesic medications), while water-soluble and biodegradable poly(vinyl alcohol) served as the polymer matrix. The FDM filament was prepared by mixing milled PVA with the powdered drugs, and then a filament with a diameter of 1.75 mm containing 5 mass % and 10 mass % drugs was formed using a desktop extrusion system. The 3D design of dosage forms is performed in the same way as the design of other items for 3D printing using any computer-aided design system. Paracetamol and caffeine were successfully combined in one dosage form owing to the use of a general-purpose desktop 3D printer with two extruders, which allowed simultaneous printing of two materials (no special bioprinter was required to solve this task; printing was carried out at 200 °C, and the layer height was 0.2 mm). The dissolution of the layered structure with parallel layers (Fig. 20 *a*) under conditions mimicking a biological medium shows equal release rates for different drugs. The core – shell type capsules (Fig. 20 *b*) are designed for delayed release of the drug from the core and immediate release of the drug from the shell. The dissolution of the core starts after the dissolution of the shell; therefore, the

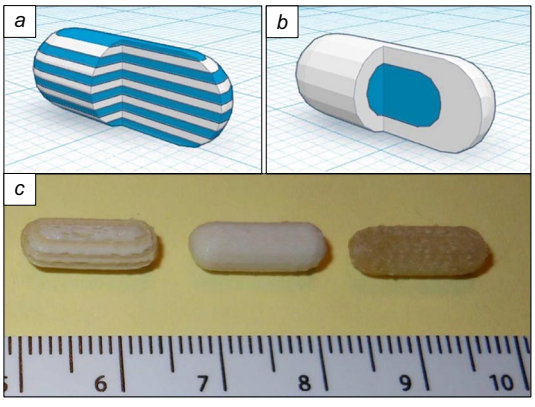


Figure 20. Examples of 3D-printed dosage forms.[428] (*a*, *b*) Models of dosage forms containing two different drugs in the layers shown in different colours; (*c*) finished dosage forms: the capsule on the left contains alternating PVA + paracetamol and PVA + caffeine layers; the capsule in the middle contains PVA + caffeine in the outer shell and PVA + paracetamol in the central core; and the far right capsule has PVA + paracetamol in the outer shell and PVA + caffeine in the core.

thickness of the shell may serve as a tool for controlling the delay time before core dissolution. However, the solubility of the drug-loaded material depends not only on the solubility of the polymer matrix, although it is the major component, but also on the interaction between the matrix and the drug. In particular, if caffeine is loaded in the outer layer of the capsule, paracetamol starts to be released after 50 min, whereas paracetamol in the shell results in a 130 min delay before caffeine release from the core, *i.e.*, the addition of paracetamol decreases the solubility of the material. The core–shell architecture of the capsule is an example of a dosage form combining delayed release for the drug located in the core and the simultaneous delivery of several drugs.[428]

The pulsed release of API is implemented in the dosage forms of a layered structure in which the layers containing API (10% diltiazem, a drug for the treatment of cardiovascular diseases) alternate with layers of API-free polymer matrix (HPMC).[435] Drug release from the outer layer starts immediately after drug administration into the body; the dissolution of the outer layer exposes the layer of neat polymer, and the release is interrupted; after the dissolution of the neat polymer, the release is resumed. The number of layers, *i.e.*, API release periods, can be easily changed by adding more layers; the delay time between the release periods can be adjusted by varying the thickness of the neat polymer layers. As in the above example, the diltiazem dissolution rate in the body can be varied by changing the infill density: 100% infill density results in the slowest drug release to the external medium.[435]

The delayed drug release does not necessarily require a dosage form fabricated from an API-loaded plastic; in some cases, it is sufficient to fabricate only the shell, which would prevent immediate dissolution of the drug in the body. For example, it was shown that delayed release can be achieved by using PVA capsules filled with powdered or liquid API, which was placed inside the capsule during FDM printing. Depending on the thickness of the shell, drug release took place in different parts of the gastrointestinal tract.[436]

In addition to monolithic dosage forms, assembled structures consisting of several parts in which API is also loaded as a powder were proposed for oral drug administration. As in the previous example, in these systems, the material of the capsule does not contain API, and controlled drug release is attained only due to the design of the capsule. For example, dismountable H-shaped capsules for the delivery of two drugs were proposed.[437] A capsule consists of a cylindrical chamber separated into two compartments by a partition. The compartments are covered by caps. Owing to the different wall thicknesses of the caps, this design can ensure pulsed release of drugs: the thinner outer wall is the first to dissolve, and then the thicker wall is dissolved. The caps can be made of materials characterized by different solubilities, *e.g.*, one cap is made of the PVA–poly(ethylene glycol) copolymer, and the other cap is made of HPMC, which also provides time-separated release of two drugs. Synchronous release is possible when the material and thickness of the caps are identical.[437]

A similar design with an H-shaped central chamber made of polylactic acid was proposed for the delivery of the anti-tuberculosis drugs isoniazid and rifampicin as a part of combined therapy for tuberculosis.[438] In this design, one compartment is fully open; therefore, the first drug starts to be released immediately, whereas the second compartment is closed by a PVA cap; the time of cap dissolution constitutes the delay before the release of the second drug.

Another design consisting of two concentric cylindrical compartments closed by one common cap was proposed, implementing an analogous pulsed mechanism of drug release. When the capsule enters the body, the external wall dissolves first, and the drug of the outer compartment is released. Then, the inner compartment (core) of the capsule is dissolved.[439]

The delayed drug release can be controlled by a set of factors: type of matrix, shell thickness and matrix and drug composite solubilities. It is noteworthy that the effect of additives on drug composite solubility is intricate and depends on numerous parameters: intermolecular forces in the polymer matrix and between the drug molecules and the polymer matrix, the degree of dispersion of the drug and the amount of the drug in the material.

Modified-release dosage forms were obtained by FDM printing. The modified release implies that the rate of API release from the dosage form into the body has changed in comparison with that for the standard dosage form. For example, a mixture of PVA with Budesonide (an anti-allergic and anti-inflammatory drug used for the therapy of asthma and inflammatory diseases of parts of the digestive system) was prepared by HME and then used to fabricate monolithic capsules for oral administration. The capsules were coated by a polymer that is used for coating solid dosage forms widely present in the market. The commercial drugs Entocort and Cortiment with the same active ingredient were used for comparison. Using *in vitro* measurements, it was found that the release of Budesonide from the Entocort capsule is fast, whereas the release from the Cortiment capsule is very slow. Drug release from the FDM-printed capsule was found to proceed at an intermediate rate suitable for the therapy of intestinal inflammatory diseases.[440]

It should be noted that the dynamics of API release from FDM-printed dosage forms also depend on the porosity of products obtained by the given 3D printing technology. For example, for modified-drug release dosage forms containing the antimicrobial drug nitrofurantoin, a polymer matrix comprising a polylactic acid and HPMC mixture was proposed. This matrix allows up to 40% content of the drug with retention of the possibility of FDM printing. As the nitrofurantoin content increases, the microporosity of the dosage forms manufactured as flattened cylindrical tablets increases.[441] The FDM technique allows for some degree of control of the porosity of the resulting products using parameters such as the extrusion width, volumetric feed rate (feed factor) and layer height, while the macroporosity can be controlled by varying the infill density of the products. Therefore, varying the porosity of dosage forms during 3D printing can be considered an additional tool for controlling the drug release rate.[442]

A set of dosage forms shaped like flattened cylinders with different thicknesses (0.0, 0.4 and 1.6 mm) of the shell containing no API and different infill densities (20%, 80% and 100%) were proposed to illustrate the effect of porosity on the API release dynamics.[443] In this

case, the matrix was made of HPMC, and paracetamol served as the drug. Tablets with 100% infill density were monolithic structures, whereas intermediate infill densities give rise to a porous network structure: the lower the porosity, the greater the fraction of voids in the inner space of the product. The tablets with high porosity (20% infill density) exhibit fast drug release, so that more than 90% of paracetamol was in the free state after 2 h. Meanwhile, in the case of monolithic tablets, only ~40% of the active ingredient passed to the external medium (data for a tablet without a shell). The variation in the shell thickness also had a considerable effect on the drug release rate: as the shell thickness increased, the rate of release substantially decreased.[443]

For compositions consisting of an ethylcellulose and HPMC blend (3 : 1) with Ibuprofen as the API, it was shown that the optimal drug content is 20%, as this provides the fastest drug release (within 24 h), with the quality of 3D printing being slightly deteriorated.[444] In this case, water-soluble HPMC was added to the mixture as a modifier of API release. The variation in the amount of the modifier is a way to control the rate of release. The addition of HPMC or sodium alginate led to the highest rate of API release in comparison with the addition of other modifiers, such as PVA or xanthane gum. The increase in the infill density of the dosage form facilitates an increase in the released dose of the drug as long as water from the external medium is free to penetrate into the porous internal scaffold structure, but as the infill density approaches 100%, the drug release sharply slows down.

In some cases, immediate release of a drug rather than delayed or prolonged release is required. A block design was proposed for FDM-printed capsules to accelerate drug release.[445] In this design, the cylindrical capsule was composed of blocks (0.5 – 1.5 mm wide) separated by gaps and connected by thin bridges that kept the blocks together. When this capsule entered water, thin bridges rapidly dissolved, and the capsule was split into blocks, which also rapidly dissolved because of their small size. The highest rate of API release (theophylline used to treat respiratory tract diseases) was attained when the space between the blocks was no less than 1 mm.

Thus, 3D printing makes it possible to fabricate objects with a specified porosity to control the rate of drug release. This is difficult to attain using conventional methods for the production of dosage forms.

One type of dosage form that may benefit from the use of 3D printing is invasive implants that are used for the chemotherapy of tumours. Antitumour drugs are often aggressive compounds that have adverse effects on the whole body. One of the therapeutic approaches for decreasing adverse effects is the topical use of drugs. For this purpose, a drug is placed into a capsule and implanted into the injured tissue in which the active ingredient is gradually released and locally destroys the tumour cells. A challenge in the use of invasive implants is to control drug release to achieve a stable antitumour effect. For this goal, PLA implants fabricated by FDM printing were proposed; they represented small (10 mm high) capsules with an internal cavity and with predesigned square pores in the sidewall.[446] The pores are meant to increase the contact area between the implant and the environment. To change the API release rate, the implants can be coated by a PLA film from a solution of the polymer in dichloromethane. The dynamics of API release from these implants was tested in relation to Cytoxan, an antitumour drug with a broad spectrum of action. Drug loading was performed by immersing the implant into a solution of Cytoxan in acetone followed by drying. The drug release *in vitro* from the implants without film coating took 4 h, whereas film coating resulted in release times ranging from 4 days to 30 days, depending on the film thickness.[446] Thus, porous FDM-printed implants are quite suitable for the controlled release of pharmaceutical drugs over a broad range of rates.

Pharmaceutical drugs can also be incorporated into photopolymer compositions for the subsequent printing of dosage forms by photopolymerization. However, the number of relevant publications is still much smaller than the number of publications describing FDM printing. In particular, the addition of paracetamol (5.7%) and 4-aminosalicylic acid (5.4%) into a composition consisting of PEGDA and diphenyl(2,4,6-trimethylbenzoyl)-phosphine oxide as the photoinitiator did not hamper photopolymerization, which resulted in the preparation of solid dosage forms for oral administration.[447] It was shown that both APIs are released under conditions mimicking the medium of the gastrointestinal tract. The photopolymerization of PEGDA affords a network polymer structure; therefore, the control of API release can be attained by adding compounds that decrease the cross-linking density in the polymer. For example, the introduction of poly(ethylene glycol) (PEG 300), unable to form cross-links due to the absence of acrylate groups, considerably accelerates the release of API from the finished dosage form; the higher the fraction of PEG and the lower the fraction of PEGDA, the higher the release rate.[447] The successful release of model APIs (paracetamol and aspirin) from the SLA-printed dosage forms was demonstrated for a composition containing a mixture of PEGDA and poly(caprolactone)triol monomers.[448] Poly(caprolactone)triol devoid of photopolymerizable groups was added for the same purpose as PEG, namely, to decrease the cross-linking density in the resulting 3D polymer network and, hence, to increase the rate of API release.

A benefit of photopolymerization is the ease of adding any API into the polymer since the initial composition is liquid, *i.e.*, no additional preparation stage for the API-loaded material (which is needed in the FDM method) is required in this case. Additionally, photopolymerization methods do not require considerable heating during printing, which rules out thermal decomposition of drugs unstable on heating.

The fabrication of dosage forms by additive methods may provide a high degree of personalization of pharmaceutics. Here, personalization consists of controlled drug release, which means higher bioavailability and optimized dosage. This benefit is largely a direct consequence of the infinite possibilities of 3D printing in the manufacturing of items of complex shape using several materials. Personalization is most relevant in the case of selection of individual dosages of drugs. For example, a two-layer dosage form, with one layer containing the antidiabetic drug Metformin and the other layer containing the antidiabetic drug Glimepiride, was proposed for the combined therapy of type 2 diabetes mellitus.[449] The use

of two drugs for the treatment of type 2 diabetes mellitus has a number of advantages over monotherapy: the combined effect improves the control of the patient's blood glucose level and allows one to reduce the dose of each drug, thus Mitigating the adverse effects; moreover, Glimepiride improves the therapeutic effect of metformin. The dosage of antidiabetic drugs is adjusted individually and depends on the blood glucose level, patient age and other factors. In this case, fast 3D printing of dosage forms with the required combination of drugs, taking into account personal doses, may be in high demand.

One more example of the necessity of personalized dosing of API is thrombus formation, which is treated and prevented by pharmaceuticals that suppress blood clotting, which are called blood thinners. The doses of blood thinners should be adjusted personally for each patient, since too high doses may cause haemorrhage. The dose is selected on the basis of the patient's complete blood count, considering the possible interactions with other drugs. For Warfarin, a frequently used blood thinner, FDM-printed dosage forms were proposed for safer and more controllable dosage regimens.[450]

A convenient tool for personal dosing of API is the coextrusion of a material containing API and a material free from the drug.[451] Coextrusion is fundamentally different from multimaterial 3D printing using FDM printers with two (or more) extruders. In the printing with several extruders, a separate heating element and a separate nozzle are present for each material, *i.e.*, there is clear boundary between the materials in the printed product. In the case of coextrusion, both materials are fed to the same nozzle, but the degree of their mixing is relatively low. In this case, the pure polymer acts as the diluent for the drug-loaded polymer. With this approach, it is possible to avoid the manufacture of FDM filaments for each drug concentration, but to prepare some amount of filaments with a definite concentration in advance. The change in the API content for personal use is performed during additive manufacturing of the dosage forms.

One more important advantage of the 3D printing of dosage forms is promptness, *i.e.*, the possibility of printing 'on demand'. Since dosage forms are small items, despite the relatively low speed of most additive manufacturing techniques, printing of a batch of tablets or capsules would not take long time. However, the preparation of drug-loaded material, if the process implies the use of a mixture of the matrix and API, should also be included in the duration of the production. Even in the case of FDM, which is the slowest 3D printing technology, printing 'on demand' is possible by combining the production of the drug-loaded FDM filament and the 3D printing of dosage forms in one manufacturing cycle in a small space.

In view of the above-noted features of 3D printing of dosage forms, this method can apparently be considered a component of personalized medicine, but not a method for mass production of therapeutic agents.[452–454]

Currently, the 3D printing of drugs is still at the stage of active scientific research and development. Presumably, pharmaceutical 3D printing would enter people's lives and would enable the preparation of a set of tablets containing a combination of drugs prescribed by physicians in personally adjusted doses.

4.5. Additive technologies in chemical education

3D printing has found extensive use in educational activity, and 3D printers are encountered not only in universities but also in schools, centres for professional advancement and libraries (modern libraries have a special publicly available space for research and engineering activity, so-called makerspace, in which a set of tools and equipment are present for public use[455]). Whereas 3D printers were used to teach proper additive manufacturing methods until recently, 3D printing is currently a potent auxiliary tool for teaching any discipline related to studying material objects and phenomena. First, this refers to education in the field of mechanical engineering and architecture and design, both industrial and artistic. Students can not only make drawings, illustrations or models that require labour-consuming manual work but also create any prototypes and functional models for better demonstration and fine-tuning of their projects. For example, in the field of industrial design, it became possible to quickly make a small series of prototypes of the designed device, without significant material expenses, to verify the convenience of decive operation. Owing to digital manufacturing, teachers can themselves produce physical models most appropriate for a particular training course with minimum expenses. Modern education offers numerous examples of using 3D printing in biology (models of biological molecules), chemistry, physics (functional models of mechanical devices), engineering, pharmacology (enzyme models), mathematics (geometric shapes), anatomy, paleontology and so on.[456–458]

Fundamental chemical research, *e.g.*, study of reactivity issues, is based on the concept of molecular structure, which represents the spatial arrangement of atoms determined by the electronic structure of a molecule or a crystal. A detailed and logically complete interpretation of the reactivity of compounds is gained by studying the spatial distribution of electrons in the molecule, areas characterized by electron accumulation or electron deficiency, types and energies of chemical bonds and spatial accessibility of particular functional groups in a chemical reaction. Mechanistic studies of chemical reactions consist of determining of the possible changes in the molecular structures of reactants resulting in the formation of products. The reactivities of proteins and other biological molecules are determined by their spatial structures. The ideas of the spatial structure of molecules crucially affected not only physical chemistry but also whole chemical science, having become a part of its fundamentals. Quite a number of chemical concepts, theories and considerations are based on the geometry of chemical objects; therefore, visualization is very important for chemistry (Fig. 21).

Chemistry teachers often use molecular model kits for the construction of ball-and-stick and other models of molecules. These kits can serve not only for demonstration of molecular structures but also for illustration of conformational behaviour of molecules if the links between groups are movable. A drawback of commercial molecular kits is that the molecules can be built only of standard functional groups that are included in the kit. If a teacher or a student faces the task of assembling a nontrivial molecular structure, for example, a carbon nanotube, a fullerene or a metal cluster (see Fig. 8 *a* and Fig. 22), a special molecular kit containing the necessary parts would be needed; otherwise, the only option is to demonstrate the model on a computer's display. However, dealing with physical models, which can

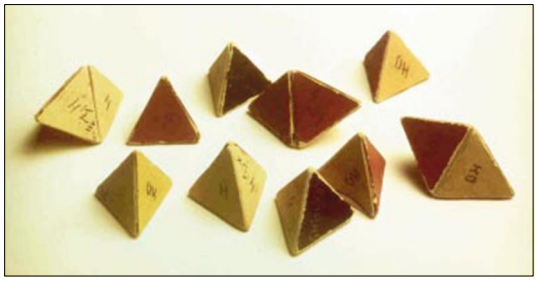


Figure 21. Spatial models of asymmetric molecules manufactured by Jacobus Henricus van't Hoff in 1875 to explain the phenomenon of optical activity of molecules.[459]

be handled, and, the more so, manual assembly of these models, lead students to a more in-depth understanding of the spatial structures of molecules than working with electronic demonstrations.

3D printing is a very efficient and convenient tool for the fabrication of any molecular model and other illustrative models in chemistry, while 3D printing is a universal 'molecular model kit'. The illustrative chemical models are printed using general-purpose plastics, PLA, PLA + and ABS.

A 3D model of a molecule or a crystal can be derived from the standard **.cif*- or **.pdb* file. Any other file format for molecular structures, xyz, mol, mol2, *etc.*, can also be used. The structure (*i.e.*, coordinates of atoms) can be determined by X-ray diffraction or by quantum chemical modelling. Then, the 'molecular' format can be converted to **.stl*, or can be used for preparing the model for 3D printing with the aid of molecular visualization and analysis software such as CCDC Mercury,[460] VMD[461] or UCSF Chimera.[462] Thus, the molecular structure model can be gained without the use of conventional 3D graphics editors, *i.e.*, in this case, there is often no need to deal with the actual 3D modelling.

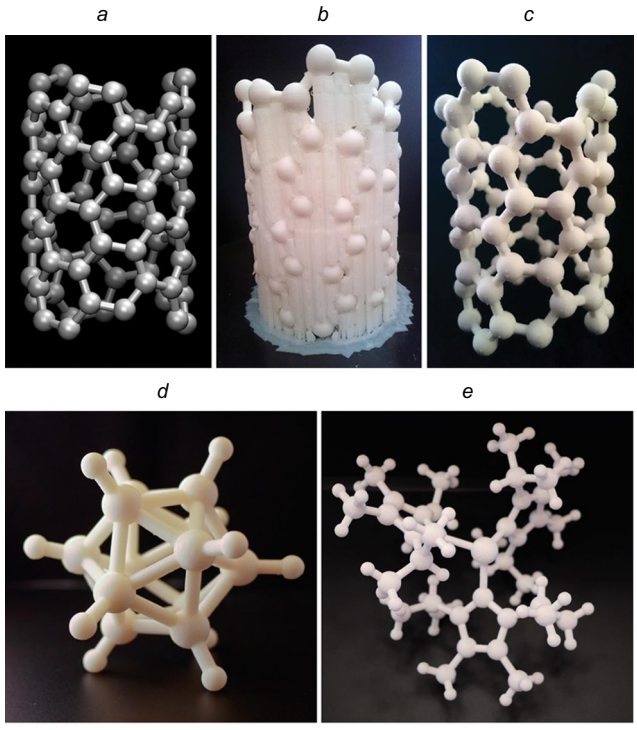


Figure 22. FDM 3D-printed molecular models. (*a*) Digital 3D model of carbon nanotube; (*b*) nanotube model printed using PLA plastic with a support; (*c*) nanotube model after removal of the support;[464] (*d*) $[B_{12}H_{12}]^{2-}$ polyhedral dianion of I_h group of symmetry (ABS plastic); (*e*) germanium complex with *N*-heterocyclic ligands $[Ge(Pr^i_2NHC)_3]^{2+}$ (ABS plastic).[465]

The model of a molecule can be fabricated either as a whole or in parts, which are then assembled together. The models are made in parts if it is necessary to construct a large-size object to demonstrate in the classroom. The built chambers of desktop 3D printers allow printing of objects with outer dimensions up to ~20 – 25 cm. To fabricate larger objects, the model should be cut into pieces, each piece is printed separately, and then the entire molecular model is glued together. The fabrication in parts is also appropriate when the model is multicoloured: the atoms of different elements are printed with plastics of different colours, if FDM printing is used. An obvious disadvantage of assembling the models from parts is laboriousness. The digital 3D molecular model should be manually split into pieces that can be printed; this is not always an easy task for a beginner in 3D modelling if chemical bonds are connected to atoms at intricate angles. However, software tools have recently appeared for automated splitting of a complex molecular model into fragments.[463]

Of course, the most facile method for fast production of a complex molecular model is fabrication in one piece, as a single whole object (see Fig. 22). As a rule, molecular structures comprise overhanging parts; therefore, printing of a model 'as a single whole' requires the use of supports (see Fig. 22 *b*). If postprocessing of the printed model is not planned, then it is desirable to use soluble supports, which would be separated from the model without noticeable surface damage.

Physical models are very useful for studying the symmetry properties of molecules,[466] especially for complex symmetric structures with high-order symmetry axes such as the $[B_{12}H_{12}]^{2-}$ polyhedral dianion with a fivefold axis corresponding to the I_h point group of symmetry (Fig. 22 *d*). The search for symmetry elements is much easier in three-dimensional digital models than in static drawings, but physical models embodied in a material make elements of symmetry even more vivid and easier to identify since the symmetry can be held in hands.

Crystal fragment models can be obtained directly from the crystallographic data contained in the cif file.[467] The contrast between atoms of different elements is achieved either by varying the sizes of the corresponding spheres or by using different-colour plastics in the case of FDM 3D printers with several extruders (Fig. 23).

Not only the molecular, but also the electronic structures of compounds can be visualized or interpreted using material models. Rigid rod models illustrating the Woodward – Hoffman rules of conservation of orbital symmetry in reactions of unsaturated organic compounds were presented back in 1969.[469]

The planetary model of atom and models of atomic orbitals were proposed as simple basic examples for high school students and first-year university students (Fig. 24 *a*,*b*). In the model of the atoms, the electrons (blue) can move along the circular orbitals, which in turn

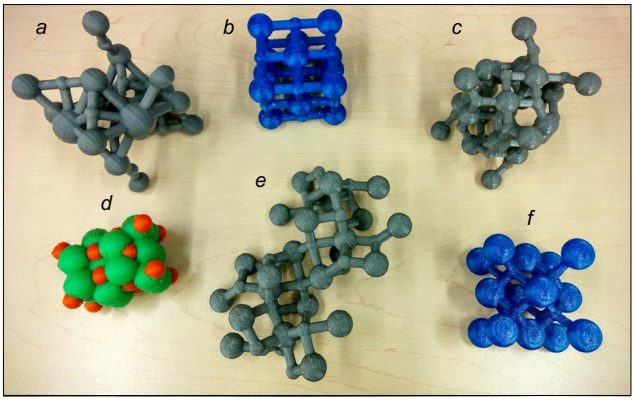


Figure 23. Models of crystal fragments of various compounds FDM-printed on the basis of crystallographic data.[468] (*a*) Perovskite, (*b*) halite (salt rock), (*c*) spinel, (*d*) spinel as a set of overlapping spheres of different colours, (*e*) corundum, (*f*) fluorite.

rotate around the axis passing through the atomic nucleus (red). A set of atomic models is fabricated for the lesson, and students are asked to determine which of the elements of the Periodic Table is represented by each of the models.

A model of a propylene molecule in which different types of bonds are shown with different plastic colour was proposed to illustrate hybridization of the atomic orbitals of carbon (Fig. 24 *c*). In this model, students are asked to identify the types of bonds, discuss the differences in carbon atom hybridization and show on the model how these differences affect the geometry of the molecule. Most students have a positive attitude towards working with such models, but some of them note that using the models resembles a lab, while at the lecture, they would prefer to just listen to the teacher and take notes; therefore, personal characteristics of students should be taken into account while planning the classes.[470]

In the concept of atomic structure in the physical chemistry course, a fundamental issue is the spatial

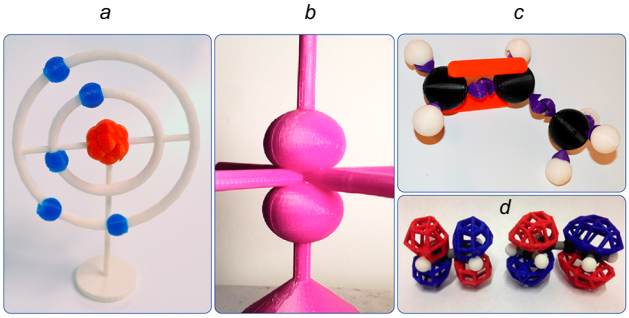


Figure 24. FDM-printed models of electronic structures of atoms and molecules. (*a*) Planetary model of the boron atom,[470] (*b*) model of $2p_y$ atomic orbital;[471] (*c*) mechanical model of propylene molecule illustrating different hybridizations of carbon atoms (σ-bonds are made of violet plastic, π-bond is made of orange plastic);[470] (*d*) model of the lowest unoccupied molecular orbital of the ethylene molecule and the highest occupied molecular orbital of the 1,3-diene molecule (red and blue colours correspond to different signs of the wave function).[472]

structure of atomic orbitals. The atomic orbital models proposed in commercial educational kits only mimic the orbital shape, but they are not physically strict isosurfaces of the electron density function. The combination of relevant software and 3D printing enables the fabrication of any atomic orbitals for analysis of their spatial structure. The first stage is the construction of a strict mathematical model of some hydrogen-like atomic orbitals, which would be the square of the wave function, resulting in the product of the squares of the radial and angular parts of the wave function. The three-dimensional model obtained in this way is exported to the *stl* format owing to the ability of modern mathematical software to convert a mathematical surface to the 3D model geometric format. The three-dimensional model obtained in this way is printed on a 3D printer (Fig. 24 *b*).[471] Certainly, atomic orbitals of the complex shape (d and f) are most relevant for educational purposes since the students are not always able to obtain a full idea of the shape of these orbitals from a textbook picture. The models of d and f atomic orbitals provide a better understanding of the geometry of transition metal complexes.

From the models of atomic orbitals, it is reasonable to pass to molecular orbital (MO) models. The spatial structure of molecular orbitals is of fundamental importance for determining the reactivity of a molecule. Among all molecular orbitals inherent in a given molecular structure, the most important are the frontier MOs: the highest occupied (HOMO) and lowest unoccupied (LUMO) molecular orbitals. In particular, HOMO characterizes the electron-donating (nucleophilic) properties of the molecule, while LUMO determines the electron-withdrawing (electrophilic) properties. The geometric match between the frontier MOs of the reactant molecules is a key factor determining the occurrence of a chemical reaction. For example, the models of ethylene and 1,3-diene frontier MOs shown in Fig. 24 *d* clearly show the spatial structures of the ethylene LUMO and diene HOMO.[472] Students who manipulate these models by hand easily find the relative positions of two molecules where the same signs of wave function match, *i.e.*, the red-coloured HOMO of the diene coincides with the red-coloured LUMO of ethylene. Thus, using models of the frontier MOs of the reactants, students obtain a clear illustration of the possibility for the Diels–Alder reaction (diene synthesis) to occur. The spatial structure of MOs is derived from quantum chemical modelling. Most of the popular program packages for quantum chemical modelling (both commercial and free packages) offer the option for saving the spatial structures of MOs in a separate file, which can be visualized using molecular visualization software. After adjustment of the 3D view of the chosen MO, the spatial model of the orbital can be exported to the *stl* format (this option is provided by the VMD and UCSF Chimera programs) for the subsequent printing on a 3D printer.

The use of 3D printing in biochemical education has some specific features. Many biochemical issues are closely related to studying intermolecular interactions, which determine the relative orientations of two separate molecules or two moieties of the same molecule, *i.e.*, the supramolecular organization of compounds is highly important for biochemistry. To teach the regularities of this organization to students, dynamic molecular models

have been proposed. Parts of the models are either fully separated from each other, such as meccano parts, or can move or deform, *i.e.*, models of biological molecules should not be static, like models of simple organic molecules or crystals, but should be dynamic and interactive to enable studying of the molecular dynamics at a simplified level.

For example, deformable DNA and RNA models have been proposed, which allow students to view the difference between the structures of these nucleic acids and study the formation of nucleosomes by wrapping an elastic DNA strand around a histone protein model to gain an idea of the mechanisms of packing of DNA molecules in chromosomes.[473] An original model of binding of one transcription factor (a protein involved in the formation template RNA based on DNA) to a definite site of DNA molecule was proposed to illustrate the initial stages of protein biosynthesis. In this model, DNA atoms binding the protein were implemented as spherical magnets, and similar magnets were present in the transcription factor model. Some parts of the protein model could be detached, together with magnetic holders. This detachment of protein parts simulates protein mutation. Protein mutations influence the attraction force between the transcription factor and DNA site. Thus, students can physically feel with their own hands how much mutations affect biochemical processes.

Dynamic models are also useful for studying the levels of protein organization in which the spatial shape of a molecule is dictated by nonbonded interactions (mainly hydrogen bonds) between parts of the polypeptide chain. Researchers from the University of Texas used FDM printing to develop a training model of a small protein with mobile connectors between amino acid residues so that side groups capable of hydrogen bonding could approach each other in an optimal way to form a hydrogen bond network.[474]

Another type of molecular model also serving as a demonstration of the supramolecular organization of biological molecules deserves attention, particularly models based on molecular surfaces. In this case, the molecules are too complex to be fabricated with atomic resolution and are represented as a solid body described by a surface accessible to a solvent, which is most often water in biochemistry (other types of molecular surfaces can also be used). The nucleophilic and electrophilic sites are marked by different colours on the surface of the molecule. Two molecules (*e.g.*, enzyme and its substrate) should be arranged in space to enable electrophilic sites of one molecule to interact with nucleophilic sites of the other molecule. By handling models of this type, students easily learn the molecular recognition principle, according to which proteins (*e.g.*, enzymes) bind other molecules.[475,476] This approach is actively used to study the relationship between the protein structure and properties and for the development of new drugs.

Although the use of 3D printing in chemical education is mainly related to molecular models of various types,[477–484] this versatile method is also used to fabricate other physicochemical models, in particular, 3D models of 2D NMR spectra,[485] 3D models of the time dependences of concentrations of compounds derived from the data of IR and NMR spectroscopic monitoring of chemical reactions,[486] models of block copolymer organization at the micro-level,[487] potential energy surfaces (PES),[488,489] *etc.*

A potential energy surface is the dependence of the potential energy of a molecule on the coordinates of atomic nuclei incorporated in the molecule. This dependence is the main subject of discussion in mechanistic studies of chemical reactions and is based on the results of quantum chemical modelling. The PES has local minima corresponding to intermediates, the global minimum characterizing the most stable state of the reacting system and saddle points corresponding to transition states of a multistep process. By analyzing PES, one can calculate the heats of reactions and estimate the potential barriers for all steps. Potential energy surfaces of multistep reactions have complex shapes; therefore, scientific publications and textbooks usually discuss only the PES profile obtained as a cross-section along the reaction coordinate and projected on the plane of the drawing, rather than PES as a whole. Therefore, students often conceive the reaction path as a planar line connecting the reactants, the transition states and products. The actual reaction coordinate is the minimum energy path, which has a complex three-dimensional geometry even for elementary chemical reactions. The planar two-dimensional profiles of the reaction coordinates do not reflect either the complexity of the coordinate shape or the minimality of the energy characterizing the coordinate; furthermore, they hide the possibility for the reaction to follow several paths.

The 3D PES models for educational purposes were developed back in the mid-20th century. An example is the gypsum-made PES model of 1957, which was based on the data of semiempirical calculations to describe the reaction of a hydrogen molecule with a bromine atom ($H_2 + Br \rightarrow H + HBr$) (see Fig. 25 *a*,*b*).[490] The arrowed

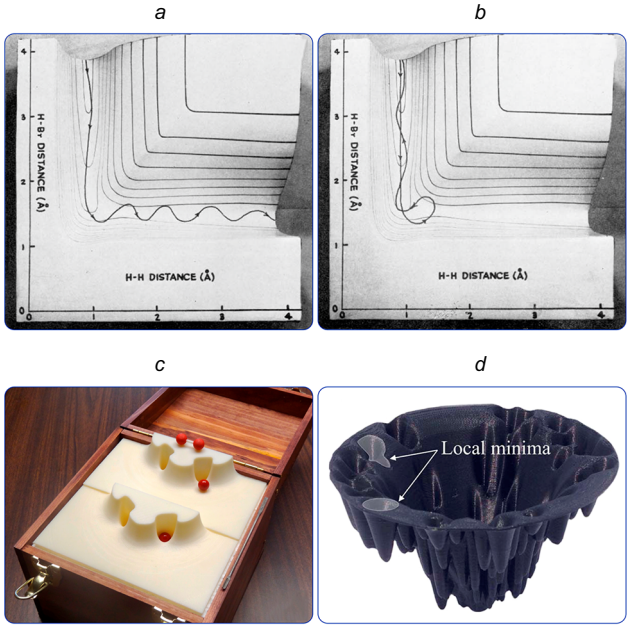


Figure 25. PES models for various chemical processes. (*a*, *b*) PES model for the reaction of hydrogen molecules with a bromine atom manufactured from gypsum by conventional methods;[490] (*c*) FDM 3D-printed PES models for the formation of ozone molecules;[491] (*d*) FDM-printed PES model for folding of a protein molecule.[492]

line shows a reactive collision of molecules, inducing transition of the system to the valley of the products (see Fig. 25 *a*), or a non-reactive collision of molecules, which does not allow the molecules to pass over the potential barrier and brings the system back to the valley of the reactants (Fig. 25 *b*). Since the reaction follows the minimum energy path, the shown lines represent the trajectory of a ball rolling on the bottom of PES, since a ball tends to occupy the lowest positions on the surface to minimize its potential energy.

3D printing makes it possible to fabricate much more intricate PES models with numerous local minima. Figure 25 *c* shows the models of two PESs corresponding to the formation of ozone molecules upon the addition of an oxygen atom to an oxygen molecule. This process is highly important for studying atmospheric chemistry. Both surfaces have two symmetrically located minima, each corresponding to the reaction product, O_3. The symmetrical positions of the minima are due to the symmetry of the oxygen molecule: an oxygen atom can approach the molecule from either of the sides, and both cases give ozone. The PES shown at the back has reefs (potential barriers) in front of wells, whereas the PES at the front is corrected and has no such reefs. Due to this difference, a ball corresponding to the oxygen atom, while approaching the O_2 molecule, is stopped by the barrier in the first PES and cannot enter the well (no ozone is formed), whereas the motion over the corrected PES is not retarded in this way, and ozone is formed without obstacles. The second, corrected PES better corresponds to experimental data, since this process is known to proceed at low temperature. These PES models show students that even small changes in the PES can significantly affect the course of chemical reactions.

If a chemical structure has many degrees of freedom, then the processes involving this structure will be characterized by numerous local minima. These systems can be exemplified by protein molecules. The model of the potential energy surface of folding of one of the protein molecules is shown in Fig. 25 *d*. Each well on this surface is a local minimum corresponding to the state that can be acquired by a folded protein molecule; the molecule then remains in this state unless some external impact forces it out. The general view of the surface resembles a funnel, the lowest point of which is the global free energy minimum corresponding to the most energetically favourable protein structure. If upon folding, the protein molecule remains in the local minimum, the biological functions of this molecule can be disrupted.

Along with models pertaining to structural and physical chemistry, additive technologies are actively used to fabricate educational equipment for experimental chemistry. Chemical reactors of various types,[493,494] accessory equipment for colorimetric and polarimetric measurements,[495,496] even the model of atomic force microscope[497] and a lot of other engineering solutions can be implemented using 3D printing by students or teachers without specific engineering training. The key educational goal is to encourage students towards creative engineering activity as applied to chemical experiments. Although the purpose of this work is educational, the strategy towards such design is the same as that used to solve professional research problems. Students are expected to design and manufacture, by their own, a setup or its components to carry out a chemical experiment with the highest efficiency and compare the benefits and drawbacks of various approaches.

The application of 3D printing in chemical education is evidently in high demand, as it supplements the educational process with a new teaching element unusual for chemistry teaching, namely, the design of molecular structures of any complexity and topology and the design and creation of reactors and other equipment for experimental laboratory work performed by students on their own. A chemistry teacher, especially a university lecturer, can ask students who are interested in printing 3D models of various molecules as an extra assignment;[498] *i.e.*, students who still have no opportunity to perform real chemical synthesis can 'synthesize' structurally interesting compounds using a 3D printer. This is highly important for education, as it helps students to perceive chemistry as a creative activity aimed at the design of compounds.

It should be noted that teaching the fundamentals of additive technologies using personal 3D printers may be partly included in chemistry courses (or even fully included, if additive technologies are not considered in other education courses) as extra training, since this subject covers many important chemical and physicochemical processes. Using FDM printing as an example, it is possible to illustrate the behaviour of thermoplastic polymers on heating and consider the extrusion process as a method for polymer processing. The use of compact systems for the extrusion of polymer filaments is perfectly suited for the fabrication of polymer compositions with various fillers and for studying the possibility of polymer recycling by remelting products of poor quality or spent support. Laser stereolithography methods provide the possibility to become acquainted with photochemical polymerization processes.

5. Conclusion

Until quite recently, personal 3D printing with inexpensive 3D printers was mainly considered an interesting hobby for enthusiastic makers. The advancement of designs of personal 3D printers, expansion of the range of printing materials and development of convenient relevant software made personal 3D printing a full-fledged production method, which is increasingly used in various fields of chemistry and biochemistry (Fig. 26).

Most of the 3D printed products considered in this review could have also been manufactured by classical manufacturing methods, but in that case, the production would have consisted of several stages and would have taken much more time. Conventional processing equipment (processing machines, casting moulds, *etc.*) is not often encountered in a chemical laboratory since the use of conventional methods for manufacturing objects with intricate shapes requires a special workshop and high production skills, absent in the vast majority of research chemists. Due to the expected high time and material expenditures associated with conventional manufacturing methods, many design ideas of equipment promising for a chemical experiment are never implemented in reality. Additive technologies simplified the fabrication of intricate objects to such an extent that the strategy towards solving production problems has fundamentally changed. Additive manufacturing methods with personal 3D printers do not require special engineering skills of the user or

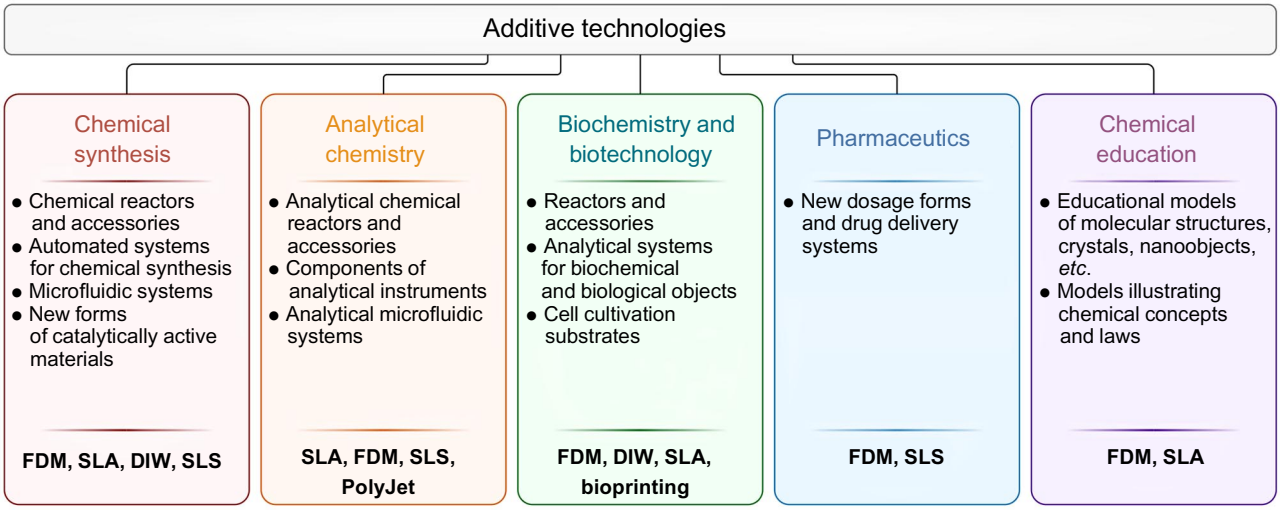


Figure 26. Key applications of additive technologies in chemistry and related fields. The additive manufacturing methods used most frequently in each field are indicated.

a special workshop; therefore, the extrusion melting of thermoplastic materials and various types of stereolithography have become everyday tools in many chemical laboratories.

The major advantage of additive technologies is versatility. 3D printing is a flexible tool suitable for creating any shape from a material. The manufacturing time depends little on the complexity of the product topology: a conventional test tube rack or a laboratory chemical reactor with a coiled inner channel can be fabricated using the same 3D printer on a laboratory bench.

An important benefit of 3D printing, which is especially inherent in extrusion methods, is the possibility to fabricate materials adapted to solving particular research tasks. This enables the design of catalytic systems with a strictly ordered geometry, the production of new types of adsorbents, the invention of more effective dosage forms of drugs, and the printing of biocompatible scaffolds. Owing to this feature of additive methods, a new trend called bioprinting has appeared in regenerative medicine.

In view of the vigorous growth of the number of scientific publications devoted to the use of additive technologies in all areas of chemical science, the integration of 3D printing into the routine research activities of chemical laboratories will undoubtedly continue since new opportunities open up the way for the implementation of new ideas.

Figures 4 *b*,*c*,*d* are published under the license of Creative Commons Attribution (CC BY); Figures 5, 9, 16 *a*, 17 *b* are published under the license of Creative Commons Attribution 3.0 Unported License; Figures 15 *a*,*c*,*d* are published with the permission of *Springer*. Figure 6 *a* is published under the license of Creative Commons Attribution 2.0 Generic (https://creativecommons.org/licenses/by/2.0/, creativetools.se, www.flickr.com/photos/creative_tools/24203075010/). Figures 12 and 16 *c*,*e* are published under the license of Creative Commons Attribution 4.0 International License (http://creativecommons.org/licenses/by/4.0/). Figure 17 *a* is published under the license of Attribution-Non-Commercial-NoDerivatives 4.0 International (CC BY-NC-ND 4.0, https://creativecommons.org/licenses/by-nc-nd/4.0/). Figures 6 *b*,*c*, 10, 19 *a* are published with the permission of *Royal Society of Chemistry*. Figures 7 *a*, 14, 16 *d*, 18 *d*,*e* are published with the permission of *Elsevier*. Figure 16 *b* is published with the permission of *The American Association for the Advancement of Science*. Figures 18 *a* – *c*, 20, 22 *a* – *c*, 23, 24, 25 are published with the permission of *American Chemical Society*. Figures 22 *d*,*e* are published under the license of *ACS Author-Choice or ACS Editors Choice* (https://pubs.acs.org/page/policy/authorchoice_termsofuse.html). Figure 19 *b* is published with the permission of *Springer Nature*. Figures 13, 21 are published with the permission of *John Wiley and Sons*.

The following acronyms are used in the review:

ABS — acrylonitrile butadiene styrene,
AM — additive manufacturing,
API — active pharmaceutical ingredient,
ASTM — American Society for Testing and Materials,
BJ — binder jetting,
CAD — computer-aided design,
CDLP — continuous digital light processing,
CFRT — continuous fiber reinforced thermoplastics,
CLIP — continuous liquid interface production,
DED — directed energy deposition,
DIW — direct-ink-writing,
DLP — digital light processing,
DMD — direct metal deposition,
DMLS — direct metal laser sintering,
DOD — drop-on-demand,
3DP — 3D printing,
EBM — electron beam melting,
FDA — Food and Drug Administration,
FDM — fused deposition modelling,
FFF — fused filament fabrication,
HDPE — high-density polyethylene,
HIPS — high impact polystyrene,
HME — hot-melt extrusion,
HOMO — higher occupied molecular orbital
HPMC — hydroxypropyl methylcellulose,
ISO — international organization for standardization,
LCD — liquid crystal display,
LDM — liquid deposition modelling,

LENS — laser engineered net shaping,
LMD — laser metal deposition,
LOM — laminated object manufacturing,
LTP — low-temperature plasma,
LUMO — lowest unoccupied molecular orbital
ME — material extrusion,
MJ — material jetting,
MJF — Multi Jet Fusion,
MJP — MultiJet Printing,
MO — molecular orbital,
NPJ — NanoParticle Jetting,
PA — polyamides,
PC — polycarbonate,
PCL — polycaprolactone,
PDMS — polydimethylsiloxane,
PE — polyethylene,
PEEK — poly(ether ether ketone),
PEG — polyethylene glycol,
PEGDA — polyethylene glycol diacrylate,
PEI — polyetherimide,
PEKK — poly(ether ketone ketone),
PES — potential energy surface,
PETG — poly(ethylene terephthalate)-glycol,
PHA — polyhydroxyalkanoate,
PLA — polylactic acid,
PLGA — poly(lactic-co-glycolic acid),
POC — point-of-collection (diagnostics),
POM — polyoxymethylene,
PP — polypropylene,
PPSU — polyphenylsulfone,
PSI — paper spray ionization,
PVA — polyvinyl alcohol,
PVDF — polyvinylidene fluoride,
SDL — selective deposition lamination,
SEBS — styrene – ethylene – butylene – styrene,
SECM — scanning electrochemical microscopy,
SFRT — short fiber reinforced thermoplastics,
SL — sheet lamination,
SLA — stereolithography apparatus,
SLM — selective laser melting,
SLS — selective laser sintering,
TEEE — thermoplastic ester ether elastomer,
TLC — thin layer chromatography,
TPU — thermoplastic polyurethane,
UAM — ultrasonic additive manufacturing,
VP — vat photopolymerization.

References

1. A.Silver. *Nature (London)*, **565**, 123 (2019); https://doi.org/10.1038/d41586-018-07853-5
2. M.Zastrow. *Nature (London)*, **578**, 20 (2020); https://doi.org/10.1038/d41586-020-00271-6
3. A.H.Tullo. *C&EN*, **95** (41), 30 (2017); https://doi.org/10.1021/cen-09541-cover
4. O.Diegel, A.Nordin, D.Motte. *A Practical Guide to Design for Additive Manufacturing*. (Singapore: Springer, 2019); https://doi.org/10.1007/978-981-13-8281-9
5. B.Berman. *Bus. Horiz.*, **55**, 155 (2012); https://doi.org/10.1016/j.bushor.2011.11.003
6. A.Gebhardt, J.-S.Hötter. *Additive Manufacturing: 3D Printing for Prototyping and Manufacturing*. (Hanser Publishers, 2016)
7. U.M.Dilberoglu, B.Gharehpapagh, U.Yaman, M.Dolen. *Proc. Manuf.*, **11**, 545 (2017); https://doi.org/10.1016/j.promfg.2017.07.148
8. A.Ciabara, Ş.L.Burlea, M.Axinte, R.Cimpoeşu, D.L.Chicet, V.Manole, G.Burlea, N.Cimpoeşu. *IOP Conf. Ser.: Mater. Sci. Eng.*, **374**, 012066 (2018); https://doi.org/10.1088/1757-899X/374/1/012066
9. J.Feng, J.Fu, Z.Lin, C.Shang, B.Li. *Vis. Comput. Ind. Biomed. Art*, **1**, 5 (2018); https://doi.org/10.1186/s42492-018-0004-3
10. N.B.Palaganas, J.D.Mangadlao, A.C.C.de Leon, J.O.Palaganas, K.D.Pangilinan, Y.J.Lee, R.C.Advincula. *ACS Appl. Mater. Interfaces*, **9**, 34314 (2017); https://doi.org/10.1021/acsami.7b09223
11. T.D.Ngo, A.Kashani, G.Imbalzano, K.T.Q.Nguyen, D.Hui. *Composites, Part B*, **143**, 172 (2018); https://doi.org/10.1016/j.compositesb.2018.02.012
12. L.Bourdon, J.-C.Maurin, K.Gritsch, A.Brioude, V.Salles. *ACS Biomater. Sci. Eng.*, **4**, 3927 (2018); https://doi.org/10.1021/acsbiomaterials.8b00810
13. S.K.Saha, J.S.Oakdale, J.A.Cuadra, C.Divin, J.Ye, J.-B.Forien, L.B.B.Aji, J.Biener. *ACS Appl. Mater. Interfaces*, **10**, 1164 (2018); https://doi.org/10.1021/acsami.7b12654
14. J.Rühe. *ACS Nano*, **11**, 8537 (2017); https://doi.org/10.1021/acsnano.7b05593
15. A.J.Capel, R.P.Rimington, M.P.Lewis, S.D.R.Christie. *Nat. Rev. Chem.*, **2**, 422 (2018); https://doi.org/10.1038/s41570-018-0058-y
16. ISO/ASTM52900-15. *Standard Terminology for Additive Manufacturing — General Principles — Terminology*. (West Conshohocken, PA: ASTM International, 2015); www.astm.org; https://doi.org/10.1520/ISOASTM52900-15
17. GOSTR 57589-2017. *Natsionalnyi Standart Rossiiskoi Federatsii, Additivnye Tekhnologicheskie Protsessy. Bazovye Printsipy — Chast' 2. Materialy dlya Additivnykh Tekhnologicheskikh Protsessov. Obshchie Trebovaniya*. (National Standard of the Russian Federation, Additive Technological Processes. Basic Principles — Part 2. Materials for Additive Manufacturing Processes. General Requirements). (Moscow: Standartinform, 2017). 12 p.
18. Patent US 005204055A (1993)
19. N.Travitzky, A.Bonet, B.Dermeik, T.Fey, I.Filbert-Demut, L.Schlier, T.Schlordt, P.Greil. *Adv. Eng. Mater.*, **16**, 729 (2014); https://doi.org/10.1002/adem.201400097
20. P.Kunchala, K.Kappagantula. *Mater. Design*, **155**, 443 (2018); https://doi.org/10.1016/j.matdes.2018.06.009
21. D.Snelling, Q.Li, N.Meisel, C.B.Williams, R.C.Batra, A.P.Druschitz. *Adv. Eng. Mater.*, **17**, 923 (2015); https://doi.org/10.1002/adem.201400524
22. S.R.Mogali, W.Y.Yeong, H.K.J.Tan, G.J.S.Tan, P.H.Abrahams, N.Zary, N.Low-Beer, M.A.Ferenczi. *Anatom. Sci. Ed.*, **11**, 54 (2017); https://doi.org/10.1002/ase.1703
23. Patent US 006046426A (2000)
24. B.Heer, A.Bandyopadhyay. *Mater. Lett.*, **216**, 16 (2018); https://doi.org/10.1016/j.matlet.2017.12.129
25. A.Saboori, A.Aversa, G.Marchese, S.Biamino, M.Lombardi, P.Fino. *Appl. Sci.*, **9**, 3316 (2019); https://doi.org/10.3390/app9163316
26. N.Tepylo, X.Huang, P.C.Patnaik. *Adv. Eng. Mater.*, **21**, 1900617 (2019); https://doi.org/10.1002/adem.201900617

27. T.Yamazaki. *Proc. CIRP*, **42**, 81 (2016); https://doi.org/10.1016/j.procir.2016.02.193
28. Patent US 005121329A (1989)
29. M.Seel, R.Akerboom, U.Knaack, M.Oechsner, P.Hof, J.Schneider. *Mater. Sci. Eng. Technol. (Materialwiss. Werkstofftech.)*, **49**, 870 (2018); https://doi.org/10.1002/mawe.201800075
30. J.Klein, M.Stern, G.Franchin, M.Kayser, C.Inamura, S.Dave, J.C.Weaver, P.Houk, P.Colombo, M.Yang, N.Oxman. *3D Print. Addit. Manuf.*, **2**, 92 (2015); https://doi.org/10.1089/3dp.2015.0021
31. D.G. Moore, L.Barbera, K.Masania, A.R. Studart. *Nat. Mater.*, **19**, 212 (2020); https://doi.org/10.1038/s41563-019-0525-y
32. E.G.Gordeev, A.S.Galushko, V.P.Ananikov. *PLoS ONE*, **13**, e0198370 (2018); https://doi.org/10.1371/journal.pone.0198370
33. O.A.Mohamed, S.H.Masood, J.L.Bhowmik. *Adv. Manuf.*, **3**, 42 (2015); https://doi.org/10.1007/s40436-014-0097-7
34. L.Geoffroy, F.Samyn, M.Jimenez, S.Bourbigot. *Polym. Adv. Technol.*, **30**, 1878 (2019); https://doi.org/10.1002/pat.4620
35. T.W.Kerekes, H.Lim, W.Y.Joe, G.J.Yun. *Addit. Manuf.*, **25**, 532 (2019); https://doi.org/10.1016/j.addma.2018.11.008
36. T.Sonsalla, A.L.Moore, W.J.Meng, A.D.Radadia, L.Weiss. *Polym. Test.*, **70**, 389 (2018); https://doi.org/10.1016/j.polymertesting.2018.07.018
37. E.Peng, D.Zhang, J.Ding. *Adv. Mater.*, **30**, 1802404 (2018); https://doi.org/10.1002/adma.201802404
38. K.Lin, R.Sheikh, S.Romanazzo, I.Roohani. *Materials*, **20**, 2660 (2019); https://doi.org/10.3390/ma12172660
39. R.D.Farahani, M.Dubé. *Adv. Eng. Mater.*, **20**, 1700539 (2018); https://doi.org/10.1002/adem.201700539
40. R.D.Farahani, M.Dubé, D.Therriault. *Adv. Mater.*, **28**, 5794 (2016); https://doi.org/10.1002/adma.201506215
41. N.van de Werken, H.Tekinalp, P.Khanbolouki, S.Ozcan, A.Williams, M.Tehrani. *Addit. Manuf.*, **31**, 100962 (2020); https://doi.org/10.1016/j.addma.2019.100962
42. Patent US 006259962B1 (2001)
43. R.Udroiu, C.Braga. *MATEC Web Conf.*, **112**, 03011 (2017); https://doi.org/10.1051/matecconf/201711203011
44. T.J.Snyder, M.Andrews, M.Weislogel, P.Moeck, J.Stone-Sundberg, D.Birkes, M.P.Hoffert, A.Lindeman, J.Morrill, O.Fercak, S.Friedman, J.Gunderson, A.Ha, J.McCollister, Y.Chen, J.Geile, A.Wollman, B.Attari, N.Botnen, V.Vuppuluri, J.Shim, W.Kaminsky, D.Adams, J.Graft. *3D Print. Addit. Manuf.*, **1**, 169 (2014); https://doi.org/10.1089/3dp.2014.1502
45. Patent US 7993123 B2 (2011)
46. M.Simonelli, N.Aboulkhair, M.Rasa, M.East, C.Tuck, R.Wildman, O.Salomons, R.Hague. *Addit. Manuf.*, **30**, 100930 (2019); https://doi.org/10.1016/j.addma.2019.100930
47. A.Bandyopadhyay, B.Heer. *Mater. Sci. Eng. R*, **129**, 1 (2018); https://doi.org/10.1016/j.mser.2018.04.001
48. G.H.Loh, E.Pei, D.Harrison, M.D.Monzón. *Addit. Manuf.*, **23**, 34 (2018); https://doi.org/10.1016/j.addma.2018.06.023
49. Patent US 4863538 (1989)
50. S.Singh, V.S.Sharma, A.Sachdeva. *Mater. Sci. Technol.*, **32**, 760 (2016); https://doi.org/10.1179/1743284715Y.0000000136
51. A.Nazarov, I.Skornyakov, I.Shishkovsky. *Machines*, **6** (1), 11 (2018); https://doi.org/10.3390/machines6010011
52. S.Yuan, F.Shen, C.K.Chua, K.Zhou. *Prog. Polym. Sci.*, **91**, 141 (2019); https://doi.org/10.1016/j.progpolymsci.2018.11.001
53. S.Sing, W.Yeong, F.Wiria, B.Tay, Z.Zhao, L.Zhao, Z.Tian, S.Yang. *Rapid Prototyp. J.*, **23**, 611 (2017); https://doi.org/10.1108/RPJ-11-2015-0178
54. A.Zocca, P.Colombo, C.M.Gomes, J.Günster. *J. Am. Ceram. Soc.*, **98**, 1983 (2015); https://doi.org/10.1111/jace.13700
55. *Laser Additive Manufacturing: Materials, Design, Technologies, and Applications*. (Ed. M.Brandt). (Woodhead Publishing, 2017). 498 p.; https://doi.org/10.1016/C2014-0-03891-9
56. D.Sofia, M.Granese, D.Barletta, M.Poletto. *Proc. Eng.*, **102**, 749 (2015); https://doi.org/10.1016/j.proeng.2015.01.180
57. J.-P.Kruth, G.Levy, F.Klocke, T.H.C.Childs. *CIRP Ann.*, **56**, 730 (2007); https://doi.org/10.1016/j.cirp.2007.10.004
58. Y.Chivel. *Phys. Proc.*, **83**, 891 (2016); https://doi.org/10.1016/j.phpro.2016.08.093
59. A.G.Demir, B.Previtali. *Manuf. Lett.*, **11**, 8 (2017); https://doi.org/10.1016/j.mfglet.2017.01.002
60. N.Ahmed. *J. Manuf. Process.*, **42**, 167 (2019); https://doi.org/10.1016/j.jmapro.2019.05.001
61. A.Arabi-Hashemi, X.Maeder, R.Figi, C.Schreiner, S.Griffiths, C.Leinenbach. *Appl. Mater. Today*, **18**, 100512 (2020); https://doi.org/10.1016/j.apmt.2019.100512
62. P.Toensmeier. *Plast. Eng.*, **73** (2), 12 (2017); https://doi.org/10.1002/j.1941-9635.2017.tb01655.x
63. J.Romeo. *Plast. Eng.*, **75** (9), 40 (2019); https://doi.org/10.1002/peng.20202
64. B.Gutmann, M.Köckinger, G.Glotz, T.Ciaglia, E.Slama, M.Zadravec, S.Pfanner, M.C.Maier, H.Gruber-Wölfler, C.O.Kappe. *React. Chem. Eng.*, **2**, 919 (2017); https://doi.org/10.1039/c7re00176b
65. S.H.Khajavi, M.Baumers, J.Holmström, E.Özcan, J.Atkin, W.Jackson, W.Li. *Comput. Ind.*, **98**, 100 (2018); https://doi.org/10.1016/j.compind.2018.01.022
66. A.H.Espera, A.D.Valino, J.O.Palaganas, L.Souza, Q.Chen, R.C.Advincula. *Macromol. Mater. Eng.*, 1800718 (2019); https://doi.org/10.1002/mame.201800718
67. Patent US 4752352 (1988)
68. G.D.Janaki Ram, C.Robinson, Y.Yang, B.E.Stucker. *Rapid Prototyp. J.*, **13**, 226 (2007); https://doi.org/10.1108/13552540710776179
69. B.Mueller, D.Kochan. *Comput. Ind.*, **39**, 47 (1999); https://doi.org/10.1016/S0166-3615(98)00127-4
70. I.Gibson, D.Rosen, B.Stucker. *Additive Manufacturing Technologies: 3D Printing, Rapid Prototyping, and Direct Digital Manufacturing*. (2nd Ed.). (New York: Springer Verlag, 2015); https://doi.org/10.1007/978-1-4939-2113-3
71. H.K.Park, M.Shin, B.Kim, J.W.Park, H.Lee. *NPG Asia Mater.*, **10**, 82 (2018); https://doi.org/10.1038/s41427-018-0021-x

72. A.L.Jardini, R.M.Filho, A.F.Scarparo, S.R.Andrade, L.F.M.Moura. *Int. J. Mater. Prod. Tecnol. (IJMPT)*, **21**, 241 (2004); https://doi.org/10.1504/IJMPT.2004.004940
73. *Stereolithography: Materials, Processes and Applications*. (Ed. P.J.Bártolo). (Springer, US, 2011); https://doi.org/10.1007/978-0-387-92904-0
74. H.Kodama. *Rev. Sci. Instrum.*, **52**, 1770 (1981); https://doi.org/10.1063/1.1136492
75. A.J.Herbert. *J. Appl. Photogr. Eng.*, **8** (4), 185 (1982)
76. Patent US 4575330 (1986)
77. O.Okafor, A.Weihard, J.A.Fernandes, E.Karjalainen, R.Goodridge, V.Sans. *React. Chem. Eng.*, **2**, 129 (2017); https://doi.org/10.1039/c6re00210b
78. R.Jafari, C.Cloutier, A.Allahdini, G.Momen. *Int. J. Adv. Manuf. Technol.*, **103**, 1225 (2019); https://doi.org/10.1007/s00170-019-03630-4
79. S.-H.Park, D.-Y.Yang, K.-S.Lee. *Laser. Photon. Rev.*, **3** (1 – 2), 1 (2009); https://doi.org/10.1002/lpor.200810027
80. A.N.Nguyen, R.J.Narayan. *Mater. Today*, **20** (6), 314 (2017); https://doi.org/10.1016/j.mattod.2017.06.004
81. K.B.Fritzler, V.Ya.Prinz. *Physics-Uspekhi*, **62**, 54 (2019); https://doi.org/10.3367/UFNe.2017.11.038239
82. T.Tanaka, H.-B.Sun, S.Kawata *Appl. Phys. Lett.*, **80**, 312 (2002); https://doi.org/10.1063/1.1432450
83. J.R.Tumbleston, D.Shirvanyants, N.Ermoshkin, R.Janusziewicz, A.R.Johnson, D.Kelly, K.Chen, R.Pinschmidt, J.P.Rolland, A.Ermoshkin, E.T.Samulski, J.M.DeSimone. *Science*, **347** (6228), 1349 (2015); https://doi.org/10.1126/science.aaa2397
84. L.Behalek, J.Safka, M.Seidl, J.Habr, J.Bobek. *MM Sci. J.*, 2722 (2018); https://doi.org/10.17973/MMSJ.2018_12_2018117
85. M.Dawoud, I.Taha, S.J.Ebeid. *J. Manuf. Proc.*, **21**, 39 (2016); https://doi.org/10.1016/j.jmapro.2015.11.002
86. J.E.Seppala, S.H.Han, K.E.Hillgartner, C.S.Davis, K.B.Migler. *Soft Matter*, **13**, 6761 (2017); https://doi.org/10.1039/c7sm00950j
87. S.Jiang, M.Zhan, M.Sun, W.Dai, C.Zhao. *Shock Vibrat.*, 1219435 (2019); https://doi.org/10.1155/2019/1219435
88. T.D.McLouth, J.V.Severino, P.M.Adams, D.N.Patel, R.J.Zaldivar. *Addit. Manuf.*, **18**, 103 (2017); https://doi.org/10.1016/j.addma.2017.09.003
89. S.Ahn, M.Montero, D.Odell, S.Roundy, P.Wright. *Rapid Prototyp. J.*, **8**, 248 (2002); https://doi.org/10.1108/13552540210441166
90. K.S.Erokhin, E.G.Gordeev, V.P.Ananikov. *Sci. Rep.*, **9**, 20177 (2019); https://doi.org/10.1038/s41598-019-56350-w
91. G.Weisgrab, A.Ovsianikov, P.F.Costa. *Adv. Mater. Technol.*, **4**, 1900275 (2019); https://doi.org/10.1002/admt.201900275
92. S.C.Daminabo, S.Goel, S.A.Grammatikos, H.Y.Nezhad, V.K.Thakur. *Mater. Today Chem.*, **16**, 100248 (2020); https://doi.org/10.1016/j.mtchem.2020.100248
93. R.D.Bintara, I.Z.Aminnudin, F.R.Arbianto, D.Prasetiyo. *J. Mech. Eng. Sci. Technol.*, **3** (1), 35 (2019); https://doi.org/10.17977/um016v3i12019p035
94. S.Rosales, S.Ferrándiz, M.J.Reig, J.Seguí. *Proc. Manuf.*, **13**, 833 (2017); https://doi.org/10.1016/j.promfg.2017.09.188
95. F.Ni, G.Wang, H.Zhao. *J. Appl. Polym. Sci.*, **134**, 44966 (2017); https://doi.org/10.1002/APP.44966
96. O.S.Carneiro, A.F.Silva, R.Gomes. *Mater. Design*, **83**, 768 (2015); https://doi.org/10.1016/j.matdes.2015.06.053
97. E.G.Gordeev, V.P.Ananikov. *3D Printing with Support Material*, (2020); https://doi.org/10.6084/m9.figshare.12640763.v1
98. V.Mazzanti, L.Malagutti, F.Mollica. *Polymers*, **11**, 1094 (2019); https://doi.org/10.3390/polym11071094
99. A.M.Peterson. *Addit. Manuf.*, **27**, 363 (2019); https://doi.org/10.1016/j.addma.2019.03.030
100. S.Farah, D.G.Anderson, R.Langer. *Adv. Drug Deliv. Rev.*, **107**, 367 (2016); https://doi.org/10.1016/j.addr.2016.06.012
101. J.T.Belter, A.M.Dollar. *PLoS ONE*, **10**, e0122915 (2015); https://doi.org/10.1371/journal.pone.0122915
102. B.M.Tymrak, M.Kreiger, J.M.Pearce. *Mater. Design*, **58**, 242 (2014); https://doi.org/10.1016/j.matdes.2014.02.038
103. J.Kiendl, C.Gao. *Composites, Part B*, **180**, 107562 (2020); https://doi.org/10.1016/j.compositesb.2019.107562
104. A.Rodríguez-Panes, J.Claver, A.M.Camacho. *Materials*, **11**, 1333 (2018); DOI:10.3390/ma11081333
105. E.G.Gordeev, V.P.Ananikov. *3D Printed Fullerene Model* (2020); https://doi.org/10.6084/m9.figshare.12090570.v1
106. E.G.Gordeev, V.P.Ananikov. *3D Printed Stand for Operational Work with Microcentrifuge Tubes in a Chemical Laboratory* (2020); https://doi.org/10.6084/m9.figshare.12090594.v1
107. B.Wittbrodt, J.M.Pearce. *Addit. Manuf.*, **8**, 110 (2015); https://doi.org/10.1016/j.addma.2015.09.006
108. P.Minetola, M.Galati, L.Iuliano, E.Atzeni, A.Salmi. *Proc. CIRP*, **67**, 203 (2018); https://doi.org/10.1016/j.procir.2017.12.200
109. F.M.Mwema, E.T.Akinlabi, O.S.Fatoba. *Mater. Today: Proc.*, **26**, 1520 (2020); https://doi.org/10.1016/j.matpr.2020.02.313
110. L.P.Bressan, C.B.Adamo, R.F.Quero, D.P.de Jesus, J.A.F.da Silva. *Anal. Methods*, **11**, 1014 (2019); https://doi.org/10.1039/c8ay02092b
111. J.Korpela, A.Kokkari, H.Korhonen, M.Malin, T.Närhi, J.Seppälä. *J. Biomed. Mater. Res., B*, **101**, 610 (2013); https://doi.org/10.1002/jbm.b.32863
112. K.Liang, S.Carmone, D.Brambilla, J.-C.Leroux. *Sci. Adv.*, **4**, eaat2544 (2018); https://doi.org/10.1126/sciadv.aat2544
113. F.Ning, W.Cong, J.Qiu, J.Wei, S.Wang. *Composites, Part B*, **80**, 369 (2015); https://doi.org/10.1016/j.compositesb.2015.06.013
114. N.Mohan, P.Senthil, S.Vinodh, N.Jayanth. *Virt. Phys. Prototyp.*, **12** (1), 47 (2017); https://doi.org/10.1080/17452759.2016.1274490
115. Y.Liu, T.-W.Chou. *Mater. Today Adv.*, **5**, 100045 (2020); https://doi.org/10.1016/j.mtadv.2019.100045
116. L.Yang, S.Li, X.Zhou, J.Liu, Y.Li, M.Yang, Q.Yuan. *Synt. Met.*, **253**, 122 (2019); https://doi.org/10.1016/j.synthmet.2019.05.008
117. M.Murariu, P.Dubois. *Adv. Drug Deliv. Rev.*, **107**, 17 (2016); https://doi.org/10.1016/j.addr.2016.04.003
118. V.Mirón, S.Ferrándiz, D.Juárez, A.Mengual. *Proc. Manuf.*, **13**, 888 (2017); https://doi.org/10.1016/j.promfg.2017.09.151
119. H.Mei, X.Yin, J.Zhang, W.Zhao. *Adv. Eng. Mater.*, **21**, 1800539 (2019); https://doi.org/10.1002/adem.201800539

120. Q.Ding, X.Li, D.Zhang, G.Zhao, Z.Sun. *J. Appl. Polym. Sci.*, **137**, 48786 (2020); https://doi.org/10.1002/APP.48786
121. J.Ye, T.Chu, J.Chu, B.Gao, B.He. *ACS Sust. Chem. Eng.*, **7**, 18048 (2019); https://doi.org/10.1021/acssuschemeng.9b04980
122. X.Li, Z.Ni, S.Bai, B.Lou. *IOP Conf. Ser.: Mater. Sci. Eng.*, **322**, 022012 (2018); https://doi.org/10.1088/1757-899X/322/2/022012
123. M.Kariz, M.Sernek, M.Obućina, M.K.Kuzman. *Mater. Today Commun.*, **14**, 135 (2018); https://doi.org/10.1016/j.mtcomm.2017.12.016
124. D.Depuydt, M.Balthazar, K.Hendrickx, W.Six, E.Ferraris, F.Desplentere, J.Ivens, A.W.Van Vuure. *Polym. Compos.*, **40**, 1951 (2019); https://doi.org/10.1002/pc.24971
125. H.Liu, H.He, X.Peng, B.Huang, J.Li. *Polym. Adv. Technol.*, **30**, 910 (2019); https://doi.org/10.1002/pat.4524
126. X.Zhang, L.Chen, T.Mulholland, T.A.Osswald. *Polym. Adv. Technol.*, **30**, 2122 (2019); https://doi.org/10.1002/pat.4645
127. L.Chen, X.Zhang, Y.Wang, T.A.Osswald. *Polym. Compos.*, **41**, 1356 (2020); https://doi.org/10.1002/pc.25459
128. J.Lee, H.Lee, K.-H.Cheon, C.Park, T.-S.Jang, H.-E.Kim. *Addit. Manuf.*, **30**, 100883 (2019); https://doi.org/10.1016/j.addma.2019.100883
129. W.Liu, N.Wu, K.Pochiraju. *Composites, Part A*, **108**, 1 (2018); https://doi.org/10.1016/j.compositesa.2018.02.017
130. J.C.Camargo, Á.R.Machado, E.C.Almeida, E.F.M.S.Silva. *Int. J. Adv. Manuf. Technol.*, **103**, 2423 (2019); https://doi.org/10.1007/s00170-019-03532-5
131. H.S.Patanwala, D.Hong, S.R.Vora, B.Bognet, A.W.K.Ma. *Polym. Compos.*, **39** (S2), E1060 (2018); https://doi.org/10.1002/pc.24494
132. S.-H.Su, Y.Huang, S.Qu, W.Liu, R.Liu, L.Li. *Diam. Relat. Mater.*, **81**, 161 (2018); https://doi.org/10.1016/j.diamond.2017.12.011
133. Z.Liu, Q.Lei, S.Xing. *J. Mater. Res. Technol.*, **8**, 3741 (2019); https://doi.org/10.1016/j.jmrt.2019.06.034
134. Y.Zhuang, W.Song, G.Ning, X.Sun, Z.Sun, G.Xu, B.Zhang, Y.Chen, S.Tao. *Mater. Design*, **126**, 135 (2017); https://doi.org/10.1016/j.matdes.2017.04.047
135. G.Spinelli, P.Lamberti, V.Tucci, R.Ivanova, S.Tabakova, E.Ivanov, R.Kotsilkova, S.Cimmino, R.Di Maio, C.Silvestre. *Composites, Part B*, **167**, 467 (2019); https://doi.org/10.1016/j.compositesb.2019.03.021
136. R.H.Sanatgar, A.Cayla, C.Campagne, V.Nierstrasz. *J. Appl. Polym. Sci.*, 47040 (2019); https://doi.org/10.1002/APP.47040
137. P.F.Flowers, C.Reyes, S.Ye, M.J.Kim, B.J.Wiley *Addit. Manuf.*, **18**, 156 (2017); https://doi.org/10.1016/j.addma.2017.10.002
138. S.Fafenrot, N.Grimmelsmann, M.Wortmann, A.Ehrmann. *Materials*, **10**, 1199 (2017); https://doi.org/10.3390/ma10101199
139. G.D.Goh, Y.L.Yap, S.Agarwala, W.Y.Yeong. *Adv. Mater. Technol.*, **4**, 1800271 (2019); https://doi.org/10.1002/admt.201800271
140. P.Parandoush, D.Lin. *Compos. Struct.*, **182**, 36 (2017); https://doi.org/10.1016/j.compstruct.2017.08.088
141. R.Matsuzaki, M.Ueda, M.Namiki, T.-K.Jeong, H.Asahara, K.Horiguchi, T.Nakamura, A.Todoroki, Y.Hirano. *Sci. Rep.*, **6**, 23058 (2016); https://doi.org/10.1038/srep23058
142. B.Akhoundi, A.H.Behravesh, A.B.Saed. *J. Reinfor. Plast. Compos.*, **38**, 99 (2019); https://doi.org/10.1177/0731684418807300
143. X.Tian, T.Liu, C.Yang, Q.Wang, D.Li. *Composites, Part A*, **88**, 198 (2016); https://doi.org/10.1016/j.compositesa.2016.05.032
144. M.Heidari-Rarani, M.Rafiee-Afarani, A.M.Zahedi. *Composites, Part B*, **175**, 107147 (2019); https://doi.org/10.1016/j.compositesb.2019.107147
145. N.Li, Y.Li, S.Liu. *J. Mater. Proc. Technol.*, **238**, 218 (2016); https://doi.org/10.1016/j.jmatprotec.2016.07.025
146. A.Goyanes, M.Kobayashi, R.Martínez-Pacheco, S.Gaisford. *Int. J. Pharm.*, **514**, 290 (2016); https://doi.org/10.1016/j.ijpharm.2016.06.021
147. H.Kim, G.H.Yang, C.H.Choi, Y.S.Cho, G.H.Kim. *Int. J. Bio. Macromol.*, **120**, 119 (2018); https://doi.org/10.1016/j.ijbiomac.2018.07.159
148. C.Wang, W.Huang, Y.Zhou, L.He, Z.He, Z.Chen, X.He, S.Tian, J.Liao, B.Lu, Y.Wei, M.Wang. *Bioact. Mater.*, **5**, 82 (2020); https://doi.org/10.1016/j.bioactmat.2020.01.004
149. A.Abdal-hay, K.H.Hussein, L.Casettari, K.A.Khalil, A.S.Hamdy. *Mater. Sci. Eng. C*, **60**, 143 (2016); https://doi.org/10.1016/j.msec.2015.11.024
150. O.M.F.Marwah, N.F.Yahaya, A.Darsani, E.J.Mohamad, R.H.A.Haq, M.A.Johar, M.H.Othman. *J. Phys.: Conf. Ser.*, **1150**, 012038 (2019); https://doi.org/10.1088/1742-6596/1150/1/012038
151. Y.Choi, C.Kim, H.Jeong, J.Youn. *World J. Eng. Technol.*, **4**, 186 (2016); https://doi.org/10.4236/wjet.2016.43D022
152. I.T.S.Heikkinen, C.Kauppinen, Z.Liu, S.M.Asikainen, S.Spoljaric, J.V.Seppälä, H.Savin, J.M.Pearce. *Addit. Manuf.*, **23**, 99 (2018); https://doi.org/10.1016/j.addma.2018.07.015
153. M.Lay, N.L.N.Thajudin, Z.A.A.Hamid, A.Rusli, M.K.Abdullah, R.K.Shuib. *Composites, Part B*, **176**, 107341 (2019); https://doi.org/10.1016/j.compositesb.2019.107341
154. Z.Quan, Z.Larimore, A.Wu, J.Yu, X.Qin, M.Mirotznik, J.Suhr, J.-H.Byun, Y.Oh, T.-W.Chou. *Compos. Sci. Technol.*, **126**, 139 (2016); https://doi.org/10.1016/j.compscitech.2016.02.021
155. J.Zhang, B.Yang, F.Fu, F.You, X.Dong, M.Dai. *Appl. Sci.*, **7**, 20 (2017); https://doi.org/10.3390/app7010020
156. A.Dorigato, V.Moretti, S.Dul, S.H.Unterberger, A.Pegoretti. *Synth. Met.*, **226**, 7 (2017); https://doi.org/10.1016/j.synthmet.2017.01.009
157. Jayanth N, Senthil P. *Composites, Part B*, **159**, 224 (2019); https://doi.org/10.1016/j.compositesb.2018.09.097
158. H.K.Sezer, O.Eren. *J. Manuf. Proc.*, **37**, 339 (2019); https://doi.org/10.1016/j.jmapro.2018.12.004
159. K.A.Hamzah, Y.C.Keat, T.P.Leng, M.M.Noor, S.A.Sazali, A.Y.Yun. *Mater. Today: Proc.*, **16**, 1778 (2019); https://doi.org/10.1016/j.matpr.2019.06.050
160. B.Huang, H.He, S.Meng, Y.Jia. *Polym. Int.*, **68**, 1351 (2019); https://doi.org/10.1002/pi.5824
161. W.H.Goh, M.Hashimoto. *Micromachines*, **9**, 523 (2018); https://doi.org/10.3390/mi9100523
162. Y.Xu, A.Unkovskiy, F.Klaue, F.Rupp, J.Geis-Gerstorfer, S.Spintzyk. *Materials*, **11**, 1905 (2018); https://doi.org/10.3390/ma11101905

163. M.Kaveh, M.Badrossamay, E.Foroozmehr, A.H.Etefagh. *J. Mater. Proc. Technol.*, **226**, 280 (2015); https://doi.org/10.1016/j.jmatprotec.2015.07.012
164. D.Yadav, D.Chhabra, R.K.Garg, A.Ahlawat, A.Phogat. *Mater. Today: Proc.*, **21**, 1583 (2020); https://doi.org/10.1016/j.matpr.2019.11.225
165. K.Durgashyam, M.I.Reddy, A.Balakrishna, K.Satyanarayana. *Mater. Today: Proc.*, **18**, 2052 (2019); https://doi.org/10.1016/j.matpr.2019.06.082
166. M.Ajay Kumar, M.S.Khan, S.B.Mishra. *Mater. Today: Proc.*, (2020); https://doi.org/10.1016/j.matpr.2020.01.291
167. K.Szykiedans, W.Credo, D.Osiński. *Proc. Eng.*, **177**, 455 (2017); https://doi.org/10.1016/j.proeng.2017.02.245
168. J.Herzberger, J.M.Sirrine, C.B.Williams, T.E.Long. *Prog. Polym. Sci.*, **97**, 101144 (2019); https://doi.org/10.1016/j.progpolymsci.2019.101144
169. K.Kim, J.Park, J.Suh, M.Kim, Y.Jeong, I.Park. *Sens. Actuators, A*, **263**, 493 (2017); https://doi.org/10.1016/j.sna.2017.07.020
170. M.M.Ali, D.Maddipatla, B.B.Narakathu, A.A.Chlaihawi, S.Emamian, F.Janabi, B.J.Bazuin, M.Z.Atashbar. *Sens. Actuators, A*, **274**, 109 (2018); https://doi.org/10.1016/j.sna.2018.03.003
171. J.F.Christ, N.Aliheidari, A.Ameli, P.Pötschke. *Mater. Design*, **131**, 394 (2017); https://doi.org/10.1016/j.matdes.2017.06.011
172. E.O.Bachtiar, O.Erol, M.Millrod, R.Tao, D.H.Gracias, L.H.Romer, S.H.Kang. *J. Mech. Behav. Biomed. Mater.*, **104**, 103649 (2020); https://doi.org/10.1016/j.jmbbm.2020.103649
173. J.E.Lee, S.J.Park, Y.Yoon, Y.Son, S.-H.Park. *J. Mech. Behav. Biomed. Mater.*, **91**, 193 (2019); https://doi.org/10.1016/j.jmbbm.2018.12.020
174. M.Jin, R.Giesa, C.Neuber, H.-W.Schmidt. *Macromol. Mater. Eng.*, **303**, 1800507 (2018); https://doi.org/10.1002/mame.201800507
175. M.Spoerk, J.Gonzalez-Gutierrez, C.Lichal, H.Cajner, G.R.Berger, S.Schuschnigg, L.Cardon, C.Holzer. *Polymers*, **10**, 490 (2018); https://doi.org/10.3390/polym10050490
176. M.Spoerk, F.Arbeiter, I.Raguž, G.Weingrill, T.Fischinger, G.Traxler, S.Schuschnigg, L.Cardon, C.Holzer. *Macromol. Mater. Eng.*, **303**, 1800179 (2018); https://doi.org/10.1002/mame.201800179
177. B.Kaynak, M.Spoerk, A.Shirole, W.Ziegler, J.Sapkota. *Macromol. Mater. Eng.*, **303**, 1800037 (2018); https://doi.org/10.1002/mame.201800037
178. M.Spoerk, C.Savandaiah, F.Arbeiter, G.Traxler, L.Cardon, C.Holzer, J.Sapkota. *Composites, Part A*, **118**, 95 (2018); https://doi.org/10.1016/j.compositesa.2018.06.018
179. M.Spoerk, C.Holzer, J.Gonzalez-Gutierrez. *J. Appl. Polym. Sci.*, **136**, 48545 (2019); https://doi.org/10.1002/a48545
180. A.M.Cadena-Perez, I.Yañez-Flores, S.Sanchez-Valdes, O.S.Rodriguez-Fernandez, S.Fernandez-Tavizon, L.F.R.de Valle, T.Lozano-Ramirez, J.G.Martinez-Colunga, J.L.Sanchez-Cuevas. *Int. J. Mater. Form.*, **10**, 233 (2017); https://doi.org/10.1007/s12289-015-1272-5
181. G.Sodeifian, S.Ghaseminejad, A.A.Yousefi. *Results Phys.*, **12**, 205 (2019); https://doi.org/10.1016/j.rinp.2018.11.065
182. M.Spoerk, C.Savandaiah, F.Arbeiter, J.Sapkota, C.Holzer. *Polym. Compos.*, **40**, 638 (2019); https://doi.org/10.1002/pc.24701
183. M.Spoerk, J.Sapkota, G.Weingrill, T.Fischinger, F.Arbeiter, C.Holzer. *Macromol. Mater. Eng.*, 1700143 (2017); https://doi.org/10.1002/mame.201700143
184. S.W.Kwok, H.K.H.Goh, Z.D.Tan, S.T.M.Tan, W.W.Tjiu, J.Y.Soh, Z.J.G.Ng, Y.Z.Chan, H.K.Hui, K.E.J.Goh. *Appl. Mater. Today*, **9**, 167 (2017); https://doi.org/10.1016/j.apmt.2017.07.001
185. M.P.Browne, E.Redondo, M.Pumera. *Chem. Rev.*, **120**, 2783 (2020); https://doi.org/10.1021/acs.chemrev.9b00783
186. N.E.Zander, J.H.Park, Z.R.Boelter, M.A.Gillan. *ACS Omega*, **4**, 13879 (2019); https://doi.org/10.1021/acsomega.9b01564
187. F.Kucherov, E.Gordeev, A.Kashin, V.Ananikov. *Angew. Chem., Int. Ed.*, **56**, 15931 (2017); https://doi.org/10.1002/anie.201708528
188. Q.Tarrés, J.K.Melbø, M.Delgado-Aguilar, F.X.Espinach, P.Mutjé, G.Chinga-Carrasco. *Composites, Part B*, **153**, 70 (2018); https://doi.org/10.1016/j.compositesb.2018.07.009
189. A.S.M.Sayem, H.Shahariar, J.Haider. *Encycl. Renew. Sustain. Mater.*, **2**, 839 (2020); https://doi.org/10.1016/B978-0-12-803581-8.10942-7
190. F.A.C.Sanchez, H.Boudaoud, M.Camargo, J.M.Pearce. *J. Clean. Prod.*, **264**, 121602 (2020); https://doi.org/10.1016/j.jclepro.2020.121602
191. G.Scotti, S.M.E.Nilsson, M.Haapala, P.Pöhö, G.Boije af Gennäs, J.Yli-Kauhaluoma, T.Kotiaho. *React. Chem. Eng.*, **2**, 299 (2017); https://doi.org/10.1039/c7re00015d
192. S.Chong, G.-T.Pan, M.Khalid, T. C.-K.Yang, S.-T.Hung, C.-M.Huang. *J. Polym. Environ.*, **25**, 136 (2017); https://doi.org/10.1007/s10924-016-0793-4
193. C.G.Schirmeister, T.Hees, E.H.Licht, R.Mülhaupt. *Addit. Manuf.*, **28**, 152 (2019); https://doi.org/10.1016/j.addma.2019.05.003
194. M.Nabipour, B.Akhoundi, A.B.Saed. *Inc. J. Appl. Polym. Sci.*, **137**, 48717 (2020); https://doi.org/10.1002/a48717
195. M.A.Kreiger, M.L.Mulder, A.G.Glover, J.M.Pearce. *J. Clean. Prod.*, **70**, 90 (2014); https://doi.org/10.1016/j.jclepro.2014.02.009
196. K.G.Mostafa, C.Montemagno, A.J.Qureshi. *Proc. Manuf.*, **26**, 753 (2018); https://doi.org/10.1016/j.promfg.2018.07.086
197. E.Verdejo de Toro, J.C.Sobrino, A.M.Martínez, V.M.Eguía. *Proc. Manuf.*, **41**, 731 (2019); https://doi.org/10.1016/j.promfg.2019.09.064
198. T.N.A.T.Rahim, A.M.Abdulla, H.M.Akil, D.Mohamad, Z.A.Rajion. *J. Reinfor. Plast. Compos.*, **34**, 1628 (2015); https://doi.org/10.1177/0731684415594692
199. Q.He, H.Wang, K.Fu, L.Ye. *Compos. Sci. Technol.*, **191**, 108077 (2020); https://doi.org/10.1016/j.compscitech.2020.108077
200. T.N.A.T.Rahim, A.M.Abdullah, H.Md Akil, D.Mohamad, Z.A.Rajion. *eXPRESS Polym. Lett.*, **11**, 963 (2017); https://doi.org/10.3144/expresspolymlett.2017.92
201. S.Lüftl, P.M.Visakh, S.Chandran. *Polyoxymethylene Handbook: Structure, Properties, Applications and Their Nanocomposites*. (Scrivener Publishing LLC, 2014); https://doi.org/10.1002/9781118914458
202. I.Muro-Fraguas, E.Sainz-García, A.Pernía-Espinoza, F.Alba-Elías. *Plasma Process Polym.*, **16**, e1900020 (2019); https://doi.org/10.1002/ppap.201900020

203. K.Von Petersdorff-Campen, Y.Hauswirth, J.Carpenter, A.Hagmann, S.Boës, M.S.Daners, D.Penner, M.Meboldt. *Appl. Sci.*, **8**, 1275 (2018); https://doi.org/10.3390/app8081275
204. W.C.Smith, R.W.Dean. *Polym. Test.*, **32**, 1306 (2013); https://doi.org/10.1016/j.polymertesting.2013.07.014
205. C.-H.Lee, H.Takagi, H.Okamoto, M.Kato. *J. Appl. Polym. Sci.*, **127**, 530 (2013); https://doi.org/10.1002/a37838
206. C.-H.Lee, H.Takagi, H.Okamoto, M.Kato. *Polym. J.*, **47**, 639 (2015); https://doi.org/10.1038/pj.2015.39
207. S.J.Park, J.E.Lee, H.B.Lee, J.Park, N.-K.Lee, Y.Son, S.-H.Park. *Addit. Manuf.*, **31**, 100974 (2020); https://doi.org/10.1016/j.addma.2019.100974
208. N.Momenzadeh, H.Miyanaji, D.A.Porter, T.A.Berfield. *Rapid Prototyp. J.*, **26**, 156 (2020); https://doi.org/10.1108/RPJ-08-2018-0203
209. A.Almazrouei, R.A.Susantyoko, C.-H.Wu, I.Mustafa, A.Alhammadi, S.Almheiri. *Sci. Rep.*, **9**, 9618 (2019); https://doi.org/10.1038/s41598-019-45992-5
210. H.Kim, F.Torres, D.Villagran, C.Stewart, Y.Lin, T.-L.B.Tseng. *Macromol. Mater. Eng.*, **302**, 1700229 (2017); https://doi.org/10.1002/mame.201700229
211. B.Valentan, Ž.Kadivnik, T.Brajlih, A.Anderson, I.Drstvenšek. *Mater. Technol.*, **47**, 715 (2013)
212. M.J.Harding, S.Brady, H.O'Connor, R.Lopez-Rodriguez, M.D.Edwards, S.Tracy, D.Dowling, G.Gibson, K.P.Girard, S.Ferguson. *React. Chem. Eng.*, **5**, 728 (2020); https://doi.org/10.1039/c9re00408d
213. A.C.de Leon, Q.Chen, N.B.Palaganas, J.O.Palaganas, J.Manapat, R.C.Advincula. *React. Funct. Polym.*, **103**, 141 (2016); https://doi.org/10.1016/j.reactfunctpolym.2016.04.010
214. L.O.Dandy, G.Oliveux, J.Wood, M.J.Jenkins, G.A.Leeke. *Polym. Degrad. Stab.*, **112**, 52 (2015); https://doi.org/10.1016/j.polymdegradstab.2014.12.012
215. S.A.Muhsin, P.V.Hatton, A.Johnson, N.Sereno, D.J.Wood. *Saudi Dental J.*, **31**, 382 (2019); https://doi.org/10.1016/j.sdentj.2019.03.005
216. W.Wu, P.Geng, G.Li, D.Zhao, H.Zhang, J.Zhao. *Materials*, **8**, 5834 (2015); DOI:10.3390/ma8095271
217. J.H.Bannock, S.H.Krishnadasan, M.Heeney, J.C.de Mello. *Mater. Horiz.*, **1**, 373 (2014); https://doi.org/10.1039/c4mh00054d
218. M.Rinaldi, T.Ghidini, F.Cecchini, A.Brandao, F.Nanni. *Composites, Part B*, **145**, 162 (2018); https://doi.org/10.1016/j.compositesb.2018.03.029
219. P.Geng, J.Zhao, W.Wu, W.Ye, Y.Wang, S.Wang, S.Zhang. *J. Manuf. Process.*, **37**, 266 (2019); https://doi.org/10.1016/j.jmapro.2018.11.023
220. S.Najeeb, M.S.Zafar, Z.Khurshid, F.Siddiqui. *J. Prosthodont. Res.*, **60** (1), 12 (2016); https://doi.org/10.1016/j.jpor.2015.10.001
221. F.Rahmitasari, Y.Ishida, K.Kurahashi, T.Matsuda, M.Watanabe, T.Ichikawa. *Dent. J.*, **5**, 35 (2017); https://doi.org/10.3390/dj5040035
222. X.Han, D.Yang, C.Yang, S.Spintzyk, L.Scheideler, P.Li, D.Li, J.Geis-Gerstorfer, F.Rupp. *J. Clin. Med.*, **8**, 240 (2019); https://doi.org/10.3390/jcm8020240
223. A.Haleem, M.Javaid. *Clin. Epidemiol. Global Health*, **7**, 571 (2019); https://doi.org/10.1016/j.cegh.2019.01.003
224. J.R.C.Dizon, A.H.Espera Jr., Q.Chen, R.C.Advincula. *Addit. Manuf.*, **20**, 44 (2018); https://doi.org/10.1016/j.addma.2017.12.002
225. H.Wu, W.P.Fahy, S.Kim, H.Kim, N.Zhao, L.Pilato, A.Kafi, S.Bateman, J.H.Koo. *Prog. Mater. Sci.*, **111**, 100638 (2020); https://doi.org/10.1016/j.pmatsci.2020.100638
226. E.Sacco, S.K.Moon. *Int. J. Adv. Manuf. Technol.*, **105**, 4123 (2019); https://doi.org/10.1007/s00170-019-03786-z
227. C.M.González-Henríquez, M.A.Sarabia-Vallejos, J.Rodriguez-Hernandez. *Prog. Polym. Sci.*, **94**, 57 (2019); https://doi.org/10.1016/j.progpolymsci.2019.03.001
228. G.Cicala, G.Ognibene, S.Portuesi, I.Blanco, M.Rapisarda, E.Pergolizzi, G.Recca. *Materials*, **11**, 285 (2018); https://doi.org/10.3390/ma11020285
229. C.Zawaski, C.Williams. *Addit. Manuf.*, **33**, 101111 (2020); https://doi.org/10.1016/j.addma.2020.101111
230. Values of Yield Strength and Bending Temperature under Load for Materials are Given in Accordance with the *Database MatWeb* (www.matweb.com)
231. L.E.Visscher, H.P.Dang, M.A.Knackstedt, D.W.Hutmacher, P.A.Tran. *Mater. Sci. Eng., C*, **87**, 78 (2018); https://doi.org/10.1016/j.msec.2018.02.008
232. Z.Jiao, B.Luo, S.Xiang, H.Ma, Y.Yu, W.Yang. *Adv. Ind. Eng. Polym. Res.*, **2**, 196 (2019); https://doi.org/10.1016/j.aiepr.2019.09.003
233. B.T.Duymaz, F.B.Erdiler, T.Alan, M.O.Aydogdu, A.T.Inan, N.Ekren, M.Uzun, M.Sahin, E.Bulus, F.N.Oktar, S.S.Selvi, E.T.Oner, O.Kilic, M.S.Bostan, M.S.Eroglu, O.Gunduz. *Eur. Polym. J.*, **119**, 426 (2019); https://doi.org/10.1016/j.eurpolymj.2019.08.015
234. F.Ghorbani, D.Li, S.Ni, Y.Zhou, B.Yu. *Mater. Today Commun.*, **22**, 100979 (2020); https://doi.org/10.1016/j.mtcomm.2020.100979
235. A.J.Guerra, P.Cano, M.Rabionet, T.Puig, J.Ciurana. *Polym. Adv. Technol.*, **29**, 2327 (2018); https://doi.org/10.1002/pat.4344
236. A.J.Guerra, J.Ciurana. *Mater. Design*, **137**, 430 (2018); https://doi.org/10.1016/j.matdes.2017.10.045
237. Y.-Q.Zhao, J.-H.Yang, X.Ding, X.Ding, S.Duan, F.-J.Xu. *Bioact. Mater.*, **5**, 185 (2020); https://doi.org/10.1016/j.bioactmat.2020.02.006
238. Y.Thompson, J.Gonzalez-Gutierrez, C.Kukla, P.Felfer. *Addit. Manuf.*, **30**, 100861 (2019); https://doi.org/10.1016/j.addma.2019.100861
239. B.Liu, Y.Wang, Z.Lin, T.Zhang. *Mater. Lett.*, **263**, 127252 (2020); https://doi.org/10.1016/j.matlet.2019.127252
240. O.A.Mohamed, S.H.Masood, J.L.Bhowmik, M.Nikzad, J.Azadmanjiri. *J. Mater. Eng. Perform.*, **25**, 2922 (2016); https://doi.org/10.1007/s11665-016-2157-6
241. M.Kumar, R.Ramakrishnan, A.Omarbekova. *J. Mech. Sci. Technol.*, **33**, 5219 (2019); https://doi.org/10.1007/s12206-019-1011-9
242. V.Tambrallimath, R.Keshavamurthy, D.Saravanabavan, P.G.Koppad, G.S.Pradeep Kumar. *Compos. Commun.*, **15**, 129 (2019); https://doi.org/10.1016/j.coco.2019.07.009
243. F.Peng, H.Jiang, A.Woods, P.Joo, E.J.Amis, N.S.Zacharia, B.D.Vogt. *ACS Appl. Polym. Mater.*, **1**, 275 (2019); https://doi.org/10.1021/acsapm.8b00186
244. A.S.de León, A.Domínguez-Calvo, S.I.Molina. *Mater. Design*, **182**, 108044 (2019); https://doi.org/10.1016/j.matdes.2019.108044
245. N.Decker, A.Yee. *Int. J. Addit. Subtract. Mater. Manufact.*, **1**, 161 (2017); https://doi.org/10.1504/IJASMM.2017.088203

246. H.Kim, E.Park, S.Kim, B.Park, N.Kim, S.Lee. *Proc. Manuf.*, **10**, 887 (2017); https://doi.org/10.1016/j.promfg.2017.07.076
247. R.Singh, R.Kumar, I.Farina, F.Colangelo, L.Feo, F.Fraternali. *Polymers*, **11**, 62 (2019); https://doi.org/10.3390/polym11010062
248. D.G.Bekas, Y.Hou, Y.Liu, A.Panesar. *Composites, Part B*, **179**, 107540 (2019); https://doi.org/10.1016/j.compositesb.2019.107540
249. J.-Y.Lee, J.An, C.K.Chua. *Appl. Mater. Today*, **7**, 120 (2017); https://doi.org/10.1016/j.apmt.2017.02.004
250. G.I.Peterson, M.B.Larsen, M.A.Ganter, D.W.Storti, A.J.Boydston. *ACS Appl. Mater. Interfaces*, **7**, 577 (2015); https://doi.org/10.1021/am506745m
251. A.D.Valino, J.R.C.Dizon, A.H.Espera Jr., Q.Chen, J.Messman, R.C.Advincula. *Prog. Polym. Sci.*, **98**, 101162 (2019); https://doi.org/10.1016/j.progpolymsci.2019.101162
252. J.A.Lewis. *Curr. Opin. Solid State Mater. Sci.*, **6**, 245 (2002); https://doi.org/10.1016/S1359-0286(02)00031-1
253. S.Zhao, W.Xiao, M.R.Rahaman, D.O'Brien, J.W.Seitz-Sampson, B.S.Bal. *Int. J. Appl. Ceram. Technol.*, **14**, 117 (2017); https://doi.org/10.1111/ijac.12633
254. D.M.Kirchmajer, R.Gorkin III, M.in het Panhuis. *J. Mater. Chem., B*, **3**, 4105 (2015); https://doi.org/10.1039/c5tb00393h
255. S.Naghieh, M.D.Sarker, N.K.Sharma, Z.Barhoumi, X.Chen. *Appl. Sci.*, **10**, 292 (2020); https://doi.org/10.3390/app10010292
256. T.Jungst, W.Smolan, K.Schacht, T.Scheibel, J.Groll. *Chem. Rev.*, **116**, 1496 (2016); https://doi.org/10.1021/acs.chemrev.5b00303
257. M.Guvendiren, J.Molde, R.M.D.Soares, J.Kohn. *ACS Biomater. Sci. Eng.*, **2**, 1679 (2016); https://doi.org/10.1021/acsbiomaterials.6b00121
258. S.Ji, M.Guvendiren. *Front. Bioeng. Biotechnol.*, **5**, 23 (2017); https://doi.org/10.3389/fbioe.2017.00023
259. J.M.Lee, W.Y.Yeong. *Adv. Healthcare Mater.*, **5**, 2856 (2016); https://doi.org/10.1002/adhm.201600435
260. Z.Chen, Z.Li, J.Li, C.Liu, C.Lao, Y.Fu, C.Liu, Y.Li, P.Wang, Y.He. *J. Eur. Ceram. Soc.*, **39**, 661 (2019); https://doi.org/10.1016/j.jeurceramsoc.2018.11.013
261. J.Gonzalez-Gutierrez, S.Cano, S.Schuschnigg, C.Kukla, J.Sapkota, C.Holzer *Materials*, **11**, 840 (2018); https://doi.org/10.3390/ma11050840
262. J.A.Lewis, J.E.Smay, J.Stuecker, J.Cesarano III. *J. Am. Ceram. Soc.*, **89**, 3599 (2006); https://doi.org/10.1111/j.1551-2916.2006.01382.x
263. E.Feilden, E.García-Tuñón Blanca, F.Giuliani, E.Saiz, L.Vandeperre. *J. Eur. Ceram. Soc.*, **36**, 2525 (2016); https://doi.org/10.1016/j.jeurceramsoc.2016.03.001
264. C.F.Revelo, H.A.Colorado. *Ceram. Int.*, **44**, 5673 (2018); https://doi.org/10.1016/j.ceramint.2017.12.219
265. A.R.Studart. *Chem. Soc. Rev.*, **45**, 359 (2016); https://doi.org/10.1039/c5cs00836k
266. U.Kalsoom, P.N.Nesterenko, B.Paull. *RSC Adv.*, **6**, 60355 (2016); https://doi.org/10.1039/c6ra11334f
267. J.Bonada, E.Xuriguera, L.Calvo, L.Poudelet, R.Cardona, J.A.Padilla, M.Niubó, F.Fenollosa. *Proc. Manuf.*, **41**, 666 (2019); https://doi.org/10.1016/j.promfg.2019.09.056
268. C.Xu, Q.Wu, G.L'Espérance, L.L.Lebel, D.Therriault. *Mater. Design*, **160**, 262 (2018); https://doi.org/10.1016/j.matdes.2018.09.024
269. P.Wei, H.Leng, Q.Chen, R.Advincula, E.B.Pentzer. *ACS Appl. Polym. Mater.*, **1**, 885 (2019); https://doi.org/10.1021/acsapm.9b00118
270. K.Chizari, M.A.Daoud, A.R.Ravindran, D.Therriault. *Small*, **12**, 6076 (2016); https://doi.org/10.1002/smll.201601695
271. J.H.Kim, S.Lee, M.Wajahat, H.Jeong, W.S.Chang, H.J.Jeong, J.-R.Yang, J.T.Kim, S.K.Seol. *ACS Nano*, **10**, 8879 (2016); https://doi.org/10.1021/acsnano.6b04771
272. H.Guo, R.Lv, S.Bai. *Nano Mater. Sci.*, **1**, 101 (2019); https://doi.org/10.1016/j.nanoms.2019.03.003
273. Y.Li, Z.Feng, L.Huang, K.Essa, E.Bilotti, H.Zhang, T.Peijs, L.Hao. *Composites, Part A*, **124**, 105483 (2019); https://doi.org/10.1016/j.compositesa.2019.105483
274. A.E.Jakus, E.B.Secor, A.L.Rutz, S.W.Jordan, M.C.Hersam, R.N.Shah. *ACS Nano*, **9**, 4636 (2015); https://doi.org/10.1021/acsnano.5b01179
275. Q.Zhang, F.Zhang, S.P.Medarametla, H.Li, C.Zhou, D.Lin. *Small*, **12**, 1702 (2016); https://doi.org/10.1002/smll.201503524
276. B.G.Compton, J.A.Lewis. *Adv. Mater.*, **26**, 5930 (2014); https://doi.org/10.1002/adma.201401804
277. S.C.Ligon, R.Liska, J.Stampfl, M.Gurr, R.Mülhaupt. *Chem. Rev.*, **117**, 10212 (2017); https://doi.org/10.1021/acs.chemrev.7b00074
278. A.Bagheri, J.Jin. *ACS Appl. Polym. Mater.*, **1**, 593 (2019); https://doi.org/10.1021/acsapm.8b00165
279. B.Ch.Kholkhoev, K.N.Bardakova, N.V.Minaev, O.S.Kupriyanova, E.N.Gorenskaia, T.M.Zharikova, P.S.Timashev, V.F.Burdukovskii. *Mendeleev Commun.*, **29**, 223 (2019); https://doi.org/10.1016/j.mencom.2019.03.037
280. S.Barone, P.Neri, A.Paoli, A.V.Razionale, F.Tamburrino. *Proc. Manuf.*, **38**, 1017 (2019); https://doi.org/10.1016/j.promfg.2020.01.187
281. A.K.Papadopoulou, A.Cantele, G.Polychronis, S.Zinelis, T.Eliades. *Materials*, **12**, 2406 (2019); https://doi.org/10.3390/ma12152406
282. Z.Weng, Y.Zhou, W.Lin, T.Senthil, L.Wu. *Composites. Part A*, **88**, 234 (2016); https://doi.org/10.1016/j.compositesa.2016.05.035
283. H.Korhonen, L.H.Sinh, N.D.Luong, P.Lehtinen, T.Verho, J.Partanen, J.Seppälä. *Phys. Status Solidi A*, **213**, 982 (2016); https://doi.org/10.1002/pssa.201532761
284. F.Kotz, K.Arnold, W.Bauer, D.Schild, N.Keller, K.Sachsenheimer, T.M.Nargang, C.Richter, D.Helmer, B.E.Rapp. *Nature (London)*, **544**, 337 (2017); https://doi.org/10.1038/nature22061
285. Z.C.Eckel, C.Zhou, J.H.Martin, A.J.Jacobsen, W.B.Carter, T.A.Schaedler. *Science*, **351**, 58 (2016); https://doi.org/10.1126/science.aad2688
286. M.Layani, X.Wang, S.Magdassi. *Adv. Mater.*, **30**, 1706344 (2018); https://doi.org/10.1002/adma.201706344
287. M.R.Hartings, Z.Ahmed. *Nat. Rev. Chem.*, **3**, 305 (2019); https://doi.org/10.1038/s41570-019-0097-z
288. V.Gupta, P.Nesterenko, B.Paull. *3D Printing in Chemical Sciences: Applications Across Chemistry*. (Cambridge: RSC, 2019); https://doi.org/10.1039/9781788015745
289. F.M.Mwema, E.T.Akinlabi. *Fused Deposition Modeling. Strategies for Quality Enhancement*. (Springer, 2020); https://doi.org/10.1007/978-3-030-48259-6
290. S.Rossi, A.Puglisi, M.Benaglia. *ChemCatChem*, **10**, 1512 (2018); https://doi.org/10.1002/cctc.201701619

291. P.J.Kitson, S.Glatzel, W.Chen, C.-G.Lin, Y.-F.Song, L.Cronin. *Nat. Prot.*, **11**, 920 (2016); https://doi.org/10.1038/nprot.2016.041
292. A.Ambrosi, M.Pumera. *Chem. Soc. Rev.*, **45**, 2740 (2016); https://doi.org/10.1039/c5cs00714c
293. C.Hurt, M.Brandt, S.S.Priya, T.Bhatelia, J.Patel, P.R.Selvakannan, S.Bhargava. *Catal. Sci. Technol.*, **7**, 3421 (2017); https://doi.org/10.1039/C7CY00615B
294. E.G.Gordeev, E.S.Degtyareva, V.P.Ananikov. *Russ. Chem. Bull.*, **65**, 1637 (2016) https://doi.org/10.1007/s11172-016-1492-y
295. E.O.Pentsak, D.B.Eremin, E.G.Gordeev, V.P.Ananikov. *ACS Catal.*, **9**, 3070 (2019); https://doi.org/10.1021/acscatal.9b00294
296. P.J.Kitson, M.D.Symes, V.Dragone, L.Cronin. *Chem. Sci.*, **4**, 3099 (2013); https://doi.org/10.1039/c3sc51253c
297. P.J.Kitson, G.Marie, J.-P.Francoia, S.S.Zalesskiy, R.C.Sigerson, J.S.Mathieson, L.Cronin. *Science*, **359**, 314 (2018); https://doi.org/10.1126/science.aao3466
298. J.M.Neumaier, A.Madani, T.Klein, T.Ziegler. *Beilstein J. Org. Chem.*, **15**, 558 (2019); https://doi.org/10.3762/bjoc.15.50
299. C.R.Tubío, J.Azuaje, L.Escalante, A.Coelho, F.Guitián, E.Sotelo, A.Gil. *J. Catal.*, **334**, 110 (2016); https://doi.org/10.1016/j.jcat.2015.11.019
300. C.Zhu, Z.Qi, V.A.Beck, M.Luneau, J.Lattimer, W.Chen, M.A.Worsley, J.Ye, E.B.Duoss, C.M.Spadaccini, C.M.Friend, J.Biener. *Sci. Adv.*, **4**, eaas9459 (2018); https://doi.org/10.1126/sciadv.aas9459
301. P.J.Kitson, S.Glatzel, L.Cronin. *Beilstein J. Org. Chem.*, **12**, 2776 (2016); https://doi.org/10.3762/bjoc.12.276
302. J.Li, S.G.Ballmer, E.P.Gillis, S.Fujii, M.J.Schmidt, A.M.E.Palazzolo, J.W.Lehmann, G.F.Morehouse, M.D.Burke. *Science*, **347**, 1221 (2015); https://doi.org/10.1126/science.aaa5414
303. S.Steiner, J.Wolf, S.Glatzel, A.Andreou, J.M.Granda, G.Keenan, T.Hinkley, G.Aragon-Camarasa, P.J.Kitson, D.Angelone, L.Cronin. *Science*, **363**, eaav2211 (2019); https://doi.org/10.1126/science.aav2211
304. P.J.Kitson, R.J.Marshall, D.Long, R.S.Forgan, L.Cronin. *Angew. Chem., Int. Ed.*, **53**, 12723 (2014); https://doi.org/10.1002/anie.201402654
305. M.D.Symes, P.J.Kitson, J.Yan, C.J.Richmond, G.J.T.Cooper, R.W.Bowman, T.Vilbrandt, L.Cronin. *Nat. Chem.*, **4**, 349 (2012); https://doi.org/10.1038/nchem.1313
306. S.S.Zalesskiy, P.J.Kitson, P.Frei, A.Bubliauskas, L.Cronin. *Nat. Commun.*, **10**, 5496 (2019); https://doi.org/10.1038/s41467-019-13328-6
307. A.J.Capel, S.Edmondson, S.D.R.Christie, R.D.Goodridge, R.J.Bibb, M.Thurstans. *Lab Chip*, **13**, 4583 (2013); https://doi.org/10.1039/c3lc50844g
308. S.Rossi, R.Porta, D.Brenna, A.Puglisi, M.Benaglia. *Angew. Chem., Int. Ed.*, **56**, 4290 (2017); https://doi.org/10.1002/anie.201612192
309. Z.X.Rao, B.Patel, A.Monaco, Z.J.Cao, M.Barniol-Xicota, E.Pichon, M.Ladlow, S.T.Hilton. *Eur. J. Org. Chem.*, 6499 (2017); https://doi.org/10.1002/ejoc.201701111
310. A.K.Au, W.Huynh, L.F.Horowitz, A.Folch. *Angew. Chem., Int. Ed.*, **55**, 3862 (2016); https://doi.org/10.1002/anie.201504382
311. C.K.Dixit, K.Kadimisetty, J.Rusling. *Trends Anal. Chem.*, **106**, 37 (2018); https://doi.org/10.1016/j.trac.2018.06.013
312. R.D.Sochol, E.Sweet, C.C.Glick, S.-Y.Wu, C.Yang, M.Restaino, L.Lin. *Microelectron. Eng.*, **189**, 52 (2018); https://doi.org/10.1016/j.mee.2017.12.010
313. N.Bhattacharjee, A.Urrios, S.Kang, A.Folch. *Lab Chip*, **16**, 1720 (2016); https://doi.org/10.1039/c6lc00163g
314. H.S.Santana, M.S.A.Palma, M.G.M.Lopes, J.Souza, G.A.S.Lima, O.P.Taranto, J.L.Silva Jr. *Ind. Eng. Chem. Res.*, **59**, 3794 (2020); https://doi.org/10.1021/acs.iecr.9b03787
315. D.J.Cocovi-Solberg, P.J.Worsfold, M.Miró. *TrAC Trend. Anal. Chem.*, **108**, 13 (2018); https://doi.org/10.1016/j.trac.2018.08.007
316. P.N.Nge, C.I.Rogers, A.T.Woolley. *Chem. Rev.*, **113**, 2550 (2013); https://doi.org/10.1021/cr300337x
317. B.K.Gale, A.R.Jafek, C.J.Lambert, B.L.Goenner, H.Moghimifam, U.C.Nze, S.K.Kamarapu. *Inventions*, **3**, 60 (2018); https://doi.org/10.3390/inventions3030060
318. N.P.Macdonald, J.M.Cabot, P.Smejkal, R.M.Guijt, B.Paull, M.C.Breadmore. *Anal. Chem.*, **89**, 3858 (2017); https://doi.org/10.1021/acs.analchem.7b00136
319. P.J.Kitson, M.H.Rosnes, V.Sans, V.Dragone, L.Cronin. *Lab Chip*, **12**, 3267 (2012); https://doi.org/10.1039/c2lc40761b
320. S.Begolo, D.V.Zhukov, D.A.Selck, L.Li, R.F.Ismagilov. *Lab Chip*, **14**, 4616 (2014); https://doi.org/10.1039/c4lc00910j
321. K.C.Bhargava, B.Thompson, N.Malmstadt. *PNAS*, **111** (42), 15013 (2014); https://doi.org/10.1073/pnas.1414764111
322. R.D.Sochol, E.Sweet, C.C.Glick, S.Venkatesh, A.Avetisyan, K.F.Ekman, A.Raulinaitis, A.Tsai, A.Wienkers, K.Korner, K.Hanson, A.Long, B.J.Hightower, G.Slatton, D.C.Burnett, T.L.Massey, K.Iwai, L.P.Lee, K.S.J.Pister, L.Lin. *Lab Chip*, **16**, 668 (2016); https://doi.org/10.1039/c5lc01389e
323. C.Parra-Cabrera, C.Achille, S.Kuhn, R.Ameloot. *Chem. Soc. Rev.*, **47**, 209 (2018); https://doi.org/10.1039/c7cs00631d
324. J.S.Manzano, Z.B.Weinstein, A.D.Sadow, I.I.Slowing. *ACS Catal.*, **7**, 7567 (2017); https://doi.org/10.1021/acscatal.7b02111
325. A.S.Díaz-Marta, S.Yáñez, C.R.Tubío, V.L.Barrio, Y.Piñeiro, R.Pedrido, J.Rivas, M.Amorín, F.Guitián, A.Coelho. *ACS Appl. Mater. Interfaces*, **11**, 25283 (2019); https://doi.org/10.1021/acsami.9b08119
326. S.Rossi, A.Puglisi, L.M.Raimondi, M.Benaglia. *Catalysts*, **10**, 109 (2020); DOI:10.3390/catal10010109
327. C.-R.Chang, X.-F.Yang, B.Long, J.Li. *ACS Catal.*, **3**, 1693 (2013); https://doi.org/10.1021/cs400344r
328. A.Lackmann, C.Mahr, A.Rosenauer, M.Bäumer, A.Wittstock. *Catalysts*, **9**, 416 (2019); https://doi.org/10.3390/catal9050416
329. E.Bulatov, E.Lahtinen, L.Kivijärvi, E.Hey-Hawkins, M.Haukka. *ChemCatChem*, **12**, 4831 (2020); https://doi.org/10.1002/cctc.202000806
330. M.R.Penny, S.T.Hilton. *React. Chem. Eng.*, **5**, 853 (2020); https://doi.org/10.1039/c9re00492k
331. D.B.Eremin, V.P.Ananikov. *Coord. Chem. Rev.*, **346**, 2 (2017); https://doi.org/10.1016/j.ccr.2016.12.021
332. B.Gross, S.Y.Lockwood, D.M.Spence. *Anal. Chem.*, **89**, 57 (2017); https://doi.org/10.1021/acs.analchem.6b04344
333. M.T.W.Hearn. *Curr. Opin. Chem. Eng.*, **18**, 90 (2017); https://doi.org/10.1016/j.coche.2017.11.003
334. P.N.Nesterenko. *Pure Appl. Chem.*, **92**, 1341 (2020); https://doi.org/10.1515/pac-2020-0206

335. U.Kalsoom, P.N.Nesterenko, B.Paull. *TrAC Trend. Anal. Chem.*, **105**, 492 (2018); https://doi.org/10.1016/j.trac.2018.06.006
336. K.B.Anderson, S.Y.Lockwood, R.S.Martin, D.M.Spence. *Anal. Chem.*, **85**, 5622 (2013); https://doi.org/10.1021/ac4009594
337. V.Romanov, R.Samuel, M.Chaharlang, A.R.Jafek, A.Frost, B.K.Gale. *Anal. Chem.*, **90**, 10450 (2018); https://doi.org/10.1021/acs.analchem.8b02356
338. S.Martínez-Jarquín, A.Moreno-Pedraza, H.Guillén-Alonso, R.Winkler. *Anal. Chem.*, **88**, 6976 (2016); https://doi.org/10.1021/acs.analchem.6b01019
339. C.Fee, S.Nawada, S.Dimartino. *J. Chromatogr., A*, **1333**, 18 (2014); https://doi.org/10.1016/j.chroma.2014.01.043
340. G.IJ.Salentijn, P.E.Oomen, M.Grajewski, E.Verpoorte. *Anal. Chem.*, **89**, 7053 (2017); https://doi.org/10.1021/acs.analchem.7b00828
341. G.Comina, A.Suska, D.Filippini. *Lab Chip*, **14**, 424 (2014); https://doi.org/10.1039/c3lc50956g
342. J.X.H.Wong, F.S.F.Liu, H.-Z.Yu. *Anal. Chem.*, **86**, 11966 (2014); https://doi.org/10.1021/ac5035727
343. A.Roda, E.Michelini, L.Cevenini, D.Calabria, M.M.Calabretta, P.Simoni. *Anal. Chem.*, **86**, 7299 (2014); https://doi.org/10.1021/ac502137s
344. M.Rezazadeh, S.Seidi, S.Lid, S.Pedersen-Bjergaard, Y.Yamini. *Trends Anal. Chem.*, **118**, 548 (2019); https://doi.org/10.1016/j.trac.2019.06.019
345. A.C.Johnson, M.T.Bowser. *Lab Chip*, **18**, 27 (2018); https://doi.org/10.1039/C7LC01105A
346. S.K.Anciaux, M.Geiger, M.T.Bowser. *Anal. Chem.*, **88**, 7675 (2016); https://doi.org/10.1021/acs.analchem.6b01573
347. S.Nayak, N.R.Blumenfeld, T.Laksanasopin, S.K.Sia. *Anal. Chem.*, **89**, 102 (2017); https://doi.org/10.1021/acs.analchem.6b04630
348. H.N.Chan, Y.Shu, B.Xiong, Y.Chen, Y.Chen, Q.Tian, S.A.Michael, B.Shen, H.Wu. *ACS Sens.*, **1**, 227 (2016); https://doi.org/10.1021/acssensors.5b00100
349. F.Li, N.P.Macdonald, R.M.Guijt, M.C.Breadmore. *Anal. Chem.*, **91**, 1758 (2019); https://doi.org/10.1021/acs.analchem.8b03772
350. C.-K.Su, S.-C.Yen, T.-W.Li, Y.-C.Sun. *Anal. Chem.*, **88**, 6265 (2016); https://doi.org/10.1021/acs.analchem.6b00272
351. E.M.McBride, P.M.Mach, E.S.Dhummakupt, S.Dowling, D.O.Carmany, P.S.Demond, G.Rizzo, N.E.Manicke, T.Glaros. *TrAC Trend. Anal. Chem.*, **118**, 722 (2019); https://doi.org/10.1016/j.trac.2019.06.028
352. L.D.da Silva, I.Pereira, T.C.de Carvalho, J.F.A.Filho, W.Romão, B.G.Vaz. *Anal. Methods*, **11**, 999 (2019); https://doi.org/10.1039/C8AY02270D
353. G.I.J.Salentijn, H.P.Permentier, E.Verpoorte. *Anal. Chem.*, **86**, 11657 (2014); https://doi.org/10.1021/ac502785j
354. L.C.Duarte, T.C.de Carvalho, E.O.Lobo-Júnior, P.V.Abdelnur, B.G.Vaz, W.K.T.Coltro. *Anal. Methods*, **8**, 496 (2016); https://doi.org/10.1039/C5AY03074A
355. J.S.Mathieson, M.H.Rosnes, V.Sans, P.J.Kitson, L.Cronin. *Beilstein J. Nanotechnol.*, **4**, 285 (2013); https://doi.org/10.3762/bjnano.4.31
356. P.I.Hendricks, J.K.Dalgleish, J.T.Shelley, M.A.Kirleis, M.T.McNicholas, L.Li, T.-C.Chen, C.-H.Chen, J.S.Duncan, F.Boudreau, R.J.Noll, J.P.Denton, T.A.Roach, Z.Ouyang, R.G.Cooks. *Anal. Chem.*, **86**, 2900 (2014); https://doi.org/10.1021/ac403765x
357. J.A.Lewis, G.M.Gratson. *Mater. Today*, **7**, 32 (2004); https://doi.org/10.1016/S1369-7021(04)00344-X
358. D.Fichou, G.E.Morlock. *Anal. Chem.*, **89**, 2116 (2017); https://doi.org/10.1021/acs.analchem.6b04813
359. N.P.Macdonald, S.A.Currivan, L.Tedone, B.Paull. *Anal. Chem.*, **89**, 2457 (2017); https://doi.org/10.1021/acs.analchem.6b04546
360. C.Fee. *Curr. Opin. Chem. Eng.*, **18**, 10 (2017); https://doi.org/10.1016/j.coche.2017.07.003
361. H.Wang, D.J.Cocovi-Solberg, B.Hu, M.Miró. *Anal. Chem.*, **89**, 12541 (2017); https://doi.org/10.1021/acs.analchem.7b03767
362. C.Calderilla, F.Maya, V.Cerdà, L.O.Leal. *Talanta*, **175**, 463 (2017); https://doi.org/10.1016/j.talanta.2017.07.028
363. E.Mattio, F.Robert-Peillard, C.Branger, K.Puzio, A.Margaillan, C.Brach-Papa, J.Knoery, J.-L.Boudenne, B.Coulomb. *Talanta*, **168**, 298 (2017); https://doi.org/10.1016/j.talanta.2017.03.059
364. M.Trojanowicz, K.Kołacińska *Analyst*, **141**, 2085 (2016); https://doi.org/10.1039/C5AN02522B
365. S.Sandron, B.Heery, V.Gupta, D.A.Collins, E.P.Nesterenko, P.N.Nesterenko, M.Talebi, S.Beirne, F.Thompson, G.G.Wallace, D.Brabazon, F.Regan, B.Paull. *Analyst*, **139**, 6343 (2014); https://doi.org/10.1039/c4an01476f
366. F.Lucklum, S.Janssen, W.Lang, M.J.Vellekoop. *Proc. Eng.*, **120**, 703 (2015); https://doi.org/10.1016/j.proeng.2015.08.761
367. Z.-X.Low, Y.T.Chua, B.M.Ray, D.Mattia, I.S.Metcalfe, D.A.Patterson. *J. Membr. Sci.*, **523**, 596 (2017); https://doi.org/10.1016/j.memsci.2016.10.006
368. J.Seo, D.I.Kushner, M.A.Hickner. *ACS Appl. Mater. Interfaces*, **8**, 16656 (2016); https://doi.org/10.1021/acsami.6b03455
369. T.Femmer, A.J.C.Kuehne, J.Torres-Rendon, A.Walther, M.Wessling. *J. Membr. Sci.*, **478**, 12 (2015); https://doi.org/10.1016/j.memsci.2014.12.040
370. C.M.B.Ho, S.H.Ng, K.H.H.Li, Y.-J.Yoon. *Lab Chip*, **15**, 3627 (2015); https://doi.org/10.1039/c5lc00685f
371. E.A.Guzzi, M.W.Tibbitt. *Adv. Mater.*, 1901994 (2019); https://doi.org/10.1002/adma.201901994
372. T.Han, S.Kundu, A.Nag, Y.Xu. *Sensors*, **19**, 1706 (2019); https://doi.org/10.3390/s19071706
373. S.He, S.Feng, A.Nag, N.Afsarimanesh, T.Han, S.C.Mukhopadhyay. *Sensors*, **20**, 703 (2020); https://doi.org/10.3390/s20030703
374. E.Peris, O.Okafor, E.Kulcinskaja, R.Goodridge, S.V.Luis, E.Garcia-Verdugo, E.O'Reilly, V.Sans. *Green Chem.*, **19**, 5345 (2017); https://doi.org/10.1039/c7gc02421e
375. R.Ciriminna, M.Pagliaro. *Org. Process Res. Dev.*, **17**, 1479 (2013); https://doi.org/10.1021/op400258a
376. M.P.Thompson, I.Peñafiel, S.C.Cosgrove, N.J.Turner. *Org. Process Res. Dev.*, **23**, 9 (2019); https://doi.org/10.1021/acs.oprd.8b00305
377. R.R.Jose, M.J.Rodriguez, T.A.Dixon, F.Omenetto, D.L.Kaplan. *ACS Biomater. Sci. Eng.*, **2**, 1662 (2016); https://doi.org/10.1021/acsbiomaterials.6b00088

378. S.Mehrotra, J.C.Moses, A.Bandyopadhyay, B.B.Mandal. *ACS Appl. Bio Mater.*, **2**, 1385 (2019); https://doi.org/10.1021/acsabm.9b00073
379. V.Mironov, N.Reis, B.Derby. *Tissue Eng.*, **12**, 631 (2006); https://doi.org/10.1089/ten.2006.12.631
380. W.Peng, P.Datta, B.Ayan, V.Ozbolat, D.Sosnoski, I.T.Ozbolat. *Acta Biomater.*, **57**, 26 (2017); https://doi.org/10.1016/j.actbio.2017.05.025
381. A.Satpathy, P.Datta, Y.Wu, B.Ayan, E.Bayram, I.T.Ozbolat. *Expert Opin. Drug Discov.*, **13**, 1115 (2018); https://doi.org/10.1080/17460441.2018.1542427
382. I.Lukin, S.Musquiz, I.Erezuma, T.H.Al-Tel, N.Golafshan, A.Dolatshahi-Pirouz, G.Orive. *Expert Opin. Drug Discov.*, **14**, 953 (2019); https://doi.org/10.1080/17460441.2019.1636781
383. D.G.Nguyen, J.Funk, J.B.Robbins, C.Crogan-Grundy, S.C.Presnell, T.Singer, A.B.Roth. *PLoS ONE*, **11** (7), e0158674 (2016); https://doi.org/10.1371/journal.pone.0158674
384. S.Massa, M.A.Sakr, J.Seo, P.Bandaru, A.Arneri, S.Bersini, E.Zare-Eelanjegh, E.Jalilian, B.H.Cha, S.Antona, A.Enrico, Y.Gao, S.Hassan, J.P.Acevedo, M.R.Dokmeci, Y.S.Zhang, A.Khademhosseini, S.R.Shin. *Biomicrofluidics*, **11** (4), 044109 (2017); https://doi.org/10.1063/1.4994708
385. X.Ma, J.Liu, W.Zhu, M.Tang, N.Lawrence, C.Yu, M.Gou, S.Chen. *Adv. Drug Deliv. Rev.*, **132**, 235 (2018); https://doi.org/10.1016/j.addr.2018.06.011
386. E.V.Koudan, A.A.Gryadunova, P.A.Karalkin, J.V.Korneva, N.Y.Meteleva, I.I.Babichenko, A.V.Volkov, S.A.Rodionov, V.A.Parfenov, F.D.A.S.Pereira, Y.D.Khesuani, V.A.Mironov, E.A.Bulanova. *Biotechnol. J.*, **15**, 1900217 (2020); https://doi.org/10.1002/biot.201900217
387. L.J.Smith, P.Li, M.R.Holland, B.Ekser. *Sci. Rep.*, **8**, 7561 (2018); https://doi.org/10.1038/s41598-018-25663-7
388. N.I.Moldovan, N.Hibino, K.Nakayama. *Tissue Eng. Part B Rev.*, **23**, 237 (2017); https://doi.org/10.1089/ten.teb.2016.0322
389. N.I.Moldovan. *J. Cell. Mol. Med.*, **22**, 2964 (2018); https://doi.org/10.1111/jcmm.13598
390. K.Alessandri, M.Feyeux, B.Gurchenkov, C.Delgado, A.Trushko, K.-H.Krause, D.Vignjević, P.Nassoy, A.Roux. *Lab Chip*, **16**, 1593 (2016); https://doi.org/10.1039/c6lc00133e
391. W.Lee, D.Kwon, W.Choi, G.Y.Jung, S.Jeon. *Sci. Rep.*, **5**, 7717 (2015); https://doi.org/10.1038/srep07717
392. Z.Li, J.Yang, X.J.Loh. *NPG Asia Mater.*, **8**, e265 (2016); https://doi.org/10.1038/am.2016.48
393. M. Winnacker.*Eur. J. Lipid Sci. Technol.*, **121**, 1900101 (2019); https://doi.org/10.1002/ejlt.201900101
394. B.A.E.Lehner, D.T.Schmieden, A.S.Meyer. *ACS Synth. Biol.*, **6**, 1124 (2017); https://doi.org/10.1021/acssynbio.6b00395
395. L.Raddatz, I.de Vries, J.Austerjost, A.Lavrentieva, D.Geier, T.Becker, S.Beutel, T.Scheper. *Eng. Life Sci.*, **17**, 931 (2017); https://doi.org/10.1002/elsc.201700055
396. A.M.Tatara, G.L.Koons, E.Watson, T.C.Piepergerdes, S.R.Shah, B.T.Smith, J.Shum, J.C.Melville, I.A.Hanna, N.Demian, T.Ho, A.Ratcliffe, J.J.J.P.van den Beucken, J.A.Jansen, M.E.Wong, A.G.Mikos. *PNAS*, **116**, 6954 (2019); https://doi.org/10.1073/pnas.1819246116
397. B.C.Gross, J.L.Erkal, S.Y.Lockwood, C.Chen, D.M.Spence. *Anal. Chem.*, **86**, 3240 (2014); https://doi.org/10.1021/ac403397r
398. H.Zhao, F.Yang, J.Fu, Q.Gao, A.Liu, M.Sun, Y.He. *ACS Biomater. Sci. Eng.*, **3**, 3083 (2017); https://doi.org/10.1021/acsbiomaterials.7b00542
399. P.F.Egan. *Materials*, **12**, 2355 (2019); https://doi.org/10.3390/ma12152355
400. I.Buj-Corral, A.Bagheri, O.Petit-Rojo. *Materials*, **11**, 1532 (2018); https://doi.org/10.3390/ma11091532
401. A.Pirosa, R.Gottardi, P.G.Alexander, R.S.Tuan. *Stem Cell Res. Therap.*, **9** (112) (2018); https://doi.org/10.1186/s13287-018-0847-8
402. A.Marrella, T.Y.Lee, D.H.Lee, S.Karuthedom, D.Syla, A.Chawla, A.Khademhosseini, H.L.Jang. *Mater. Today*, **21**, 362 (2018); https://doi.org/10.1016/j.mattod.2017.10.005
403. A.Kumar, S.Mandal, S.Barui, R.Vasireddi, U.Gbureck, M.Gelinsky, B.Basu. *Mater. Sci. Eng. R*, **103**, 1 (2016); https://doi.org/10.1016/j.mser.2016.01.001
404. M.P.Nikolova, M.S.Chavali. *Bioact. Mater.*, **4**, 271 (2019); https://doi.org/10.1016/j.bioactmat.2019.10.005
405. T.Guo, T.R.Holzberg, C.G.Lim, F.Gao, A.Gargava, J.E.Trachtenberg, A.G.Mikos, J.P.Fisher. *Biofabrication*, **9**, 024101 (2017); https://doi.org/10.1088/1758-5090/aa6370
406. H.Qu, H.Fu, Z.Han, Y.Sun. *RSC Adv.*, **9**, 26252 (2019); https://doi.org/10.1039/C9RA05214C
407. K.Kardel, A.L.Carrano, D.M.Blersch, M.Kaur. *3D Print. Addit. Manuf.*, **2** (1), 12 (2015); https://doi.org/10.1089/3dp.2014.0024
408. P.B.Allen, Z.Khaing, C.E.Schmidt, A.D.Ellington. *ACS Biomater. Sci. Eng.*, **1**, 19 (2015); https://doi.org/10.1021/ab500026f
409. N.Nivedita, P.Ligrani, I.Papautsky. *Sci. Rep.*, **7**, 44072 (2017); https://doi.org/10.1038/srep44072
410. J.Kim, J.L.Connell, M.Whiteley, A.J.Bard. *Anal. Chem.*, **86**, 12327 (2014); https://doi.org/10.1021/ac5036204
411. R.Nielson, B.Kaehr, J.B.Shear. *Small*, **5**, 120 (2009); https://doi.org/10.1002/smll.200801084
412. B.Kaehr, J.B.Shear *J. Am. Chem. Soc.*, **129**, 1904 (2007); https://doi.org/10.1021/ja068390y
413. S.H.Lim, H.Kathuria, J.J.Y.Tan, L.Kang. *Adv. Drug Deliv. Rev.*, **132**, 139 (2018); https://doi.org/10.1016/j.addr.2018.05.006
414. B.J.Park, H.J.Choi, S.J.Moon, S.J.Kim, R.Bajracharya, J.Y.Min, H.-K.Han. *J. Pharm. Invest.*, **49**, 575 (2019); https://doi.org/10.1007/s40005-018-00414-y
415. P.H.L.Tran, T.T.D.Tran. *Int. J. Pharm.*, **581**, 119274 (2020); https://doi.org/10.1016/j.ijpharm.2020.119274
416. E.Fuenmayor, M.Forde, A.V.Healy, D.M.Devine, J.G.Lyons, C.McConville, I.Major. *Int. J. Pharm.*, **558**, 328 (2019); https://doi.org/10.1016/j.ijpharm.2019.01.013
417. B.M.Wu, S.W.Borland, R.A.Giordano, L.G.Cima, E.M.Sachs, M.J.Cima. *J. Control. Release*, **40**, 77 (1996); https://doi.org/10.1016/0168-3659(95)00173-5
418. M.D.Prima, J.Coburn, D.Hwang, J.Kelly, A.Khairuzzaman, L.Ricles. *3D Print. Med.*, **2**, 1 (2016); https://doi.org/10.1186/s41205-016-0005-9
419. J.Norman, R.D.Madurawe, C.M.V.Moore, M.A.Khan, A.Khairuzzaman. *Adv. Drug Deliv. Rev.*, **108**, 39 (2017); https://doi.org/10.1016/j.addr.2016.03.001
420. M.A.Azad, D.Olawuni, G.Kimbell, A.Z.Badruddoza, S.Hossain, T.Sultana *Pharmaceutics*, **12**, 124 (2020); https://doi.org/10.3390/pharmaceutics12020124

421. A.Melocchi, F.Parietti, G.Loreti, A.Maroni, A.Gazzaniga, L.Zema. *J. Drug Deliv. Sci. Technol.*, **30**, 360 (2015); https://doi.org/10.1016/j.jddst.2015.07.016
422. P.Polamaplly, Y.Cheng, X.Shi, K.Manikandan, G.E.Kremer, H.Qin. *Proc. Manuf.*, **34**, 552 (2019); https://doi.org/10.1016/j.promfg.2019.06.219
423. R.C.R.Beck, P.S.Chaves, A.Goyanes, B.Vukosavljevic, A.Buanz, M.Windbergs, A.W.Basit, S.Gaisford. *Int. J. Pharm.*, **528**, 298 (2017); https://doi.org/10.1016/j.ijpharm.2017.05.074
424. W.Jamróz, J.Szafraniec, M.Kurek, R.Jachowicz. *Pharm. Res.*, **35**, 176 (2018); https://doi.org/10.1007/s11095-018-2454-x
425. A.Melocchi, F.Parietti, A.Maroni, A.Foppoli, A.Gazzaniga, L.Zema. *Int. J. Pharm.*, **509**, 255 (2016); https://doi.org/10.1016/j.ijpharm.2016.05.036
426. J.Skowyra, K.Pietrzak, M.A.Alhnan. *Eur. J. Pharm. Sci.*, **68**, 11 (2015); https://doi.org/10.1016/j.ejps.2014.11.009
427. A.Goyanes, A.S.B.M.Buanz, G.B.Hatton, S.Gaisford, A.W.Basit. *Eur. J. Pharm. Biopharm.*, **89**, 157 (2015); https://doi.org/10.1016/j.ejpb.2014.12.003
428. A.Goyanes, J.Wang, A.Buanz, R.Martínez-Pacheco, R.Telford, S.Gaisford, A.W.Basit. *Mol. Pharmaceut.*, **12**, 4077 (2015); https://doi.org/10.1021/acs.molpharmaceut.5b00510
429. M.F.Simões, R.M.A.Pinto, S.Simões. *Drug Discov. Today*, **24**, 1749 (2019); https://doi.org/10.1016/j.drudis.2019.05.013
430. D.K.Tan, M.Maniruzzaman, A.Nokhodchi. *Pharmaceutics*, **10**, 203 (2018); DOI:10.3390/pharmaceutics10040203
431. M.A.Repka, S.Bandari, V.R.Kallakunta, A.Q.Vo, H.McFall, M.B.Pimparade, A.M.Bhagurkar. *Int. J. Pharm.*, **535**, 68 (2018); https://doi.org/10.1016/j.ijpharm.2017.10.056
432. J.Zhang, X.Feng, H.Patil, R.V.Tiwar, M.A.Repka. *Int. J. Pharm.*, **519**, 186 (2017); https://doi.org/10.1016/j.ijpharm.2016.12.049
433. E.Prasad, M.T.Islam, D.J.Goodwin, A.J.Megarry, G.W.Halbert, A.J.Florence, J.Robertson. *Addit. Manuf.*, **29**, 100776 (2019); https://doi.org/10.1016/j.addma.2019.06.027
434. Y.Zhao, X.Xie, Y.Zhao, Y.Gao, C.Cai, Q.Zhang, Z.Ding, Z.Fan, H.Zhang, M.Liu, J.Han. *Eur. J. Pharm. Sci.*, **127**, 60 (2019); https://doi.org/10.1016/j.ejps.2018.10.020
435. H.Kadry, A.Al-Hilal, A.Keshavarz, F.Alam, C.Xu, A.Joy, F.Ahsan. *Int. J. Pharm.*, **544**, 285 (2018); https://doi.org/10.1016/j.ijpharm.2018.04.010
436. D.Smith, Y.Kapoor, A.Hermans, R.Nofsinger, F.Kesisoglou, T.P.Gustafson, A.Procopio. *Int. J. Pharm.*, **550**, 418 (2018); https://doi.org/10.1016/j.ijpharm.2018.08.055
437. A.Maroni, A.Melocchi, F.Parietti, A.Foppoli, L.Zema, A.Gazzaniga. *J. Control. Release*, **268**, 10 (2017); https://doi.org/10.1016/j.jconrel.2017.10.008
438. N.Genina, J.P.Boetker, S.Colombo, N.Harmankaya, J.Rantanen, A.Bohr. *J. Control. Release*, **268**, 40 (2017); https://doi.org/10.1016/j.jconrel.2017.10.003
439. G.Matijašić, M.Gretić, J.Vinčić, A.Poropat, L.Cuculić, T.Rahelić. *J. Drug Deliv. Sci. Technol.*, **52**, 677 (2019); https://doi.org/10.1016/j.jddst.2019.05.037
440. A.Goyanes, H.Chang, D.Sedough, G.B.Hatton, J.Wang, A.Buanz, S.Gaisford, A.W.Basit. *Int. J. Pharm.*, **496**, 414 (2015); https://doi.org/10.1016/j.ijpharm.2015.10.039
441. J.Boetker, J.J.Water, J.Aho, L.Arnfast, A.Bohr, J.Rantanen. *Eur. J. Pharm. Sci.*, **90**, 47 (2016); https://doi.org/10.1016/j.ejps.2016.03.013
442. Z.Khizer, M.R.Akram, R.M.Sarfraz, J.S.Nirwan, S.Farhaj, M.Yousaf, T.Hussain, S.Lou, P.Timmins, B.R.Conway, M.U.Ghori. *Polymers*, **11**, 1095 (2019); https://doi.org/10.3390/polym11071095
443. J.Zhang, W.Yang, A.Q.Vo, X.Feng, X.Ye, D.W.Kim, M.A.Repka. *Carbohydr. Polym.*, **177**, 49 (2017); https://doi.org/10.1016/j.carbpol.2017.08.058
444. Y.Yang, H.Wang, H.Li, Z.Ou, G.Yang. *Eur. J. Pharm. Sci.*, **115**, 11 (2018); https://doi.org/10.1016/j.ejps.2018.01.005
445. B.Arafat, M.Wojsz, A.Isreb, R.T.Forbes, M.Isreb, W.Ahmed, T.Arafat, M.A.Alhnan. *Eur. J. Pharm. Sci.*, **118**, 191 (2018); https://doi.org/10.1016/j.ejps.2018.03.019
446. N.Yang, H.Chen, H.Han, Y.Shen, S.Gu, Y.He, S.Guo. *Int. J. Pharm.*, **552**, 91 (2018); https://doi.org/10.1016/j.ijpharm.2018.09.042
447. J.Wang, A.Goyanes, S.Gaisford, A.W.Basit. *Int. J. Pharm.*, **503**, 207 (2016); https://doi.org/10.1016/j.ijpharm.2016.03.016
448. A.V.Healy, E.Fuenmayor, P.Doran, L.M.Geever, C.L.Higginbotham, J.G.Lyons. *Pharmaceutics*, **11**, 645 (2019); https://doi.org/10.3390/pharmaceutics11120645
449. C.I.Gioumouxouzis, A.Baklavaridis, O.L.Katsamenis, C.K.Markopoulou, N.Bouropoulos, D.Tzetzis, D.G.Fatouros. *Eur. J. Pharm. Sci.*, **120**, 40 (2018); https://doi.org/10.1016/j.ejps.2018.04.020
450. B.Arafat, N.Qinna, M.Cieszynska, R.T.Forbes, M.A.Alhnan. *Eur. J. Pharm. Biopharm.*, **128**, 282 (2018); https://doi.org/10.1016/j.ejpb.2018.04.010
451. W.Jamróz, M.Kurek, A.Czech, J.Szafraniec, K.Gawlak, R.Jachowicz. *Eur. J. Pharm. Biopharm.*, **131**, 44 (2018); https://doi.org/10.1016/j.ejpb.2018.07.017
452. E.Mathew, G.Pitzanti, E.Larrañeta, D.A.Lamprou. *Pharmaceutics*, **12**, 266 (2020); https://doi.org/10.3390/pharmaceutics12030266
453. C.-Y.Liaw, M.Guvendiren. *Biofabrication*, **9**, 024102 (2017); https://doi.org/10.1088/1758-5090/aa7279
454. A.Aimar, A.Palermo, B.Innocenti. *J. Healthcare Eng.*, 5340616 (2019); https://doi.org/10.1155/2019/5340616
455. N.Bharti, S.Singh. *J. Chem. Educ.*, **94**, 879 (2017); https://doi.org/10.1021/acs.jchemed.6b00745
456. S.Ford, T.Minshall. *Addit. Manuf.*, **25**, 131 (2019); https://doi.org/10.1016/j.addma.2018.10.028
457. C.W.Pinger, M.K.Geiger, D.M.Spence. *J. Chem. Educ.*, **97**, 112 (2020); https://doi.org/10.1021/acs.jchemed.9b00588
458. S.Hall, G.Grant, D.Arora, A.Karaksha, A.McFarland, A.Lohning, S.Anoopkumar-Dukie. *Curr. Pharm. Teach. Learn.*, **9**, 723 (2017); https://doi.org/10.1016/j.cptl.2017.03.029
459. E.W.Meijer. *Angew. Chem., Int. Ed.*, **40**, 3783 (2001); https://doi.org/10.1002/1521-3773(20011015)40:20<3783::AID-ANIE3783>3.0.CO;2-J
460. C.F.Macrae, I.Sovago, S.J.Cottrell, P.T.A.Galek, P.McCabe, E.Pidcock, M.Platings, G.P.Shields, J.S.Stevens, M.Towler, P.A.Wood. *J. Appl. Cryst.*, **53**, 226 (2020); https://doi.org/10.1107/S1600576719014092

461. W.Humphrey, A.Dalke, K.Schulten. *J. Mol. Graph.*, **14**, 33 (1996); https://doi.org/10.1016/0263-7855(96)00018-5
462. E.F.Pettersen, T.D.Goddard, C.C.Huang, G.S.Couch, D.M.Greenblatt, E.C.Meng, T.E.Ferrin. *J. Comput. Chem.*, **25**, 1605 (2004); https://doi.org/10.1002/jcc.20084
463. P.J.Paukstelis. *J. Chem. Educ.*, **95**, 169 (2018); https://doi.org/10.1021/acs.jchemed.7b00549
464. S.Rossi, M.Benaglia, D.Brenna, R.Porta, M.Orlandi. *J. Chem. Educ.*, **92**, 1398 (2015); https://doi.org/10.1021/acs.jchemed.5b00168
465. V.F.Scalfani, T.P.Vaid. *J. Chem. Educ.*, **91**, 1174 (2014); https://doi.org/10.1021/ed400887t
466. B.K.Niece. *J. Chem. Educ.*, **96**, 2059 (2019); https://doi.org/10.1021/acs.jchemed.9b00053
467. J.Stone-Sundberg, W.Kaminsky, T.Snyder, P.Moeck. *Cryst. Res. Technol.*, **50**, 432 (2015); https://doi.org/10.1002/crat.201400469
468. P.P.Rodenbough, W.B.Vanti, S.-W.Chan. *J. Chem. Educ.*, **92**, 1960 (2015); https://doi.org/10.1021/acs.jchemed.5b00597
469. W.B.Chipman. *J. Chem. Educ.*, **46**, 118 (1969); https://doi.org/10.1021/ed046p118
470. K.Smiar, J.D.Mendez. *J. Chem. Educ.*, **93**, 1591 (2016); https://doi.org/10.1021/acs.jchemed.6b00297
471. K.M.Griffith, R.de Cataldo, K.H.Fogarty. *J. Chem. Educ.*, **93**, 1586 (2016); https://doi.org/10.1021/acs.jchemed.6b00293
472. M.J.Robertson, W.L.Jorgensen. *J. Chem. Educ.*, **92**, 2113 (2015); https://doi.org/10.1021/acs.jchemed.5b00682
473. M.E.Howell, C.S.Booth, S.M.Sikich, T.Helikar, R.L.Roston, B.A.Couch, K.van Dijk. *Biochem. Mol. Biol. Educ.*, **47**, 303 (2019); https://doi.org/10.1002/bmb.21234
474. S.M.Kerwin. *Biochem. Mol. Biol. Educ.*, **47**, 432 (2019); https://doi.org/10.1002/bmb.21250
475. S.C.Meyer. *J. Chem. Educ.*, **92**, 2120 (2015); https://doi.org/10.1021/acs.jchemed.5b00207
476. A.E.Lohning, S.Hall, S.Dukie. *J. Chem. Educ.*, **96**, 2497 (2019); https://doi.org/10.1021/acs.jchemed.8b00965
477. O.A.H.Jones, M.J.S.Spencer. *J. Chem. Educ.*, **95**, 88 (2018); https://doi.org/10.1021/acs.jchemed.7b00533
478. F.A.Carroll, D.N.Blauch. *J. Chem. Educ.*, **94**, 886 (2017); https://doi.org/10.1021/acs.jchemed.6b00933
479. A.S.Grumman, F.A.Carroll. *J. Chem. Educ.*, **96**, 1157 (2019); https://doi.org/10.1021/acs.jchemed.8b00597
480. M.R.Penny, Z.J.Cao, B.Patel, B.Sil dos Santos, C.R.M.Asquith, B.R.Szulc, Z.X.Rao, Z.Muwaffak, J.P.Malkinson, S.T.Hilton. *J. Chem. Educ.*, **94**, 1265 (2017); https://doi.org/10.1021/acs.jchemed.6b00953
481. L.Casas, E.Estop. *J. Chem. Educ.*, **92**, 1338 (2015); https://doi.org/10.1021/acs.jchemed.5b00147
482. K.V.Wieren, H.N.Tailor, V.F.Scalfani, N.Merbouh. *J. Chem. Educ.*, **94**, 964 (2017); https://doi.org/10.1021/acs.jchemed.6b00602
483. F.A.Carroll, D.N.Blauch. *J. Chem. Educ.*, **95**, 1607 (2018); https://doi.org/10.1021/acs.jchemed.7b00987
484. R.de Cataldo, K.M.Griffith, K.H.Fogarty. *J. Chem. Educ.*, **95**, 1601 (2018); https://doi.org/10.1021/acs.jchemed.8b00078
485. M.Bakker, B.Boyd, G.A.Meints. *Concep. Magn. Reson., Part A*, **47** (1), e21470 (2019); https://doi.org/10.1002/cmr.a.21470
486. C.S.Higman, H.Situ, P.Blacklin, J.E.Hein. *J. Chem. Educ.*, **94**, 1367 (2017); https://doi.org/10.1021/acs.jchemed.7b00314
487. V.F.Scalfani, C.H.Turner, P.A.Rupar, A.H.Jenkins, J.E.Bara. *J. Chem. Educ.*, **92**, 1866 (2015); https://doi.org/10.1021/acs.jchemed.5b00375
488. D.N.Blauch, F.A.Carroll. *J. Chem. Educ.*, **91**, 1254 (2014); https://doi.org/10.1021/ed4007259
489. A.Teplukhin, D.Babikov. *J. Chem. Educ.*, **92**, 305 (2015); https://doi.org/10.1021/ed500683g
490. J.L.Dye. *J. Chem. Educ.*, **34**, 215 (1957); https://doi.org/10.1021/ed034p215
491. P.Lolur, R.Dawes. *J. Chem. Educ.*, **91**, 1181 (2014); https://doi.org/10.1021/ed500199m
492. D.S.Kaliakin, R.R.Zaari, S.A.Varganov. *J. Chem. Educ.*, **92**, 2106 (2015); https://doi.org/10.1021/acs.jchemed.5b00409
493. T.Tabassum, M.Iloska, D.Scuereb, N.Taira, C.Jin, V.Zaitsev, F.Afshar, T.Kim. *J. Chem. Educ.*, **95**, 783 (2018); https://doi.org/10.1021/acs.jchemed.7b00663
494. M.T.Vangunten, U.J.Walker, H.G.Do, K.N.Knust. *J. Chem. Educ.*, **97**, 178 (2020); https://doi.org/10.1021/acs.jchemed.9b00620
495. L.A.Porter Jr., B.M.Washer, M.H.Hakim, R.F.Dallinger. *J. Chem. Educ.*, **93**, 305 (2016); https://doi.org/10.1021/acs.jchemed.6b00041
496. P.Bernard, J.D.Mendez. *J. Chem. Educ.*, **97**, 1162 (2020); https://doi.org/10.1021/acs.jchemed.9b01083
497. D.M.Gruber, T.Perez, B.Q.Layug, M.Ohama, L.Tran, L.A.F.Rojas, A.Xavier Garcia, G.Liu, W.J.W.Miller. *J. Chem. Educ.*, **97**, 845 (2020); https://doi.org/10.1021/acs.jchemed.9b01099
498. D.Fourches, J.Feducia. *J. Chem. Educ.*, **96**, 291 (2019); https://doi.org/10.1021/acs.jchemed.8b00346